TOWARDS AUTONOMOUS MICROCYSTIN DETECTION: INVESTIGATING METHODS FOR AUTOMATION

by

Maureen Schneider

A Thesis Submitted in
Partial Fulfillment of the
Requirements for the Degree of

Master of Science
in Freshwater Sciences and Technology

at
The University of Wisconsin-Milwaukee
May 2017

ABSTRACT

TOWARDS AUTONOMOUS MICROCYSTIN DETECTION: INVESTIGATING METHODS FOR AUTOMATION

by

Maureen Schneider

The University of Wisconsin-Milwaukee, 2017
Under the Supervision of Professor Matthew C. Smith

Due to increased anthropogenic activity, severe eutrophication is occurring in bodies of water around the world. Effects include decreased water quality, decreased value of surrounding land and recreational use (estimated loss in revenue of 0.67 and 3.96 U.S. billion dollars per year), and increased occurrence of toxin producing Harmful Algal Blooms (HABs). Microcystins are cyclic peptides made up of 7 amino acids and 800-1100 Daltons in size. They are one of the most predominantly produced of these toxins, and therefore was the focus of this study. Numerous structural variants of microcystin (referred to as congeners) exist, but microcystin-LR is one of the most common, having a World Health Organization (WHO) recommended limit of 1 µg/L in drinking water. In order to make informed public health decisions on potable and recreational water, an automated *in situ* instrument for detection of microcystin and its nucleic acids is needed. Very few detection systems have reached the market (i.e. Environmental Sample Processor, McLane Laboratories, USA), but all remain prohibitively costly and complex. Currently, research in many fields is directed towards developing a more cost effective automated *in situ* detection instrument that can collect and filter environmental samples, extract toxins and nucleic acids, and detect and quantify analytes, genes, and gene transcripts. In this

study, a sample preparation method for on-filter collection, filtration, and dual extraction of microcystin and nucleic acids was developed during the summer of 2016 on environmental samples from two bodies of water, Lake Winnebago, WI and Veteran's Park Lagoon, Milwaukee, WI. Results were compared to a traditional laboratory bead beating method. Results showed that the median extraction ratios (quantified by mass spectrometry) obtained with on-filter method compared to bead beat method (comparative recovery) for microcystin congeners MC-LR, MC-YR, MC-RR, and MC-LA were 43% ± 12%, 34% ± 9%, 46% ± 10% and 44% ± 13%, respectively for Lake Winnebago. The median comparative recovery for MC-LR, MC-YR, and MC-RR was 51% ± 9%, 49% ± 12%, and 53% ± 7%, respectively, for Veteran's Park Lagoon. Total RNA extraction by the on-filter result showed lower and more inconsistent ratios. Comparative recovery values for the Veteran's Park Lagoon ranged from 6% to 27% and 5% to 64% for Lake Winnebago. Further quantification with RT-qPCR is needed to evaluate extraction efficiency of the desired gene cluster (*mcy*). Methods that were evaluated for detection of microcystin included chemical derivatization (fluorescent derivatization) and optical signal amplification (direct and indirect hybridization schemes using DNA aptamers and oligonucleotide probes, nicking enzyme assisted fluorescent signal amplification (NEFSA)). Methods evaluated for detection of nucleic acids included optical signal amplification (direct and indirect hybridization, NEFSA, cascading amplification of nucleic acids (CANA)) and nucleic acid amplification (strand displacement amplification (SDA)). Of the techniques tested, SDA gave non-specific or no amplification, fluorescent derivatization was inconsistent, and all hybridization schemes resulted in non-specific binding. Preliminary results from NEFSA and CANA showed promise, but were inconsistent. Therefore, further optimization of reaction conditions is necessary to conclude if either could be viable options for use in an automated *in*

situ detection system in combination with the on-filter sample preparation and extraction technique.

© Copyright by Maureen Schneider, 2017
All Rights Reserved

TABLE OF CONTENTS

LIST OF FIGURES

LIST OF TABLES

ACKNOWLEDGEMENTS

I would like to sincerely thank Dr. Matthew Smith for his continuous guidance and support throughout this project; it would not have been possible without him. I would also like to thank my committee members, Dr. Todd Miller and Dr. Vipin Paliwal. Dr. Miller's endless mass spectrometry expertise and advice was invaluable and Dr. Paliwal supplied significant aid with hybridization chemistry techniques. My fellow lab mates Victoria St. Martin, Stephen Binter, Sarah Kahl, and Sydney Stephens also were vital in the data collection and analysis for the bulk of this work. I am also deeply grateful to my family, friends, and husband for emotional support, proof-reading my drafts, and listening to my presentation much more than once.

1 Chapter 1: Current and Emerging Technologies for Microcystin Sensor Systems

Abstract

Eutrophication of bodies of water around the globe is increasing due to anthropogenic activity such as over fertilization and run off to surface water, industrial point source pollution, waste water, etc. In many cases, eutrophication causes an increase of Harmful Algal Blooms (HABs), of which many are capable of producing toxins. These HABs have negative environmental and economic effects including decreased water quality, decreased value of surrounding land and economic loss due to decreased recreational use. In freshwater systems, microcystin is one of the most commonly produced toxins. Numerous microcystin congeners exist, but microcystin-LR is one of the most predominantly produced. The World Health Organization recommended limits of 1 µg/L for drinking water and 10 µg /L for recreational water, while in 2015, the United States Environmental Protection Agency (EPA) recommended a limit of 0.3 µg/L for 0 through 6 years of age and 1.6 µg /L for 6 years through adults in drinking water and 20 µg /L in recreational water [1]. More recently, the EPA has drafted a new limit of 4 µg /L in recreational water, which will go into effect in early 2017 [2]. Current analytical methodologies for microcystin rely mainly on timely laboratory analysis of environmental samples. In order to make informed public health decisions on potable and recreational water, cheaper and more portable analytical methodologies are needed. One such approach is to develop an automated *in situ* instrument for detection of microcystin and/or nucleic acids involved in its biosynthesis. Very few field deployable detection systems that quantify microbial metabolites (e.g., toxins) or nucleic acids from environmental water samples have reached the market. For example, the Environmental Sample Processor (ESP) (McLane Laboratories, USA) is a

potentially flexible system that can be applied to detect a variety of microbial toxins [3], [4]. However, the system remains prohibitively costly and complex for many researchers and regulatory agencies to incorporate into routine testing. This chapter examines current research trends in development of *in situ* instruments for microcystin, as well as reviewing and assessing other emerging laboratory based detection technologies with potential for application in the development of field deployable systems for detection of microcystin and its associated nucleic acids.

1.1 Introduction

1.1.1 Harmful Algal Blooms

Cyanobacteria (Cyanophyceae), commonly referred to as blue-green algae, are the oldest oxygenic photoautotrophs on Earth. Cyanobacterial blooms often form in warm water that has high concentrations of nutrients, such as phosphorous and nitrogen. They can form a film at the air-water interface or be suspended sub-surface at different depths in a body of water [5]. Cyanobacterial blooms are increasing in their occurrence and intensity globally, primarily due to the effects of global warming, eutrophication, land use changes and other anthropogenic activity [6], [7], [8]. The increased biomass from blooms of cyanobacteria has the potential to diminish water quality, ecosystem services, and species diversity, as well as produce toxins that are dangerous to human health [6]. These negative impacts can lead to severely reduced revenue in the affected regions due to decreased tourism, land value, recreational water use, biodiversity, etc. It can also increase municipal costs from clean-up of algal mats and treatment of toxin in drinking water. Dodds et al. [8] suggested that real estate value losses and recreational water use losses are the two main components in the eutrophication cost analysis of freshwater systems in the United States. Loss of real estate value was estimated to be between 0.3 and 2.8 billion U.S. dollars per year and loss of recreational water use was estimated to be between 0.37 and 1.16 billion U.S. dollars per year [8].

Some cyanobacterial blooms are classified as harmful algal blooms (HABs), which can produce a variety of toxins. A variety of toxins are commonly found in water samples taken when blooms are visible, suggesting correlation between bloom formation and the presence of toxin [9]. However, the amount of visible cyanobacteria does not definitively correlate to toxin production because not all cyanobacterial strains are capable of producing toxins [10].

Microcystin (MC) is one of the most commonly produced cyanotoxins from HABs. From the perspectives of research in toxicity, genetic regulation, environmental dynamics and detection methodology, microcystin is one of the most studied cyanotoxins [11], [7]. However, much is still not known about the factors the drive microcystin biosynthesis in the environment, and the public health implications from short and long term exposure.

1.1.2 Microcystin

Microcystins (MC) are produced by species of *Planktothrix, Microcystis, Aphanizomenon, Nostoc* and *Anabaena*, among others, [12] through non-ribosomal synthesis using large multi- and mono-functional proteins. In *Microcystis spp.* the microcystin biosynthesis gene cluster (*mcy*) has a conserved organization and has been shown to have orthologs in other cyanobacterial genera [13]. The *mcy* gene cluster encodes multifunctional proteins with nonribosomal peptide synthetase and polyketide synthetase domains as well as monofunctional enzymes with various active domains such as ABC transporters, amino acid epimerase, hydroxy acid dehydrogenase and methylation activity [14]. Figure 1 shows *mcy* gene cluster subunits *mcyA-J*. *McyA-C* are peptide synthetase genes, *mcyD, E,* and *G* are polyketide synthase genes, and *mycF, H, I,* and *J* are tailoring enzymes. *McyE* and *G* also have regions contributing to peptide synthetases [15]. In environmental samples, the presence of the *mcy* gene cluster is not a reliable predictor of the presence of microcystin [9], [16]. However, active transcription of the *mcy* gene cluster may suggest a higher likelihood of microcystin production [17], [16].

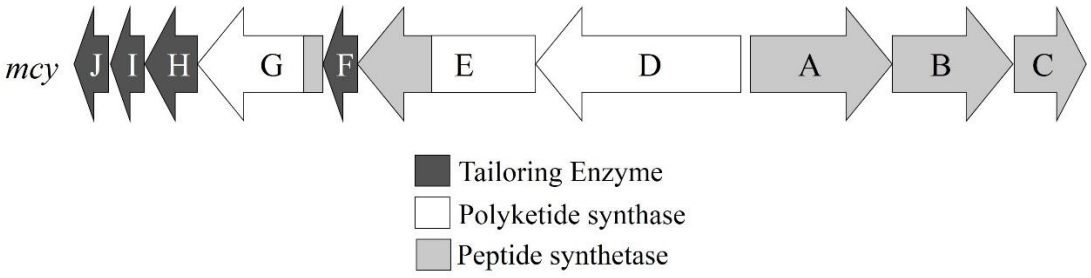

Figure 1: Example illustration showing the organization of the *mcy* gene cluster in *Microcystis spp.*, adapted from *[15]*.

Microcystins are cyclic peptides ranging in size between 800-1,100 Daltons. They are made up of 7 amino acid/amino acid constituents [18], with substitutions at positions X and Y and modifications at positions R1 (Figure 2). There are many possible structural variants of microcystin, and more than 100 microcystin congeners have been discovered in the environment [19]. The Adda amino acid ((2*S*,3*S*,8*S*,9*S*,4*E*,6*E*)-3-amino-9-methoxy-2,6,8-trimethyl-10-phenyl-4,6-decadienoic acid) is common to all variants. The hydrophobicity of the amino acids substituted at positions X and Y influences the overall hydrophobicity. Hydrophobicity of the microcystin congener determines how the toxin interacts with cell membranes, and therefore affects its specific toxicity [20].

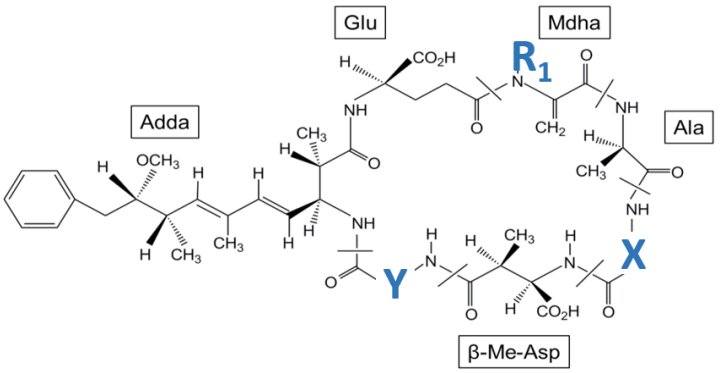

Microcystin	X	Y	R_1
MC-LR	Leu	Arg	CH_3
MC-RR	Arg	Arg	CH_3
MC-YR	Tyr	Arg	CH_3
[Dha7]MC-LR	Leu	Arg	H
MC-LA	Leu	Ala	CH_3

Figure 2: Generic Structure of Microcystin and Common congeners. Structure of microcystin showing conserved amino acids. Positions X and Y highlight sites of amino acid variations. Position R1 is a site of variable methylation. Common microcystin congeners with highlighted amino acid substitutions and methylation modifications. Adapted from *[21]*.

Microcystins are potent inhibitors of protein phosphatase 1 and 2A (PP1 and PP2A), which is widely accepted to be the main mechanism of toxicity [20]. It has also been suggested that microcystin can also interfere with aldehyde dehydrogenase II and the β subunit of ATP-synthase [20]. Phosphatases are crucial in regulating protein activity by phosphorylation/dephosphorylation [20] in cells throughout the body; microcystin is known to affect cells of the liver, blood brain-barrier, colon, etc. [22]. Microcystin can inactivate both PP1 and PP2A first by non-covalent binding, and following prolonged incubation covalent binding [20]. The mechanism of inhibition of both forms of protein phosphatase differs. However, interactions of microcystin's carboxyl residues at the amino acids d-*erythro*-β-methylaspartic acid (β-Me-Asp) and Glutamic acid (Glu), and hydrophobic interactions of the *N*-methyldehydroalanine (MdhA) and Adda residues (Figure 2).

Molecular interactions of microcystin with protein phosphatases have primarily been studied using the MC-LR congener. From X-ray crystallography of MC-LR bound to the α isoform PP1C, it was determined that binding occurred at the hydrophobic groove, C-terminal

groove, and the catalytic subunit. The hydrophobic Adda residue of MC-LR binds to the hydrophobic region of PP1c, which is adjacent to its active site. The carboxyl group of the β-Me-Asp residue of MC-LR interacts with PP1c amino acids (Arg 96 and Tyr 134), blocking access to the active site. The **α**–carboxyl of the MC-LR glutamic acid moiety interacts with the two catalytic metal atoms of PP1c. The crystal structure of MC-LR bound to PP2A showed that MC-LR bound to a surface pocket located directly above the active site of the enzyme. The bond is reinforced due to hydrophobic interactions between PP2A amino acid residues (Leu 243, Tyr 265, Cys 266, Arg 268, and Cys 269) and the hydrophobic Adda side chain of MC-LR, as well as covalent bonds between PP2A amino acid Cys 269 and the Mdha side chain of MC-LR.
This binding of microcystin to PP1 and PP2A inhibits the protein phosphatases from performing their necessary function, which causes disruption of the cytoskeleton and hepatic hemorrhage [23]. Microcystins are traditionally classed as hepatotoxins. However, they have also been shown to cross the blood-brain barrier producing neurotoxic effects and affect the colon, as well as other organs. [12].

Microcystin cannot penetrate plasma membranes without an active uptake mechanism through the aid of transporters. Organic anion transporting polypeptides (OATPs) are likely the transporter responsible for uptake of microcystin into the liver. OATPs also work as transport systems in enterocytes, hepatocytes, and renal epithelial cell types as well as in cells of the heart, lungs, spleen, pancreas, brain and blood-brain barrier. Therefore, microcystin has the potential to affect many other areas of the body, based on microcystin diffusion and OATP expression levels. Genes that are homologous to human OATP genes have been found in most animals [22], [24]. The threat that microcystin poses to human health is gaining greater attention from regulatory agencies that need to monitor toxin concentrations in the environment, such as the US

Environmental Protection Agency (EPA) and the World Health Organization (WHO). Imposing regulatory standards on algal toxins will require improved and expanded monitoring efforts, particularly if long term and low dose exposure to algal toxins at the community level are to be examined. MC-LR is the most commonly measured microcystin congener, especially in drinking water [25], [26]. Therefore, the concentration of MC-LR is often used as an approximation of the total concentration of microcystin. Microcystin-LR has acute toxicity, with a lethal dose in mice by the intraperitoneal route of approximately 100 µg/kg of body mass [27]. In 1998, WHO set a limit of 1 µg/L of MC-LR in drinking water [27]. In 2015, the EPA set a 10 day drinking water health advisory limit of 0.3 µg/L microcystin for children 6 years old or younger and 1.6 µg/L microcystin for children 6 years old through adults in drinking water and 20 µg/L in recreational water [28]. More recently, the EPA has drafted a new limit of 4 µg/L in recreational water, which will go into effect in early 2017 [29].

1.1.3 Common Laboratory Sample Preparation and Detection Methods

Microcystin can be isolated and concentrated from environmental samples or cultures using a variety of methods. In 2015, the EPA published method 544: Determination of microcystin and nodularin in drinking water by solid phase extraction (SPE) and liquid chromatography (LC)/tandem mass spectrometry (MS) [30]. In this method, environmental samples are filtered, saving both the retentate and the filtrate. The retentate is placed in a solution of 20% methanol for 1 hour in order to lyse cyanobacterial cells and release microcystin into the solution. This solution is then combined with the filtrate, and then run through an SPE column to concentrate and purify microcystin. Typical SPE purification of microcystin relies on the affinity of microcystin in an aqueous solution to bind to a column packed with non-polar octadecyl carbon chain bound silica (C18). An organic wash solvent can then be used to elute the

toxin [12], [31]. Samples are then further analyzed with (LC-MS); this method quantifies both extracellular and intracellular microcystin [30]. However, in this review, intracellular microcystin is the primary focus. For intracellular microcystin, laboratory based detection typically begins with concentration of cyanobacterial cells using centrifugation or filtration (the filter flow through is discarded). Filtration is followed by mechanical disruption of the cells using bead beating, freeze/thaw cycles, sonication etc. [32]. Depending on the chemistry of the microcystin variant of interest, certain acid-water or methanol-water combinations may be appropriate to use as solvents for extraction. Concentration of the toxin is most commonly performed using SPE [12].

Microcystin is commonly quantified in the laboratory using high performance liquid chromatography (HPLC) in combination with MS or ultraviolet absorption at 238 nm (HPLC-ABS/DAD/MWD). HPLC-MS is considered the gold-standard for quantitative microcystin detection, congener identification, and quantification, at this point in time. Different microcystin congeners have different toxicity values. Therefore, various types of bioassays are often used to assess toxicity of the total sample rather than to identify and quantify the individual microcystin structural variants. Bioassays for microcystin include use of microbes [33], invertebrate animals, vertebrate animals [33], cell culture [33], plants/plant extracts [33], enzymes (protein phosphatase inhibition assay) [34], [33], and Enzyme Linked Immunosorbent Assay (ELISA) [33]) [35]. ELISA tests can either select primarily for one congener (having varying degrees of cross reactivity to other congeners) or use an Adda moiety specific antibody to estimate total microcystin concentrations.

Typically, nucleic acids are analyzed in the laboratory by first extracting total DNA or RNA from a sample using a commercial extraction kit from a variety of manufacturers (i.e.

Qiagen, MoBio, Invitrogen, etc.). Subsequent analysis can be performed by a variety of techniques such as polymerase chain reaction (PCR) or PCR coupled with fluorescent probes/intercalating dyes, referred to as quantitative PCR (qPCR). Using PCR to detect specific loci in the *mcy* gene cluster is a rapid and sensitive laboratory technique that allows for specific detection of microcystin structural variants [36]. Real time PCR (qPCR) can be used if quantitative assessment of nucleic acids is desired. Another technique employing nucleic acids for detection is DNA Microarray technology. Arrays have been developed that allow for differentiation between types of toxin producing cyanobacteria. Other arrays have the capability to estimate molecular toxicity based on detection of gene clusters involved in microcystin synthesis [36].

1.1.4 Advantages of an Automated *In Situ* Sensor

Common laboratory methods for detection of microcystin or its corresponding nucleic acids introduce a lag-time between sampling and results. An automated, *in situ* detection instrument for intracellular microcystin and associated nucleic acids could be used as an early warning system to aid in resource management and to better inform public health decisions. Also, *in situ* sensors have the potential to reduce costs associated with continually deploying technicians to the field to obtain and transport samples to the laboratory for analysis, while increasing sample frequency, particularly at times when it is inconvenient or dangerous. Therefore, employing field deployable sensing systems for microcystin could enable near real time assessment of water quality without the need for traditional sample acquisition, storage and transport, and traditional laboratory analysis. Traditional methods such as HPLC-ABS/MS and PCR/qPCR involve large equipment that would not be easily adapted to an *in situ* detection instrument. Many require lengthy analysis times, storage of reagents at specific temperatures,

and procedural steps that are difficult to automate [37], [38]. Due to these physical restraints, a significant amount of research is directed towards developing methods that can be adapted to automated *in situ* detection of microcystin and its required nucleic acids [37], [38].

Development of an automated *in situ* sensor capable of continuous monitoring is needed because HABs are dynamic, showing a high degree of spatial and temporal variability. It is still not understood exactly what environmental factors promote cyanobacteria to produce toxins. In addition, some species of cyanobacteria have morphologically indistinguishable strains that do and do not produce toxins [11] [39]. In some cases, strains appear to be able to gain and lose the capability to produce toxins for various reasons (i.e. mutation, gene loss, virus activity, etc.) [18]. Given this uncertainty, it would be ideal to monitor toxin production at the biochemical and at the genetic expression level. Also, microcystin has a relatively long half- life compared to the RNA involved in its production, meaning that changes in microcystin levels do not necessarily correlate with how the cell is regulating toxin production in real-time. However, detection of genetic expression will can give an indicator of when the toxin is likely to be present. Coupling this information with metadata obtained from *in situ* sensors for other environmental parameters could provide further information on the ecosystem dynamics that lead to toxin production. However, the first step to achieving these *in situ* detection systems will involve the development of inexpensive, fast, high throughput analytical methods in the laboratory that have the potential for adaption to an automated *in situ* instrument.

Figure 3 breaks down the process for developing an effective detection instrument into three main stages: analytical detection method development, technology development and testing, and user considerations. Each one of these stages informs the next, but can also give feedback to the previous stage (i.e. if a certain aspect needs to re-engineered to meet the demands

of the next stage). This process can be used to evaluate the developmental stage of the technology.

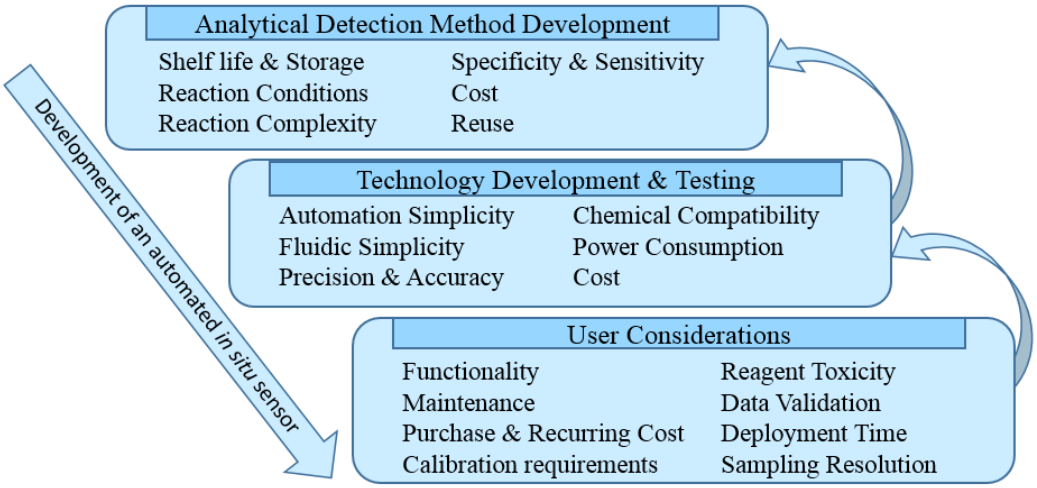

Figure 3: Evaluation Criteria for automated *in situ* sensors. The development scheme highlights a concurrent engineering approach where technological progress is advanced based on a series of design considerations. However, each subsequent stage can provide feedback and pivot points to the previous stage if technological or engineering constraints are encountered. In this review, detection chemistries are highlighted that have potential to be used in an automated *in situ* instrument capable of overcoming the challenges associated with traditional laboratory sampling and analysis. Several examples of current sensor systems and field-able assays are highlighted to represent the state of microcystin sensor research. In addition, examples of emerging sensor chemistries/technologies are presented. These systems and chemistries are evaluated by the criteria in Figure 3.

1.2 Microcystin Detection Methods with Potential for Automation or Portability

There are chemistries described in the literature for detection of microcystin, based on the analytical method development considerations outlined in Figure 3. Those that have potential to be incorporated into an automated sensor system will be highlighted below.

1.2.1 Spectroscopy

Microcystin can be detected using UV absorbance as it has a characteristic absorbance at 238 nm due to the conjugated diene present in the Adda chain [12]. However, many other

biological compounds also absorb at or near this wavelength, making this method non-specific. To overcome this, methods to increase specificity have been developed, such as chromatographic phase separation chemistries, diode array detection, etc. [12]. Raman spectroscopy can also be used to detect microcystin and distinguish between its congeners [40]. However, field amenable Raman solutions are expensive and the methodologies described in the literature would be difficult to automate as they require paper chromatography followed by Raman analysis of deposited microcystin. Additionally, a significant amount of research has been dedicated to developing methods to chemically modify microcystin by labeling or derivatization to allow for detection by UV spectroscopy with greater specificity.

1.2.1.1 Chemical Derivitization

The Adda moiety is a rare amino acid, which makes it an ideal target for use in detection strategies. Many research groups have used a Lemieux oxidation, a complex chemical reaction, in order to convert all Adda moieties to 2-methyl-3-methoxy-4-phenylbutyric acid (MMPB) [41], [42]. This allows for total microcystin detection, rather than a select variety of the variants. This MMPB compound can then be detected by mass spectrometry or by HPLC-ABS at 208 nm [42], [41]. To further increase sensitivity, MMPB can also be converted to its methyl ester form using either methylchloroformate or trifluoroborate and detected with gas chromatography [25].

Another method for derivatizing microcystin to the MMPB compound is ozonation. The ozonation process is very efficient because of its direct ozone reaction and strong indirect hydroxyl radial oxidation reaction [43]. Harada et al. [39] found that ozonolysis forms the MMPB compound in reduced times, and requires no cleanup of the reaction mixture. They directly analyzed for MMPB using thermospray-liquid or electron ionization-gas chromatography/mass spectrometry [39]. However, with different doses of ozone, different by-

products of microcystin can be formed. It has been shown that high ozone doses allow for cleavage of the Adda chain from the main ring of the toxin, which then allows for the MMPB compound to be oxidized from the Adda chain [43].

A method for toxin detection that has potential to be adapted to an automated process is high pressure liquid chromatography combined with fluorescent detection (HPLC-FLD). In order to use HPLC-FLD, toxin needs to be derivatized with a fluorescent molecule. One example of this is the derivatization of microcystin with 4-(1-pyrene) butanoic acid hydrazide (PBH) [44]. A condensation reaction binds PBH to microcystin at two conserved carboxyl groups on the microcystin molecule producing a unique di-pyrene structure with characteristic fluorescent properties (345 nm excitation, 475 nm emission). This structure can theoretically be distinguished from monopyrene conjugates and PBH monomers that emit in the range of 360-420 nm [44].

1.2.2 Chemical Signal Amplification

Chemical signal amplification can be achieved using several methods (i.e. fluorescence, luminescence, chemiluminescence, colorimetric absorption, etc.). These methods have potential to be used for detection of both the toxin, and its associated nucleic acids. They all rely on some type of mediator to modify a substrate that produces an optical signal. Chemical signal amplification can be used in combination with competitive and non-competitive hybridization techniques. A variety of approaches can be used for hybridization schemes to capture the target molecule (DNA aptamer, antibody, molecularly imprinted polymer (MIP), oligonucleotide probe, etc.) for binding of either toxin or nucleic acid (DNA/RNA), as well as some type of reporter probe.

In a non-competitive hybridization scheme, a capture probe attached to solid surface binds the target of interest. An enzyme-linked probe then binds to the target molecule. When this enzyme acts on the substrate, it produces a signal that is proportional to the amount of target molecule present in the sample. In a competitive hybridization scheme, the sample target molecule and a pre-enzyme-linked laboratory target molecule compete for binding sites on the capture molecule. When the enzyme acts on substrate, a signal is generated that is inversely proportional to the target sample concentration.

An example of chemical signal amplification is colorimetric absorption using an enzyme/substrate interaction to produce a pigment in solution that can be detected by absorbance. Examples of these enzyme-substrate complexes are Horseradish Peroxidase (HRP) enzyme and 3,3',5,5'-tetramethylbenzidine (TMB) substrate, as well as Alkaline Phosphatase (AP) enzyme and para-Nitrophenylphosphate (PNPP) substrate. When HRP acts on its substrate, TMB, a blue color is produced with maximum absorbance at 650 nm. When AP acts on its substrate, PNPP, a yellow color is produced with maximum absorbance at 405 nm. One issue with using this method for automated instrumentation is the shelf-life and storage requirements of the enzyme. However, these enzymes have been shown to be reliably stabilized and stored at room temperature with commercial products such as StabilZyme (Surmodics, USA) [45].

Other studies have developed chemiluminescent and fluorescent signal amplification techniques. Fluorescent signal amplification can be performed where the sample MC-LR competes with bound MC-LR for binding sites on a fluorescently linked antibody. A laser then excites fluorescent molecules bound to a surface through antigen/antibody interactions due to target toxin molecule, and the amount of fluorescent signal is inversely proportional to the amount of toxin present [46], [47], [48]. Chemiluminescent chemical amplification to detect

Microcystis spp. DNA can be performed using an alkaline phosphatase labeled DNA probe to cleave substrate such as commercially available fluorescent substrates (e.g. CDP-Star (Sigma Aldrich, USA). This produces a chemiluminescent signal that can be used to quantify the target nucleic acids [49].

1.2.2.1 Nucleic Acid Aptamers

Aptamers are synthesized DNA or RNA molecules that have high binding affinity to a specific target molecule [50]. They are selected by generating a large library of random oligonucleotide sequences, and selecting for the sequences that bind to the target from the sequences that do not. Aptamers have previously been used as recognition receptors for microcystin [50] and are advantageous because they are cheaper to produce and more stable than antibodies under ambient conditions [50]. Aptamers can be immobilized on solid surfaces such as silica, nanomaterials, electrodes (i.e. gold, graphene, etc.), and have been used previously in microcystin biosensing applications [50].

It is often difficult to select aptamers for low molecular weight target molecules such as cyanotoxins [50]. However, several authors have described DNA and RNA based aptamers for microcystin [51], [50], [52], [53]. For example, DNA aptamers have been reported against several congeners (i.e. MC-LR, MC-YR, and MC-LA) and have been subsequently applied in an electrochemical biosensing device [50], [51], [53], [52]. With this platform, detection limits of 0.5 µg/L, were observed; which is lower than the WHO drinking water concentration limit. This system has direct application and potential for field application using microfluidics for sensitive detection [50], [53].

1.2.2.2 Molecular DNA Probes

Molecular DNA probes are oligonucleotides that are designed to have specificity to a certain region on a nucleic acid target molecule, and therefore have potential for application to microcystin biosynthesis genes. They are usually labeled with biotin in order to bind to various types of media that have attached streptavidin linkers, or with a reporter molecule to allow for detection. Matsunaga et al. [49] designed two probes for the detection of target DNA from *Microcystis spp.* The first probe contained a biotin linker, which allowed attachment to streptavidin linked magnetic beads. This magnetic bead, DNA probe complex was used to capture the target DNA sequence. The second probe was labeled with digoxigenin, which was used in combination with an alkaline phosphatase (AP) labeled anti-digoxigenin antibody and colorimetric substrate to detect the target DNA sequence [49]. This general format can be used for designing other DNA probes targeting specific loci for use in sandwich hybridization experiments.

1.2.2.3 Molecularly Imprinted Polymers

It is often difficult to make effective antibodies or nucleic acid based aptamers for small molecular weight toxins like microcystin [37]. Molecularly imprinted polymers (MIPs) have been developed as a synthetic receptor as they are manufactured to have specific recognition sites that are complementary to the target molecule, simulating the binding site of a biological molecule [54], [55]. MIPS targeting microcystin have been developed using molecular modeling software to select monomers that are calculated to have the highest binding affinities from a virtual library of functional monomers [56]. This monomer is then cross-linked in the presence of MC-LR in order to create a receptor polymer with cavities that has high affinity for MC-LR [56]. MIPs for MC-LR have been developed with similar sensitivity to polyclonal antibodies

with a detection limit of 0.1 µg/L [56], and implemented in sensors for rapid, inexpensive detection of the toxin. The MIPs were capable of being used as a SPE substrate as well as a recognition receptor/sensing element in a piezoelectric sensor [57].

1.2.2.4 Immunoassays

There have been 2 main approaches to quantifying microcystin using immunoassays. The first approach is to target one congener of the toxin to use as a proxy for the total microcystin concentration in the sample. Many research groups have chosen to target MC-LR, as this congener is specified by regulatory agencies as the congener of concern. The alternative approach involves developing immunoassays that have broad congener specificity with the aim of quantifying total microcystin. This is most commonly achieved by generating monoclonal antibodies specific to the Adda moiety, an amino acid that is present in all forms of MC, as well as nodularin. The Adda moiety is well suited to the generation of antibodies due to its long hydrophobic side chain [58].

1.2.3 Nucleic Acid Amplification

The *mcy* nucleic acids (DNA and RNA) are difficult to directly quantify because they represent a small fraction of the total extracted nucleic acids. Therefore, detection is usually achieved using amplification strategies such as PCR or quantitative PCR (qPCR). These techniques are applicable to both DNA and RNA targets, with RNA needing to be first converted to cDNA by reverse transcription. PCR enzymes and other reagents used may have decreased long term shelf life at ambient temperature. However, some research indicates that extended shelf life of DNA polymerases used in PCR can be achieved for at least 7 days with no loss of activity [59]. However, PCR still does require precise cycling of temperatures, which would

impact the energy demand and control complexity of the instrument. Therefore, while PCR remains the gold standard in the laboratory, it is not an ideal candidate for automation.

Several methods have been developed to allow for isothermal reaction conditions using reagents that may have extended ambient temperature shelf lives, including hairpin chain reaction (HCR), nicking enzyme assisted amplification, strand displacement amplification (SDA) [60], loop mediated isothermal amplification (LAMP) [61], nucleic acid sequence based amplification (NASBA), and rolling circle amplification (RCA). All methods have inherent differences, advantages, and disadvantages (i.e. cost, primer design complexity, commercial availability, etc.). NASBA has been applied to infield applications for HABs in the marine environment [62], [63]. However, commercial formulations are expensive and in order to achieve extended shelf life, lyophilization of reagents is needed. Zhu et al. [61] developed a method for the detection of *mcyE* using LAMP. While LAMP involves more complex primer design than PCR, the authors reported real-time detection sensitivities similar to PCR. SDA primer design involves the development of 2 sets of forward and reverse loci specific primers, of which one set has contains an additional restriction site sequence. While this isothermal method has not been applied to detect *mcy* genes, there is evidence that it may be suitable to *in situ* application as some restriction endonucleases have been shown to have extended shelf life at room temperature [64]. However, it is unknown if the specific strand displacing DNA polymerases used in SDA have similar ambient storage capabilities to *Taq* DNA polymerases, which were highlighted in PCR storage studies [59].

1.3 Microcystin Sensors and Assays

Research has been directed towards developing these detection chemistries into fully functional sensor systems for many years, but few have been developed to commercially

available field-able assays or automated *in situ* instruments. To the best of our knowledge, the most complete automated *in situ* sensor to date is the Environmental Sample Processor (ESP) originally developed by the Monterey Bay Aquarium Research Institute (MBARI) [4]. The instrument has been applied to the detection of many marine toxins and microorganisms [4]. Recently, in summer 2016 it has been deployed for the first time in freshwater by National Oceanic and Atmospheric Administration, Great Lakes Environmental Research Laboratory (NOAA-GLERL) in Lake Eerie to monitor microcystin concentrations. Results have not yet been published [3].

Emerging sensor systems for microcystin have been reviewed numerous times in the literature [36], [55], [65], [50], [11], [12]. To the best of our knowledge, the most recent reviews on sensor systems for microcystin were published in 2013. Information from these reviews up until and including 2013 on different approaches to sensor/field-able assay toxin detection has been tabulated in Table 1. Sensors that have emerged post 2013 will then be reviewed in more detail according to criteria specified in Figure 3.

Table 1: Microcystin detection methods prior to 2013.

Category	Method	Detection Limit Range	References
Immunoelectric	Piezoelectric	pg/mL	[66] [67]
	Amperometric	ng/mL	[68] [69]
	Voltammetry	ng/ml	[70] [71] [72] [73]
	Impedance/Capacitive	pg/L	[74] [75]
Immuno-optical	Colorimetric	µg/L	[76] [77] [78] [79] [35]
	Fluorescent	0.03 µg/L	[46] [47] [48] [38]
	Luminescense	-	[49]
	Nuclear Magnetic Resonance	0.6 ng/g	[80]
Aptamer-electric	Voltammetry	9E-11 mol/L	[81] [50]
	Impedance	2E-11 mol/L	[53]
MIPS-electric	Piezoelectric	0.35 nM	[57] [56]
SPR	Competitive inhibition assay	70 ng/L	[37]
Enzyme inhibition-electric	Colorimetric	µg/L	[82] [83] [84]

The previously mentioned chemistries with potential for automation have been used in a variety of ways to develop unique biosensor/sensor systems in recent years. Prior to 2013, the majority of microcystin detection research focused on using electrochemical and optical immunosensors. Since 2013 several more examples of microcystin detection systems have been reported in the literature. The trend in microcystin detection systems seems to have expanded into use of aptamers and MIPS in addition to the automation of traditional immunoassay approaches.

Table 2: Microcystin sensor technologies post 2013.

Category	Method	Analyte	Sensitivity	Author/Year/Reference
Electro-chemical	Gold nanoparticles plated on gold electrode	*Microcystis spp.*	1.6×10^{-12} mol L^{-1}	Tong et al., 2015 [85]
	Modified disposable graphite electrodes	*Microcystis spp.* (MYC)	3.72 µg/mL	Sengiz et al., 2015 [86]
	Multi-walled carbon nanotube	MC-LR	<1 µg/L	Changseaok et al., 2013 [87]
	Antibodies immobilized on Au-glassy carbon electrode	MC-LR	0.017 µg/L	Du et al., 2014 [88]
	Impedimetric immunosensors	MC-LR	0.01 µg/L	Hou et al., 2016 [89]
	Functionalized carbon nanofiber modified electrode	MC-LR	1.7 ng/L	Zhang et al., 2016 [90]
MIPs	Quartz crystal microbalance	MC-LR	0.04 nM	He et al., 2015 [91]
Immunoassay	Indirect immunoassay using internal reflection fluorescence	MC-LR	0.9 µg/L	Shi et al., 2013 [38]
	Electrochemical	*Microcystis spp.*	0.01 pM	Lebogang et al., 2014 [92]
	Strip test	MC-LR	0.3 µg/L	Liu et al., 2014 [93]
	Photoelectrochemical	MC-LR	0.055 µg/L	Tian et al. 2013 [94]
	Periodic nanostructure	MC-LR	10 ng/L	Briscoe et al., 2015 [95]
	Antigen functionalized magnetic beads/antibody immobilized gold nanoparticles	MC-LR	0.51-11.7 µg/L	Neumann et al., 2015 [96]
	Single-walled carbon nanotube-based label-free chemiresistive immunosensor	MC-LR	0.6 ng/L	Tan et al., 2015 [97]
DNA aptamers	Electrochemical	MC-LR	1.9 pM	Eissa et al., 2014 [98]
	Nanoparticles	MC-LR	0.05 nM	Wang et al., 2015 [99]
	Nanoparticles	MC-LR	0.01ng/mL	Lv, et al., 2016 [100]
	Optical-fluorescence	MC-RR	80 pg/mL	Wu et al., 2016 [101]
	Fiber-optic long-period grating immunosensors	MC-LR	5 ng/mL	Tripathi et al., 2014 [102]

Electrochemical sensors have been developed using both voltammetric ([85], [86], [90]) and impedance based ([87], [88], [89], [92], [97]) detection principles. Some of these rely on electrodes functionalized with antibody/antigen ([87], [88], [89], [90], [92], [97]) and some use aptamers ([98]) to detect the toxin. Other use probes/hybridization to detect biosynthesis genes from *Microcystis spp.* ([85], [86]). Optical (i.e. fluorescent, colorimetric, photoelectric) immunoassay sensors microcystin ([96], [38], [94]) and point of use assays ([95], [93]) also have been used to detect microcystin ([96], [38]). Other optical sensors (i.e. fiber-optic, colorimetric, and fluorescent) have been developed that rely on aptamers based mechanism for capture and detection of toxin ([99], [101], [100], [102]). A quartz crystal microbalance was also developed for the detection of MC-LR [91]. Several sensor systems are highlighted to illustrate the current state of sensor research.

Tong et al. [85] developed a voltammetric electrochemical DNA biosensor for *Microcystin spp*. Gold nanoparticles were plated on a gold electrode to increase the surface area and therefore increase ssDNA probe binding to the surface. The ssDNA probes were then used to capture purified 17 base pair oligonucleotide fragments of *Microcystis spp*. DNA (in 0.01M Tris-HCl, 0.01M NaCl, pH 7.8). Once bound, the surface was then further enhanced by modification with silver. Methylene blue was used as an electrochemical indicator of DNA hybridization efficiency, based on the reduction peak current before and after hybridization. After a 3 hour incubation, the detection limit for *Microcystis spp.* DNA was 1.6×10^{-12} mol/L, but the system had yet to be tested with environmental samples.

Lebogang et al. [92] developed an automated capacitive sensing system that used an immunoelectrode consisting of a gold nanoparticle based electrode modified with an Adda specific monoclonal antibody. When microcystin is bound to the immunoelectrode in running

buffer (phosphate buffer, pH 7.2), a detectable signal is produced due to a change in capacitance. This system was capable of detecting microcystin in *Microcystis auriginosa* batch cultures at concentrations as low as 0.01 pM [92]. After detection, a glycine buffer (pH 2.5) could be used to regenerate the sensor by dissociating the microcystin from the antibody. The total analytical time was 37 minutes; this includes regeneration, which accounts for over half of the time. While this demonstration of technology was performed under laboratory conditions, based on criteria listed in Figure 3, this sensor has potential to be used as an automated *in situ* sensor for dissolved microcystin. Promising aspects include good sensitivity, capability for regeneration, and ability to compare to standard laboratory methods. However, monoclonal Adda specific antibodies are costly, require specific temperatures for hybridization, and have short shelf lives unless they are stabilized with another reagent. This method is in the technology development and testing phase, but the power consumption and instrument construction costs are unclear. The design process of the assay would not likely require complex automation and fluidics [92].

Eissa et al. [98] also developed an electrode based system that employed DNA aptamers to selectively capture purified microcystin in binding buffer (50 mM Tris, pH 7.5, 150 mM NaCl, 2 mM $MgCl_2$, pH 7.4), causing this system to have greater potential for extended shelf life of reagents at ambient temperature. In this sensor system DNA aptamers with high specificity for MC-LR (moderate specificity for MC-LA and MC-YR) were non-covalently bound to carbon nanomaterial graphene electrodes. When microcystin bound to the aptamers during a 45 minute incubation period, a dose-responsive increase in peak height (μA) occurred, with a limit of detection of 1.9 pM. This system was also applied to tap water spiked with microcystin, as well extracted and resuspended (binding buffer, pH 7.4) microcystin samples from fish tissue. It has simple fluidics and uses low cost reagents [98].

Another sensor which has been developed by Wang et al. [99] uses oriented formation of gold nanoparticle dimers. DNA aptamers specific to MC-LR was bound to the gold nanoparticles. When MC-LR was not present, these gold nanoparticles aggregate in formation with each other. When MC-LR was present, the aptamer unfolds and binds to the MC-LR, causing the gold nanoparticles to no longer be in their aggregated form resulting in a colorimetric change (543 nm to 450 nm) in the nanoparticle solution [99]. This method is advantageous because it had approximately 5 minute reaction time (in 0.5 M Tris-HCl, pH 7.5, 1.5 M NaCl, 20 mM $MgCl_2$ binding buffer), with a limit of detection of 0.05 nM. DNA aptamers are also stable over time in solution and inexpensive compared to antibodies. The system was tested with purified microcystin, as well as environmental sample. These results were compared to detection with HPLC, with no significant difference observed. Another point of interest is that this versatile system could potentially have the ability to be expanded to other biomolecules [99].

He et al. [91] developed a 20 MHz quartz crystal microbalance (QCM) sensor that was tested with purified laboratory microcystin standards, as well as microcystin spiked into environmental lake samples. The QCM was coated with *in situ* self-assembled MIPs specific to MC-LR. The limit of detection for this sensor was shown to be 0.04 nM MC-LR. It had very little cross over to other microcystin variants, showing high specificity. However, this may be a disadvantage if the total concentration of different microcystin congeners is desired. The sensor capture surface was reported as being stable over time and was capable of less than 3% variation after a regeneration procedure involving an ethanol-acetic acid solution [91].

Liu et al. [93] developed an immunochromatographic strip for detection of microcystin with a limit of detection of 0.3 µg/L. This test could be used in the field as a “dip stick”, and was applied in this study to both tap water and lake water. The presence of MC-LR generated a

colorimetric response that was inversely proportional to the concentration of MC-LR. This reaction takes place in less than 10 minutes and is capable of being performed in the field. However, the monoclonal antibodies used are either expensive to purchase or take a great deal of time to make. Antibodies do not have extended shelf life without further stabilization, so further automation for an *in situ* would be difficult [93]. A similar test has been developed and is commercially sold by Abraxis, Inc.; 20 strip tests are sold for 400-480 U.S. dollars.

1.4 Conclusions

Further research is needed on microcystin and nucleic acid detection techniques that can be used for the development of an automated *in situ* sensor for microcystin. Traditional laboratory techniques tend to be poorly suited for adaption to automated techniques due to reagent shelf life, stability, reactivity, and complexity of sample preparation and reaction steps. Research is currently being performed on DNA aptamer based assays, immunoassays (colorimetric, fluorescent, and luminescent), electrochemical assays, MIP based assays, etc. in order to find a technique that meets all criteria listed in Figure 3. Several of the techniques for both detection of microcystin and nucleic acids have shown promising results and warrant further investigation. In particular, advances in DNA aptamer methods are showing potential to reduce the reliance on antibodies in many methods, thereby lowering the cost associated with many assays. Current sensor systems described in the literature remain in the laboratory environment and there is limited information on how they perform with real world samples. For most sensors, the sample pretreatment or concentration methods that are required for the sensor to measure samples from complex environmental samples at sensitivities that are environmentally relevant are not adequately described. The increased focus on microcystin by regulatory agencies could serve as a driver for microcystin sensor development and

implementation. Additionally, as research progresses towards a field deployable sensor for microcystin, the development of cheaper and more readily performed, accurate and precise assays will also occur. This will enable greater throughput of samples in the laboratory as well as offering the potential for in field point of use application by researchers and regulatory agencies. Increased analysis of microcystin and its biosynthesis genes will further knowledge of the microbial and ecosystem processes that drive toxin production, as well as serving to better inform public health decisions.

2 Chapter 2: Dual Extraction Sample Preparation Method for Microcystin and Nucleic Acids

Abstract

Microcystin (MC) is one of the most predominantly produced toxins of HABs; MC-LR is one of the most commonly formed structural variants of microcystin. Both the World Health Organization and United Stated Environmental Protection Agency have recommended recreational standards for MC-LR. During the summer of 2016, water samples were taken from Lake Winnebago, WI on eight dates and Veteran's Park Lagoon, WI on sixteen dates. The goal of this sampling was to assess an on-filter dual extraction method for intracellular microcystin and its biosynthesis *mcy* gene cluster compared to extraction with a typical laboratory extraction method, bead beating. Microcystin concentrations from both methods were quantified using LC-MS in order to calculate median extraction ratios obtained with on-filter method compared to bead beat method (comparative recovery) for microcystin congeners. For Lake Winnebago, the comparative recoveries ± range for microcystin congeners MC-LR, MC-YR, MC-RR, and MC-LA were 43% ± 12%, 34% ± 9%, 46% ± 10% and 44% ± 13%, respectively. For Veteran's Park Lagoon, the median comparative recoveries for MC-LR, MC-YR, and MC-RR were 51% ± 9%, 49% ± 12%, and 53% ± 7%, respectively. Median recoveries overlapped with similar intervals of confidence, suggesting that the method is robust enough to be applied to bodies of water with different characteristics (i.e. water chemistry, microbial community, suspended particulate, etc.). Total RNA was measured using absorbance at 280 nm by a Nanodrop spectrophotometer, to assess the comparative recovery between methods. Comparative recoveries were poor; Veteran's Park Lagoon values ranged from 6% to 27% and Lake Winnebago values ranged from 5% to 64%. Further quantification with RT-qPCR is needed to evaluate extraction efficiency of desired *mcy* gene cluster.

2.1 Introduction

Increased anthropogenic activity causes eutrophication of freshwater sources, which often results in increased occurrence of harmful algal blooms (HABs). These blooms are considered harmful because they can have detrimental effects on the environment, including decreased water clarity, dead zones, poor overall ecosystem health, and sometimes contain toxin-producing cyanobacterial strains. Also, ecosystem dynamics that cause HABs to produce (intracellularly) and release toxin into the environment are not fully understood.

One of the most common toxins produced by HABs in freshwater systems is the 7 amino-acid cyclic peptide, microcystin (MC). Microcystin is produced nonribosomally, and is encoded for by the *mcy* gene cluster (Figure 2). As seen in Figure 2, microcystin has variable amino acids at positions X and Y and modifications at position R_1. Five common microcystin congeners (MC-LR, MC-YR, MC-RR, MC-desmethyl-LR, and MC-LA) are described in Figure 2, using the International Union of Pure and Applied Chemistry one letter abbreviation codes for amino acids [21]. For example, MC-LR has L (leucine) at position X and R (arginine) at position Y. Structural microcystin variants have different hydrophobicities depending on the amino acids incorporated at the variable positions, which can influence toxicity due to cell membrane interactions and optimal extraction protocol due to solvent solubilities.

As the purification and concentration methodologies for microcystin and nucleic acid analysis differ, traditional laboratory based methods usually involve taking and concentrating separate samples for toxin analysis and nucleic acid measurement. There are numerous laboratory methods to extract intracellular microcystin and nucleic acids from biomass in environmental water samples. Biomass is usually concentrated by filtration [32] or centrifugation [103] and subjected to mechanical (e.g., freeze thaw, bead beating, sonication [103] cell lysis

methods. Alternatively, direct chemical extraction methods have been commonly employed using alcohols (i.e. methanol [104]); acetic acid [103]; ammonium bicarbonate [105] and proprietary commercial formulations (i.e., Abraxis Quicklyse) [106]. Barco et al. [104] determined that an 80% methanol/20% water (acidified to pH 2 with trifluoroacetic acid) solvent was the optimal methanol to water ratio for extraction of total microcystin (hydrophobic and hydrophilic) from freeze dried cells, and suggested potential application for on-filter extraction [104].

For nucleic acids, cell lysis is commonly achieved using combinations of mechanical disruption methods (e.g., bead beating, boiling, freeze/thaw cycles), chemical lysis using detergents [107] enzymatic digestion, [108] or direct cell lysis with chaotrophic salts [109] or osmotic shock [108]. Subsequent purification and concentration of the nucleic acids from the cell lysate is commonly achieved using organic (e.g., phenol, chloroform) phase separations coupled with alcohol (e.g., ethanol, isopropanol) precipitation techniques. Alternatively, nucleic acids can be purified by immobilization, washing and elution from solid surfaces such as silica [109] (i.e. Qiagen DNA and RNA spin columns), silane (e.g., Dynabeads, Life Technologies) and polyhistadine (e.g., ChargeSwitch, Invitrogen). The latter solid surface extractions methods are particularly suited to developing simple field-able or automated extraction and purification methods [62], [63].

Consistent sampling of harmful algal blooms and performing subsequent in-laboratory detection methods are labor intensive and introduce a time lag between sampling and results. Also, traditional laboratory extraction methods for microcystin and nucleic acids require laboratory infrastructure that is not amenable to point of use or automated assays. One of the first steps to develop point-of-use or automated *in situ* sensors is to develop and characterize robust

sample extraction and purification methods for microcystin and/or nucleic acids. These processes should focus on methods that have minimal fluidic manipulations, are inexpensive, and do not rely on extensive laboratory infrastructure. This will enable increased sampling regimes to be performed and potentially point of use analysis of microcystin. Additionally, the toxin has a long half-life compared to its associated RNA, which means that changes in microcystin levels do not necessarily give real-time information on how the cell is regulating toxin production. Therefore, leveraging gene expression information from these samples could further our understanding of the factors driving microcystin biosynthesis. This would be particularly useful if the nucleic acid and microcystin fractions could be recovered from the same sample. Therefore, developing field-able methods for co-extraction of toxin and nucleic acid extraction would be beneficial to our understanding of microcystin biosynthesis dynamics. Furthermore, development of an instrument capable of measuring and relaying real-time data of intracellular microcystin and *mcy* RNA transcript concentrations has the potential to act as an early warning mechanism release of microcystin into the environment.

Here we investigate a method for sequential extraction of microcystin and nucleic acids from biomass collected on one filter. Common laboratory methods for extraction of microcystin and of nucleic acids have been adapted, combined, and employed in a one filter, dual extraction method for toxin and nucleic acid. This dual extraction method uses a modification of the method described by Barco et al. [104] for microcystin. Here biomass from environmental or cultured samples are first concentrated on a filter. Subsequent extraction of the microcystin fraction is then performed with 80% acidified methanol to produces an extract that is available for direct analysis by GC/MS, or with subsequent dilution ELISA. Following this, the nucleic acid fraction is extracted from the filter using a guanidine thiocyanate buffer [109]. The nucleic

acid fraction is further purified using standard RNA purification columns (Qiagen). The method was compared against traditional laboratory based extractions for microcystin and RNA using cultured cells and environmental water samples from 2 Wisconsin lakes.

2.2 Materials and Methods

2.2.1 Microcystin Hydrophobicity Calculations

Table 3 shows relative hydrophobicity values of the variable amino acids at pH 2 found in the microcystin congeners examined in this study [110]. Hydrophobicity values are based on glycine having a hydrophobicity value of 100. These values were used to determine relative microcystin variant hydrophobicity [110] (Table 3).

Table 3 Amino acid and calculated hydrophobicity for various microcystin congeners [110]**.**

Amino acid	**Relative Hydrophobicity at pH 2**	**Classification**
leucine	100	Hydrophobic
tyrosine	49	Moderately Hydrophobic
alanine	47	Moderately Hydrophobic
arginine	-26	Hydrophilic

Microcystin Variant	**Relative Hydrophobicity at pH 2**	**Classification**
MC-LA	100+47=147	Very Hydrophobic
MC-LR	100+-26=74	Hydrophobic
MC-dmLR	100+-26=74	Hydrophobic
MC-YR	49+-26=23	Slightly Hydrophobic
MC-RR	-26+-26=-52	Hydrophilic

2.2.2 Solution Preparation

Microcystin extraction solution was prepared in accordance with the method described by Barco et al. [104]. HPLC grade methanol (Fisher Scientific, USA) was diluted to 80% using 18 MΩ H_2O before adding TFA trifluoroacetic acid (TFA) (Fisher Scientific, Germany) until the solution reached pH 2. RNA extraction solution was prepared by adding 10 μL of β-

mercaptoethanol (MP Biomedicals, USA) to every 1 mL of RLT buffer (Qiagen, Germany) needed.

2.2.3 Sample Collection and Culture Conditions.

Environmental samples were collected from Veteran's Park Lagoon, Milwaukee, Wisconsin, and from Lake Winnebago, Wisconsin in autoclaved 4 L polypropylene bottles (Fisher Scientific, USA). Samples were transported back to the laboratory in the dark and on ice where they were then stored at 4 ˚C in the dark prior to processing. Samples were processed within 48 hours of sampling. Cultures of *Microcystis spp.* were maintained under ambient light and temperature conditions in the laboratory in 100 ml of BG-11 media (Sigma Aldrich, USA) in 500 ml Erlenmeyer flasks that were lightly capped with aluminum foil.

2.2.4 On-Filter Dual Extraction Method

For sample filtration, 47 mm diameter polypropylene filter housings (Advantec, USA) were assembled with GF/F glass fiber filters (Watman, GE Health Care, USA). To facilitate filtration, a nylon 1/4" Female NPT to 3/16 barb threaded adapter (New Age Industries, USA) was fitted to the top of the filter housing using PTFE thread seal tape in the threads to prevent leakage. A 10 cm long section of Tygon S-50-HL tubing (Saint-Gobin, USA) was connected to this nylon adapter, with a polypropylene barb to luer adapter (Eldon James, USA) at the opposing end of the tubing. Samples were filtered using a 50 ml luer lock syringe (BD Biosciences, USA) and flow through was discarded. The volume of culture or environmental sample filtered varied daily based on biomass density. To extract microcystin, 2 mL of 80% acidified Methanol was pushed on to each filter using a 10 ml luer lock syringe (BD Biosciences, USA) and allowed to incubate at room temperature without agitation for 10 minutes. Following

incubation, a syringe was used to push the acidified methanol through the filter where it was recovered in a 15 ml polypropylene tube (BD Biosciences, USA).

RNA extraction from the filter mimicked the process of microcystin extraction with the exception that 2 mL of RNA extraction solution was substituted for the microcystin extraction solution. Following collection of the RNA extraction solution, RNA was purified and concentrated using RNeasy mini spin columns (Qiagen, Germany) according to the manufacturer's instructions with the exception that multiple loadings of the columns with RNA extraction buffer was required due to the increased volume used over the manufacturer's method.

2.2.5 Microcystin Analysis

The collected flow through was further purified for liquid chromatography (LC) tandem (MS/MS) analysis by filtration through a prepackaged 0.2 µm, 25 mm diameter nylon filter (Fisher Scientific, Ireland). A Luna C18 column (Phenomenex, 3 µm, 150 x 3 mm) was used to separate microcystin variants (MC-LR and MC-Dha^{7}-LR (NRC); MC-RR, MC-YR, MC-LA (Sigma Aldrich)). The mobile phase was composed of HPLC water (A) and 0.1% formic acid and 5 mM ammonium formate in 95% acetonitrile (B). Mobile phase running conditions for separation was equilibration from 0-3 min at 30% B, gradient of 30-90% B from 9-15 min, step change back to 30% B at 15.01 min and then five minutes for re-equilibration, total run time 20 minutes. MS parameters were as follows: entrance potential: 10 mV; curtain gas: 15 psi; collision gas: high; ionspray voltage: 5000; source temperature: 600 °C; ion source gases 1 and 2: 70 psi. Additional MS detection factors for microcystin are listed in Table 4. Raw values measured by LC-MS/MS (not yet accounting for sample concentration factor) of less than 0.5 µg/L were below the quantitative limit of detection and were therefore considered trace values and removed from subsequent analysis.

Table 4: Microcystin HPLC-MS Detection Parameters.

Toxin	Parent Ion	Daughter Ion	Declustering Potential	Collision Energy	Collision Cell Exit Potential	Retention Time (min)
Microcystin-LR	995.619	135.3	126	115	26	8.25
	995.619	127.1	126	115	26	8.25
Microcystin-YR	1045.633	135.3	141	107	8	8.55
	1045.633	127.1	141	123	8	8.55
Microcystin-LA	910.617	776.4	106	27	8	9.37
	910.617	135.2	106	87	8	9.37
Microcystin-RR	520	135.1	81	43	8	7.48
	520	70.1	81	129	6	7.48
[Dha^{7}]-Microcystin-LR	981.531	135.3	126	101	22	8.25
	981.531	103.2	126	129	6	8.25

2.2.6 RNA Analysis

Total RNA concentration was measured at absorbance 280 nm (A280, 10 mm equivalent pate length, NanoDrop® ND-1000 spectrophotometer. Additional measurements of absorbance ratios at 260:280 nm and 230:280 nm were performed to assess RNA purity.

2.2.7 Environmental Sampling Experimental Design and Controls

To enable the method and controls to be tested in triplicate, 9 filter housings were prepared on each sampling day. Equal volumes of culture or environmental sample were filtered through each housing. Filters 1, 2, and 3 were tested using the on-filter dual extraction method. Filters 4, 5, and 6 served as a control for microcystin extraction efficiency and were removed from their filter housings and placed in bead beating tubes (Biospec Products, USA) containing 0.1 mm diameter glass zirconia beads and 2 mL of acidified methanol. Filters 7, 8, and 9 served as controls for RNA extraction efficiency and were removed from their housings and placed in bead beat (Biospec Products, USA) containing 0.1 mm diameter glass zirconia beads (Biospec Products, USA) and 2 mL of RNA extraction buffer. Samples were bead beat 3 times for one minute in a Minibeadbeater-16 (model 607) at 3400 rpm (Biospec Products, USA). Between

each minute beating, samples were removed from the bead beater and placed on ice for one minute. Following bead beating microcystin and RNA was purified using the same methods as the *on-filter* extraction samples. Therefore, these samples served as a control for microcystin and RNA extraction because they allowed for comparison of the on-filter extraction method to a traditional, standard laboratory method of cell lysis and extraction.

2.2.8 Statistical Analysis

On each sampling date, each set of three replicates for both methods were averaged. The average extraction value for the bead beat method was assumed represent the total microcystin concentration in the sample. Equation 1 was used to calculate the comparative recovery percentage (the ratio of on-filter microcystin concentration compared to the bead beat microcystin concentration) from these averages. The interquartile range method was performed on this data set of comparative recoveries in order to determine outliers, as well as calculate quartile 1, median, and quartile 2 to graphically represent the data with box and whisker plots. The interquartile range method assumes values that are greater than quartile three plus 1.5 times the interquartile range and values that are less than quartile one minus 1.5 times the interquartile range to be outliers.

$$Comperative\ Recovery\ [\%] = \frac{Average\ On\ Filter\ MC\left[\frac{\mu g}{L}\right]}{Average\ Bead\ Beat\ MC\left[\frac{\mu g}{L}\right]} * 100 \quad (1)$$

2.2.9 Characterization of Time and Volume on Microcystin Extraction

Laboratory cultures of *Microcystis aeruginosa* (strain LB2662, UTEX, University of Texas at Austin) were cultured in the laboratory in BG11 media, stored on the bench top in sunlight at room temperature. When used in experimentation, these cultures were first vortexed to minimize biomass clumping and triplicate filter housings were prepared using the same method for environmental sampling. A 50 ml Syringe was then used to filter 10 ml aliquots of

the laboratory culture onto each filter. To investigate the influence of volume on microcystin extraction, 5 replicate filters were interrogated with 7 successive 2 mL aliquots of microcystin extraction solution each with a 10 minute on-filter incubation time. Following incubation, each individual aliquot of extraction solution was pushed through the filter and collected in a sterile 15 ml polypropelene tube. Characterization of incubation time was performed in triplicate using 2 ml microcystin extraction solution with incubation for 0, 10, and 60 minutes. Each flow through volume was 0.2 μm filtered (25 mm nylon syringe filters, Fisher Scientific, Ireland) and analyzed by HPLC-MS as previously described.

2.3 Results

2.3.1 Microcystin Extraction from Environmental Samples

The lagoon in Veteran's Park, Milwaukee, WI was analyzed for 5 microcystin congeners (MC-LR, MC-YR, MC-RR, MC-desmethyl-LR, and MC-LA) 15 times between early July and early November, 2016. Environmental water samples were processed using both the proposed dual extraction method and the standard laboratory bead beating method. After LC-MS/MS analysis, 4 out of 16 of the data sets were determined to be outliers by the interquartile range statistical method and removed from subsequent plots and analysis. Figure 4.a and Figure 4.b show microcystin extraction results from all 5 measured congeners sampled using the bead beat method and the on-filter method, respectively. The extracted microcystin congeners using both methods show similar trends at each sampling point, with the on-filter method being less concentrated. For both methods, MC-dmLR was only observed at trace levels over the sampling period. However, at the final sampling point both methods showed an increase in the MC-dmLR congener while all other congener concentrations had decreased from the previous data point. Therefore, MC-dmLR also removed from subsequent analysis.

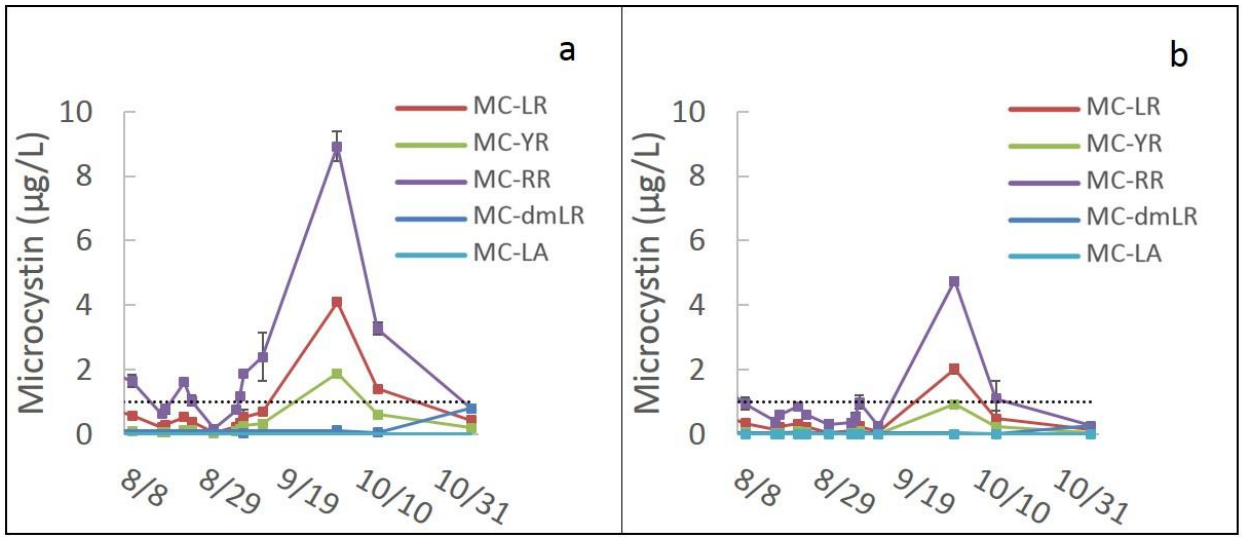

Figure 4: Microcystin concentrations for 5 congeners in Veteran's Park Lagoon. a) Bead beat extraction. b) On-filter extraction. For each sampling point, the median of the triplicate filter samples was plotted with the error bars representing the high and low concentrations.

Microcystin concentrations for the 12 sampling dates not determined to be outliers were plotted for the three relevant congeners, Figure 5.a-c. Bead beating and on-filter extraction methods showed similar overall trends in microcystin concentrations over the sampling time period. Individual microcystin congener values ranged between 0 and 10 µg/L and total microcystin concentration ranged between 0 and16 µg/L, with peaks primarily occurring in mid-August and early October. Figure 5.d shows the sum of all three microcystin congeners, to represent total microcystin in the environmental sample. In early October, the Veteran's Park Lagoon total microcystin concentration was greater than the WHO guideline for recreational microcystin levels, but the individual congener values were not. However, MC-LR and MC-RR both had early October concentration above the more recent 4 µg/L EPA regulatory recreational water limit.

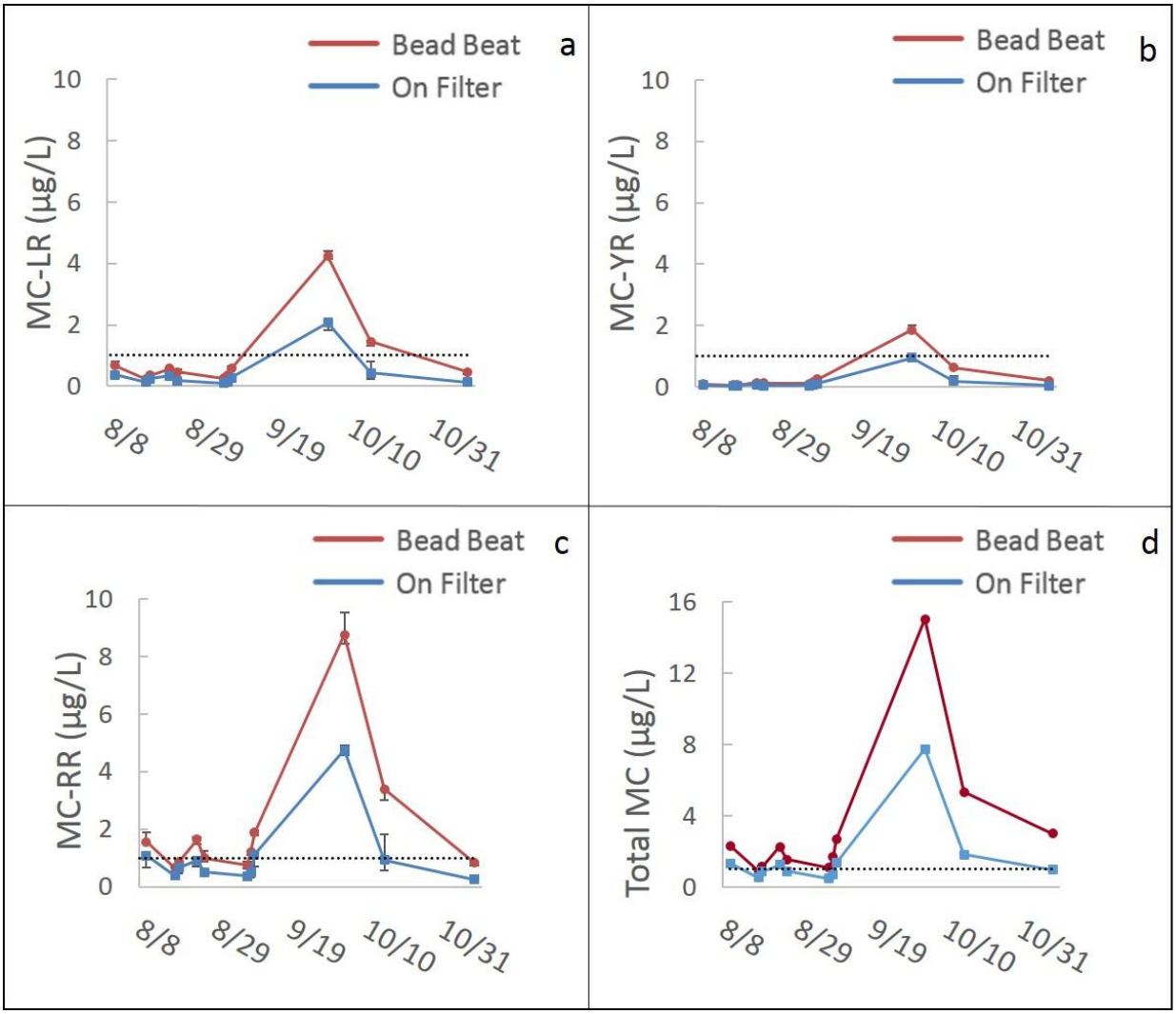

Figure 5: Veteran's Park Lagoon microcystin concentrations for individual congeners and total microcystin assessed using both the on-filter dual extraction and standard bead beat laboratory methods. The dotted line at 1 µg/L on each plot represents the World Health Organization recommended limit for microcystin in drinking water. a) MC-LR b) MC-YR c) MC-RR d) Total microcystin. a-d) For each sampling point, the median of the triplicate filter samples was plotted with standard error bars representing the high and low concentrations. e) No error bars because concentration values are sum of individual congener concentrations, each with their own standard deviation measurements.

Lake Winnebago, WI was sampled 8 times between late June and late August for 5 microcystin congeners (MC-LR, MC-YR, MC-RR, MC-desmethyl-LR, and MC-LA). Environmental water samples were processed using both the proposed dual extraction method and the standard laboratory bead beating method. After LC-MS/MS analysis, 1 out of 8 of the

data sets were determined to be outliers by the interquartile range statistical method and removed from subsequent plots and analysis. Figure 6.a and Figure 6.b show microcystin extraction results from all 5 measured congeners sampled using the bead beat method and the on-filter method, respectively. The trends between microcystin congeners for the two methods followed a similar pattern, with the exception of an increase in concentration of MC-RR in late August while all other congeners were decreasing in concentration from the previous data point. Also, the bead beat extraction method showed a peak in late July that the on-filter method did not identify. MC-dmLR was detected, but only at trace levels over the duration of the sampling period. These measurements were therefore not quantitative and so were removed from subsequent analysis.

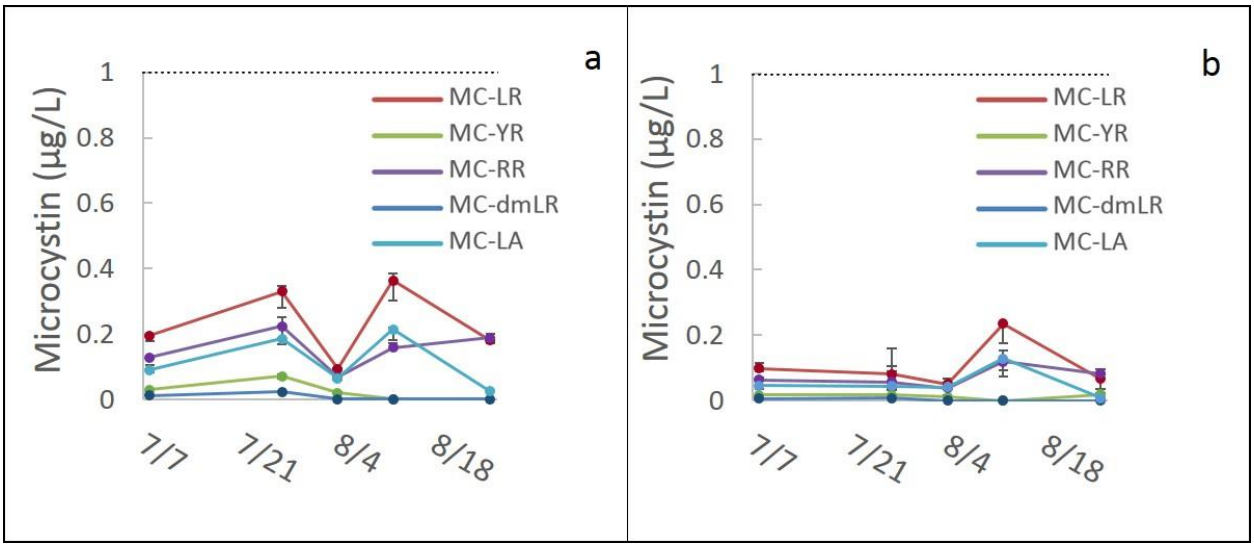

Figure 6: Microcystin concentration for 5 congeners in Lake Winnebago, WI. a) Bead beat extraction. b) On-filter extraction. For each sampling point, the median of the triplicate filter samples was plotted with standard error bars representing the high and low concentrations.

Lake Winnebago microcystin concentrations for the 7 sampling dates not determined to be outliers were plotted for each measurable congener as well as total microcystin (Figure 7.a-e).

Bead beating and on-filter extraction methods showed similar overall trends in microcystin concentrations over the sampling time period. Microcystin congener values ranged between 0 and 1 µg/L, with peaks primarily occurring in mid-July and early August. Microcystin concentrations (individual congeners or total microcystin) never exceeded the WHO drinking water guideline in Lake Winnebago.

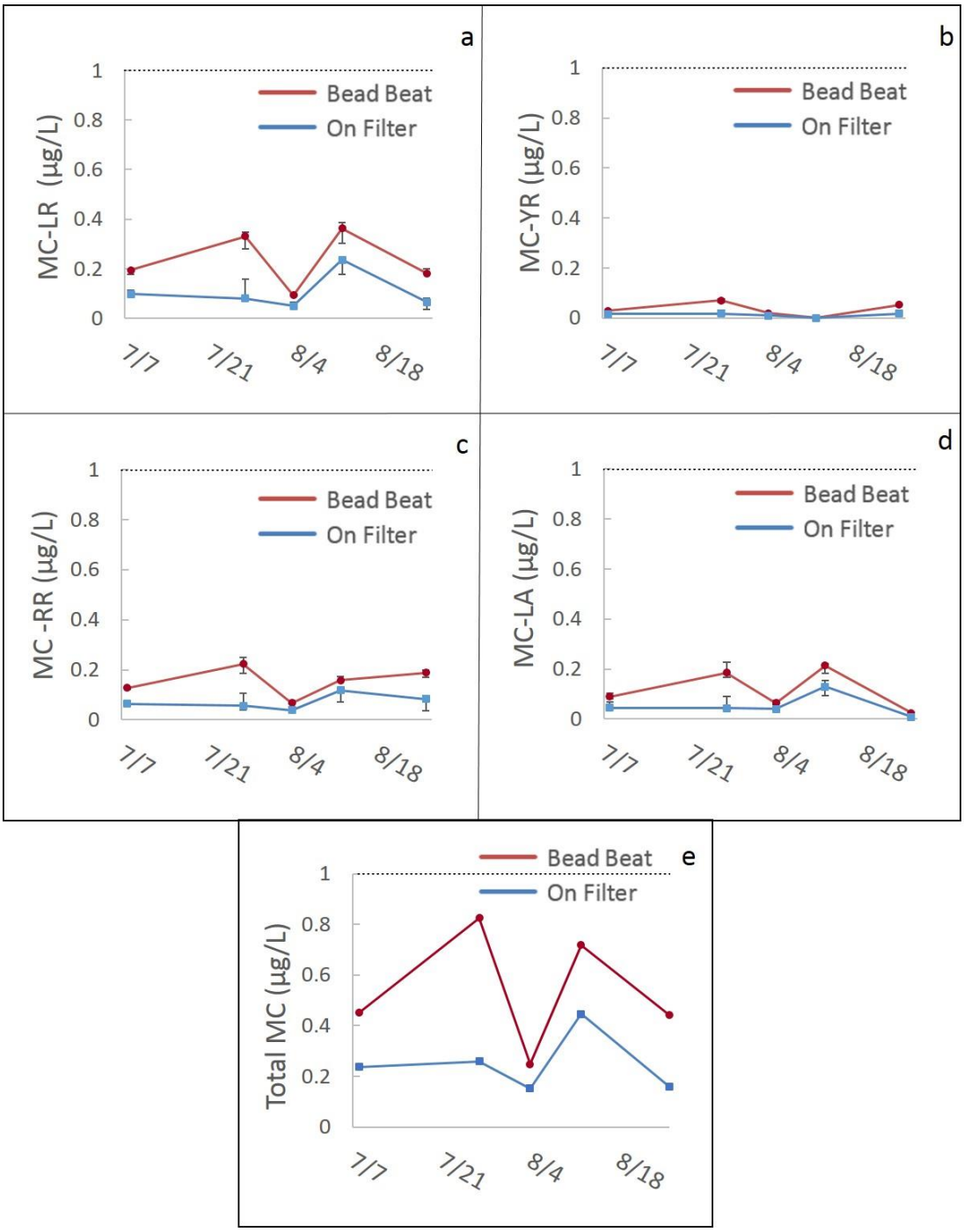

Figure 7: Lake Winnebago, WI, individual congener and total microcystin concentrations assessed using both the on-filter dual extraction and standard bead beat laboratory methods. a) MC-LR b) MC-YR c) MC-RR d) MC-LA. e) Total microcystin. The dotted line at 1 µg/L on each plot represents the World Health Organization recommended limit for microcystin in drinking water. a-d) For each sampling point, the median of the triplicate filter samples was plotted with standard error bars representing the high and low concentrations. e) No error bars because concentration values are sum of individual congener concentrations, each with their own standard deviation measurements.

In Veteran's Park Lagoon (Figure 5) and Lake Winnebago (Figure 7), ratios between extraction methods were consistent between congeners and total microcystin. Equation 1 was used to calculate the comparative recoveries between the two extraction methods for each congener on each date. Figure 8 shows box and whisker plots of the comparative recoveries for the measured congeners for both bodies of water. These plots show the three quartiles, the minimum, and the maximum data points. For Veteran's Park Lagoon, the median comparative recovery ± range for MC-LR, MC-YR, and MC-RR were 51% ± 9%, 49% ± 12%, and 53% ± 7%, respectively. For Lake Winnebago, the median comparative recovery ± range for MC-LR, MC-YR, MC-RR, and MC-LA were 43% ± 12%, 34% ± 9%, 46% ± 10% and 44% ± 13%, respectively. All ranges overlap and have a similar interval of confidence.

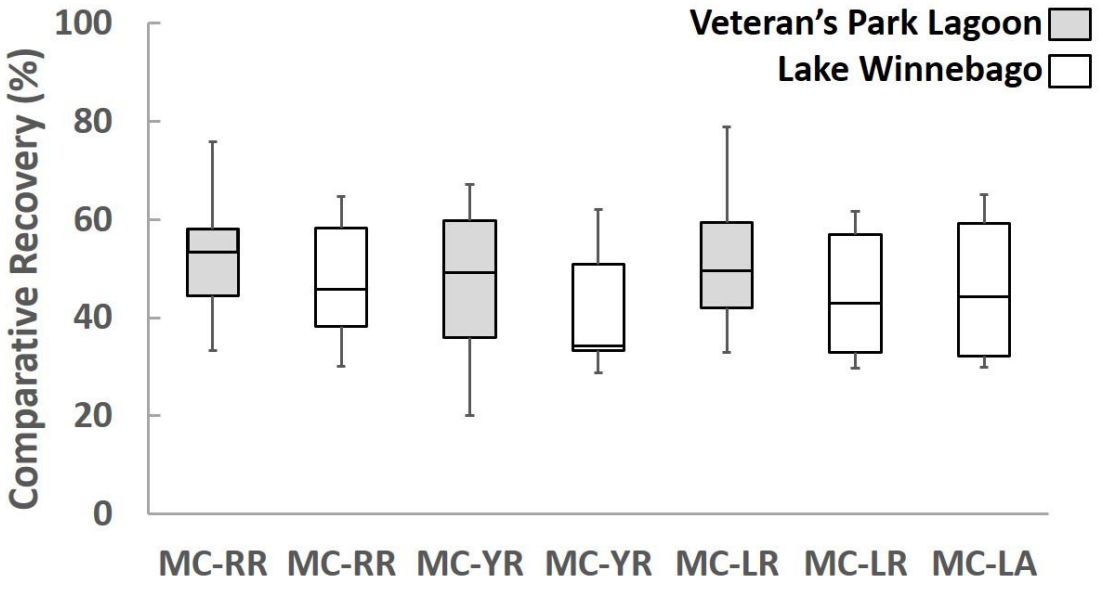

Figure 8: Box and whisker plots of comparative recoveries for on-filter compared to bead beat method for each congener in Lake Winnebago (red boxes) and Veteran's Park Lagoon (black boxes). MC-LA was not detected above trace levels in Lake Winnebago and therefore is not included in this analysis.

2.3.2 Microcystin Extraction from Sequential Filter Flushes

Figure 9.a shows the concentration of microcystin in each individual flush volume of extraction buffer after 10 minute incubation on the filter for each congener detected, with standard deviation bars representing the five replicate filters. Figure 9.b shows the sum of the congener concentrations in Figure 9.a, representing total microcystin. This total microcystin differs from cumulative elution concentration (blue) in Figure 9.c, which is total microcystin concentration as if each flush was pooled to analyze how much each sequential extraction buffer flush diluted the final sample. These values are compared to the elution concentration out of the total microcystin concentration (green) to analyze what percent of the total is collected with each sequential flush. This on-filter extraction data is then compared to the controls in Figure 9.d, which shows a bead beat control with no filter, bead beat control with filter (standard method), microcystin collected after 7 flushes, and microcystin collected after 1 flush.

A total of 4 microcystin congeners were detected in the culture of *Microcystis auerginosa* with both MC-RR and MC-LR being the most dominant. MC-RR was the most hydrophilic congener detected and MC-LR was the most hydrophobic congener detected; no clear trend in extraction characteristics based on hydrophobicity was observed. The highest concentration for all congeners was recovered in the second flush solution (Figure 9.a/b). Approximately 6-7 flushes were needed before microcystin could be only detected at trace levels, approaching 100% recovery of the total microcystin that was able to be extracted.

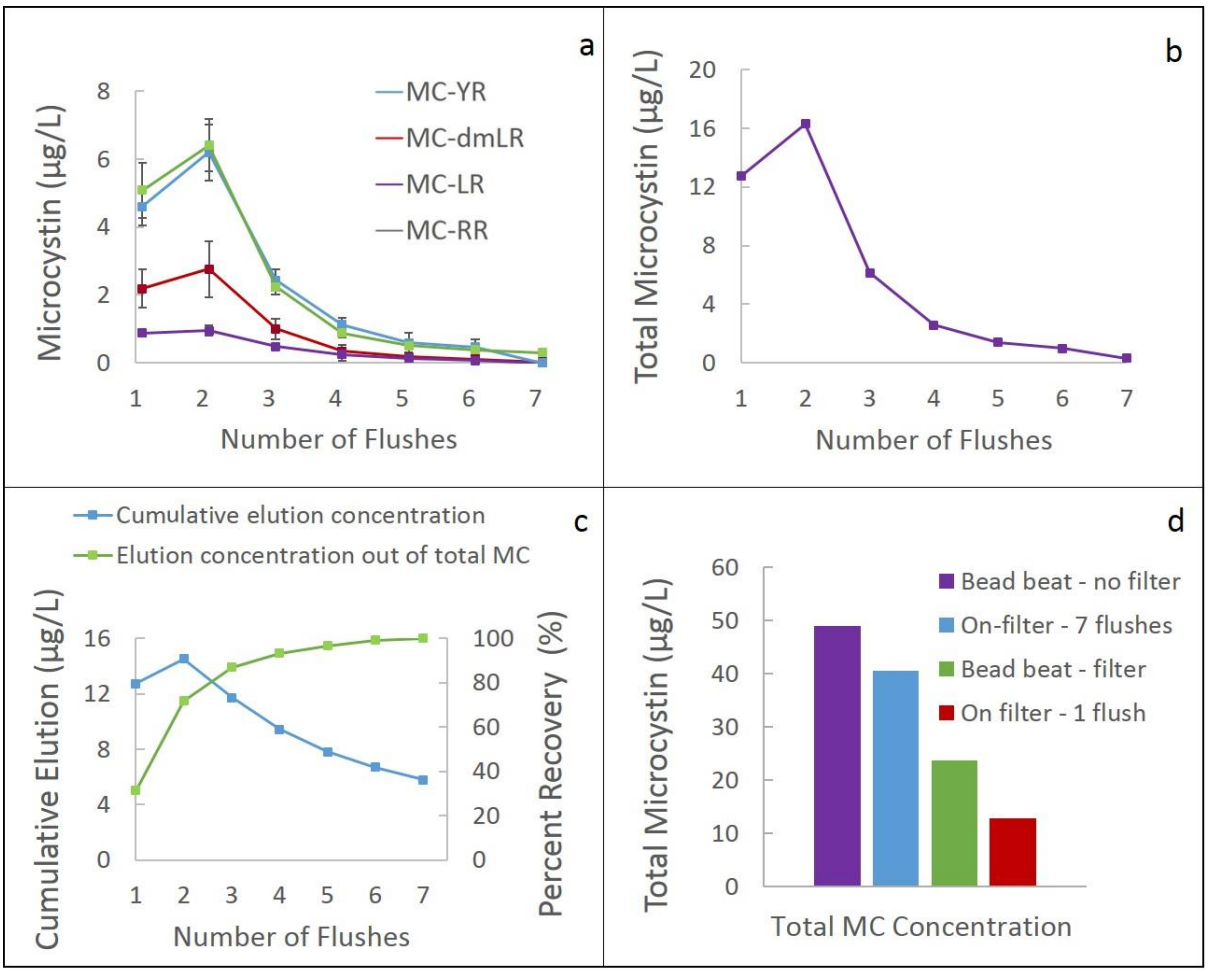

Figure 9: Filter Flush experiment to determine how many 2 mL volumes of extraction solvent are needed to extract all intracellular microcystin congeners present in biomass. a) Average concentrations of congeners MC-LR, MC-YR, MC-RR, MC-dmLR for 5 replicate filters. b) Total microcystin (sum of individual congener concentration) c) Comparison of cumulative elution concentration with each sequential flush vs. percent recovery of total microcystin. d) Comparison of on-filter extraction concentrations after 1 and 7 flushes to bead beat controls with and without filter (cells pelleted and bead beat, no filter used for biomass collection).

2.3.3 Incubation Time Dependency of Microcystin Extraction

On-filter extractions were performed to determine the effect of incubation time on microcystin extraction concentration, Figure 10. Incubation times of 0 and 10 minutes gave similar extraction profiles and concentrations, standard deviation error bars showed overlap

between the two, but the 10 minute samples were slightly greater in magnitude. The bead beat control and the 60 minute incubation time gave similar extraction concentrations, roughly double that of the 10 minute samples. They also showed similar confidence intervals.

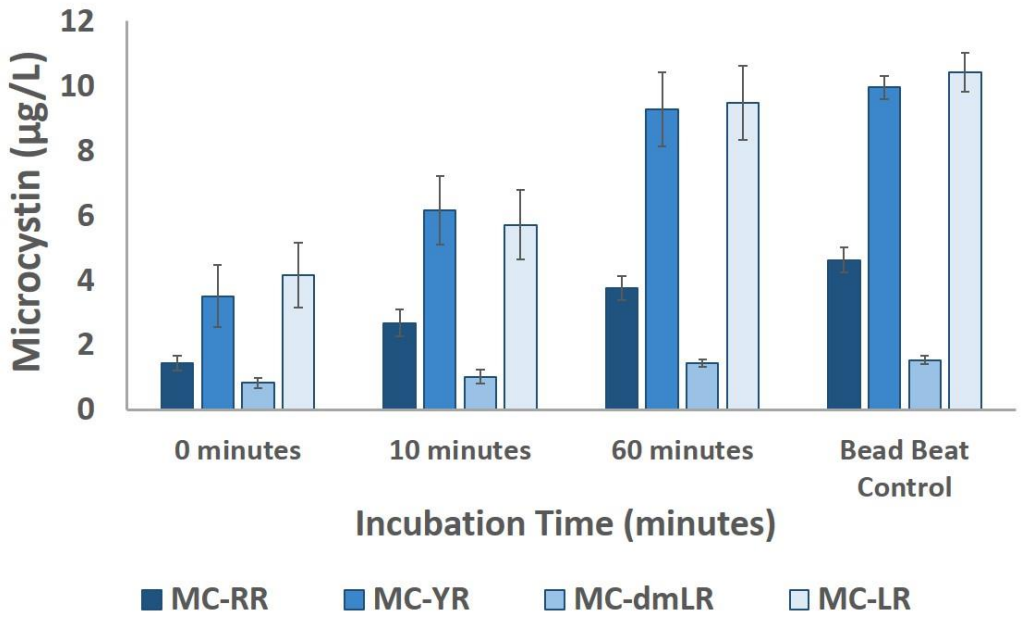

Figure 10: Incubation time dependency of microcystin extraction in 80% acidified methanol. Incubation times 0, 10, and 60 minutes compared to standard bead beat control (with filter).

2.3.4 RNA Extraction

The RNA data collected from the on-filter dual extraction method as well as the standard bead beat method was preliminarily quantified for total RNA by measuring the absorbance at 280 nm on a Nanodrop spectrophotometer. As seen in Figure 11.a/b, Nanodrop results for the dual extraction method show poor recovery of total RNA when compared to extraction using the bead beat method. Comparative recovery values for the Lagoon ranged from 6% to 27% and for Lake Winnebago the values ranged from 5% to 64% of the bead beat concentration.

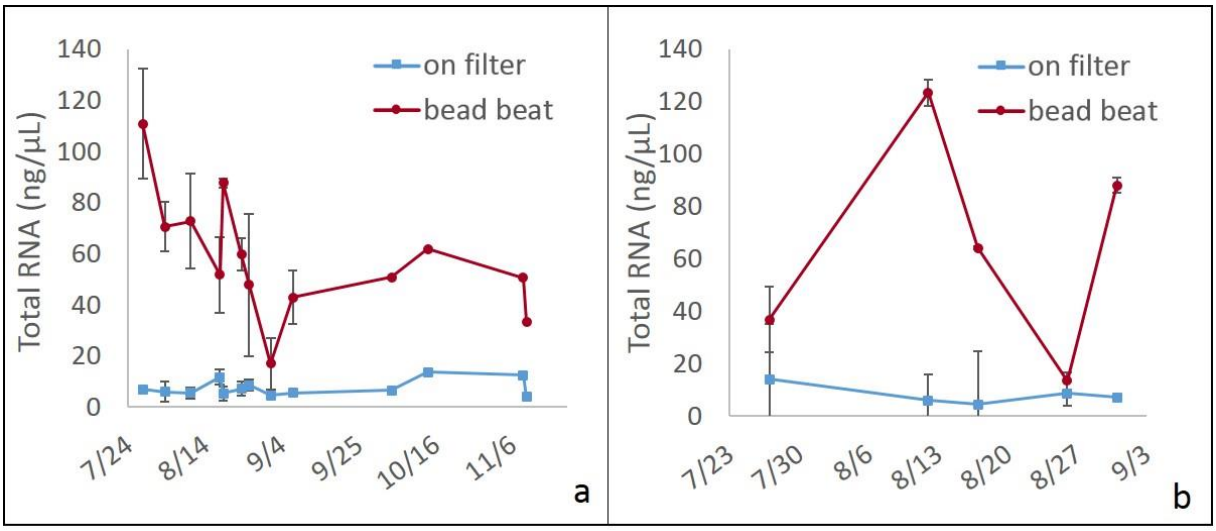

Figure 11: Total RNA concentrations for on-filter method and standard laboratory bead beat method, measured at absorbance 280 nm with Nanodrop Spectrophotometer. a) Veteran's Park Lagoon. b) Lake Winnebago.

2.4 Discussion

Extraction of microcystin directly from filtered biomass from environmental samples using a modified method described by Barco et al. [97] provided comparable results to laboratory extraction using mechanical lysis and solvent extraction. Barco et al. [104] tested various ratios of methanol and water to examine their effectiveness to extract various congeners of microcystin from freeze dried cells and limited environmental samples (only *Microcystis* and *nodularin* were examined, so extraction from other microcystin producing genera with this method is unknown). Acidified 60-70% methanol gave the highest yield for hydrophilic microcystin variants, and acidified 80-90% methanol solutions were optimal for very hydrophobic microcystin variants. However, 80% acidified methanol/20% water solution at pH 2 was optimal for extraction of the widest range of hydrophobic and hydrophilic microcystin congeners and maintaining the stability of the microcystin for prolonged storage. While the

stability of microcystin congeners using the on-filter extraction method was not tested, similar trends in congener extractions could be observed between the methods used in this study.

The environmental data demonstrates that the method is sensitive enough to be able to detect differences in production trends between microcystin congeners (Figure 5 and 7). Figure 7 also suggests that the on-filter extraction method is missing a microcystin peak for all detectable congeners in mid-July, that the bead beat method detects. However, there maybe have been underlying issues with this data set. Lake Winnebago had half the sampling points as Veteran's Park Lagoon did. If there was experimental error on one sampling date for one method, it could appear as though the whole peak was missed by that method. Also, Lake Winnebago samples were subject to logistical issues such as transportation and storage for 1-2 days before sample processing. This time lag could have influenced the accuracy of results due to cell clumping and cell settling (samples were not mixed). This provides further evidence that traditional sampling regimes may be less than ideal for processing time sensitive environmental samples.

Veteran's Park Lagoon is a recreational body of water and Lake Winnebago is a recreational and drinking water source body of water; both were analyzed with respect to the WHO drinking and recreational regulations. The on-filter method was able to extract microcystin below, at, and above the World Health Organization limit of MC-LR in drinking water of 1 µg/L. Veteran's Park comparative recovery medians range between 49% and 53 %, where Lake Winnebago medians are slightly lower, ranging between 34% and 46%. While this result could have been influenced by a number of factors including the small number of sample obtained from Lake Winnebago and the numerous sampling, storage, and transport logistics involved, it can be seen that the intervals of confidence between Veterans Park and Lake Winnebago overlap

for all congeners measured. This implies that the method is robust enough to be applied to bodies of water with difference in microbial community (microbes that are more or less well suited to cell lysis and microcystin extraction in 80% acidified methanol), suspended particulate characteristics, water chemistry, organics, inorganics, etc.

Several data sets were found to be outliers using the interquartile range method and removed from analysis. There could be several inherent errors that contributed to these outliers. In samples where the biomass density is high, the extraction of intracellular microcystin from bead beat samples may have been underestimated due to biomass adhering to the lid of the filter housing when the filter was removed for bead beating. The on-filter extraction method does not experience this loss of biomass because it does not require removal of the filter from housing for processing. In some cases, this situation was observed and potentially contributed to comparative recovery percentage greater than 100%; these values were flagged as outliers and removed from subsequent analysis. *Microcystis* and other bloom forming cyanobacteria are well known for aggregating to form large colonies, and are therefore not homogeneously distributed in a water sample. This clumping effect could lead to variability between both method replicates and extraction treatments. As sampling and extraction experiments were performed by numerous personnel over the sampling period, additional variation may have occurred from inter and intra user variability.

While the study performed here recovered approximately 50% of the bead beating method using one flush, this data suggests that, 2 flushes would not only provide the highest concentration extract, but would represent approximately 80% of the intracellular MC. Alternatively, if the final extraction volume is not a constraint and highest total yield of microcystin from the sample is desired for downstream concentration/purification, 6-7 flushes

would be required to achieve near 100% recovery of the microcystin able to be extracted with this method. Therefore, the on-filter extraction method is flexible enough to be adapted to the specific end application of the user.

Cultures of *Microcystis aeruginosa* that were filtered and subsequently bead beat (comparable to controls performed for environmental data) showed total microcystin concentrations equivalent to roughly 50% of those where the biomass was centrifuged and then bead beat, indicating that the presence of the filter influences microcystin extraction (Figure 9.d). This could be due to several factors: to the filter binding a fraction of the microcystin, some biomass being lost through the filter that is otherwise collected when pelleting cells, filtration is prematurely lysing cells due to pressure causing microcystin to be lost through the filter with the flow through, or biomass is lost when transferring filter from housing to bead beat tube. Controls could be performed with multiple additions of extraction buffer to the bead beat filter to attempt to recover a greater fraction of the microcystin. While another method such as centrifugation may be able to extract more of the total microcystin present, it is difficult to perform on board and *in situ* instrument so characterization of the on-filter method is necessary

When the total microcystin collected from the on-filter extraction-7 flushes is compared to the bead beat control performed with no filter (Figure 9.d), less microcystin is measured when the filter is present. This is likely due the binding or loss of microcystin previously mentioned. The ratio between the bead beat (standard with filter method) control and the on-filter extraction-1 flush of roughly 50% is the same approximate ratio being seen with environmental samples, further confirming the robustness of the on-filter microcystin extraction method.

Figure 10 shows that microcystin concentrations were time dependent; 0 and 10 minute incubation times resulted in microcystin concentrations with overlapping intervals of confidence.

This suggests that if time is a constraint for experimentation, a 0 minute incubation could be used to roughly estimate intracellular microcystin concentrations. The range for the bead beat control (standard method with filter) overlapped with the 60 minute incubation range. If time is no constraint and total microcystin is desired, longer incubation times could be performed. These results further support the hypothesis that intra-user error could be causing variability among the triplicate filters. Since the process is not currently automated, lag times between additions of buffer to sequential filters could be influencing results. Also, inter-user error could be contributing to variability due to slight unavoidable differences in performing the experiments by multiple users. Automation of this protocol may greatly reduce the amount of variability seen between triplicate samples.

RNA extraction with the dual on-filter extraction method is based on the hypothesis that RNA remains on-filter after Microcystin extraction in high alcohol percentage buffer, and can then be subsequently be eluted with aqueous guanidine buffer. The ability of nucleic acids (DNA and RNA) to effectively bind to glass fiber filter has been previously established and is the basis for many commercial nucleic acid spin column techniques. However, results using the described method show poor total RNA comparative recoveries between the two extraction methods (Figure 11). Total RNA may vary between the extraction methods due to recalcitrant cells that are resistant to chemicals used for cell lysis, but susceptible to mechanical lysis. Only specific gene detection techniques can determine if the organisms of interest are being effectively lysed. Preliminary data showed that a fraction of RNA appears to be retained on the filter, but some appears to be lost in the extraction buffer (data not shown). The RNA may be binding to the glass fiber filter due to effects of the guanidine salt buffer, the acidified methanol, or a combination of the two reagents. While this inhibited obtainment of dual extraction results for

the bulk of experimentation done in this study, this property may have application in downstream method development. It could potentially allow the filter to be used to purify and concentrate RNA, with elution in a different buffer. If this is not possible, different filter types would need to be investigated that do not bind the RNA fraction in the same way. Once it is determined where the microcystin biosynthesis gene fraction is being lost and it is properly detected, the next step would be to perform RT-qPCR to investigate extraction efficiency of *mcy* gene cluster, instead of using absorbance at 260 nm to measure total RNA.

2.5 Conclusion

The on-filter extraction method is promising for microcystin, but needs further optimization and investigation to identify nucleic acids extraction from microcystin producing organisms. Extraction efficiencies of the on-filter extraction method need to be correlated with a wide range of cultured microcystin producing cyanobacteria and a variety of microcystin producing microbial communities that are present during blooms in order to characterize microcystin extraction across a broad selection of genera. Further experimentation is needed in order to determine what fraction the RNA is lost in, or if it remains on the filter during the extraction protocol. If this is the case, this chemistry could also potentially be exploited for use in a nucleic acid purification step on the glass fiber filter. This method could be applied to a point of use, field-able assay immediately. Minimal equipment and time would be needed to perform *in situ* extractions of intracellular microcystin for later detection using laboratory methods (MS, ELISA, PPI assay, etc.). Filtering and extraction at the point of sampling for later analysis in the laboratory could also decease some of the logistics involved in the storage and transport of large volumes of water to centralized facilities for processing. For nucleic acids the next step is to perform RT-qPCR to for *mcyE* genes to look at the comparative RNA recovery between

extraction methods, which will provide better indication of RNA extraction efficiency specifically from microcystin producing cyanobacteria.

3 Chapter 3: Evaluation of current and emerging methods for microcystin and microcystin biosynthesis genes detection sensor systems

Abstract

Eutrophication due to increase in anthropogenic activity has caused an increase in toxin producing Harmful Algal Blooms (HABs) in freshwater bodies around the world. Microcystin is one of the most common toxins produced by HABs. A cost effective automated *in situ* detection system that can quantify intracellular microcystin before it is released into the environment is needed in order to make informed public health decisions on potable and recreational water. This study evaluated field amenable methods for detection of microcystin and or nucleic acids. Microcystin detection methods included direct fluorescent derivatization and optical signal amplification (direct and indirect hybridization schemes using DNA aptamers), nicking enzyme assisted fluorescent signal amplification (NEFSA). Methods evaluated for detection of nucleic acids included optical signal amplification (direct and indirect hybridization, NEFSA, cascading amplification of nucleic acids (CANA)) and nucleic acid amplification (Strand displacement amplification (SDA)). Of these techniques, SDA gave only non-specific amplification, fluorescent derivatization produced inconsistent reaction products, and all hybridization schemes resulted in non-specific binding. Preliminary results from NEFSA and CANA showed promise, but were inconsistent; further optimization of reaction conditions is necessary to conclude if either could be viable options for use in an automated *in situ* detection system.

3.1 Introduction

Multiple strains of cyanobacteria have the ability to produce microcystin, a potent hepatotoxin that inhibits protein phosphatase activity in the mammalian liver. Blooms of these toxic organisms are increasing in occurrence worldwide due to anthropogenic activity, and have public health implications for potable water supply, recreational exposure, and agricultural water use [104]. Toxin production is seemingly sporadic over time; little is known about the drivers of toxin production in harmful algal blooms (HABs). Currently, manual sampling and traditional laboratory analysis creates a delay between sampling and results. The development and application of *in situ* sensors to detect and quantify microcystin in near real-time would provide early warning systems for the onset of blooms and allow for more informed public health decisions. Additionally, *in situ* molecular sensors with detection capability for both microcystin and the expression of genes involved in microcystin biosynthesis will enable sustained high resolution sampling and analysis of toxin dynamics.

The overarching goal of this investigation was to develop instrumentation that can autonomously detect microcystin and the genes involved in toxin biosynthesis *in situ*. One of the first stages of this process was to identify and characterize analytical methods for both microcystin and nucleic acid detection that could be amenable to automated field deployment. Methods for the quantification of microcystin and nucleic acids were evaluated in this study based on several criteria: low reaction complexity (i.e. moderate isothermal reaction conditions; minimal fluidic manipulations), ability for prolonged deployment in the environment (i.e. reagent stability at ambient temperatures), simple detection strategies (i.e. fluorescence or colorimetric readout) and assay sensitivity and specificity over a wide dynamic range of concentrations relevant to environmental concentrations and regulatory standards (e.g., WHO and EPA

regulatory standards). Measurement of total microcystin and discrimination between individual microcystin congeners would provide additional environmentally relevant information.

Several techniques that have potential for automation were identified and assessed for the detection of microcystin as well as genes involved in its biosynthesis. Methods evaluated included fluorescent derivatization and signal amplification and methods for biosynthesis gene detection included signal amplification and nucleic acid amplification. Two of these methods could potentially be applicable to the toxin and its biosynthesis genes with minor modifications (i.e. NEFSA and CANA).

3.2 Methods Tested

3.2.1 Microcystin Derivatization: Theoretical Operation

Chemical modification of microcystin to form a fluorescent compound was described by Hayama et al. [44]. The reaction (Figure 12) relies on an isothermal (60 ˚C) condensation reaction between 2 conserved carboxyl groups on the microcystin molecule and the fluorescent monopyrene molecule 4-(1-pyrene) butanoic acid hydrazide (PBH). The authors suggest that resulting dipyrene structure has a unique fluorescent spectra, enabling it to be discriminated from unreacted monopyrene molecules. Certain aspects of this method are ideal for automation; the reaction relies on 2 chemical components to derivatize microcystin and it occurs under moderate isothermal heating conditions. However, the reaction occurs in an organic solvent, so additional design considerations to account for chemical compatibility would be required [44].

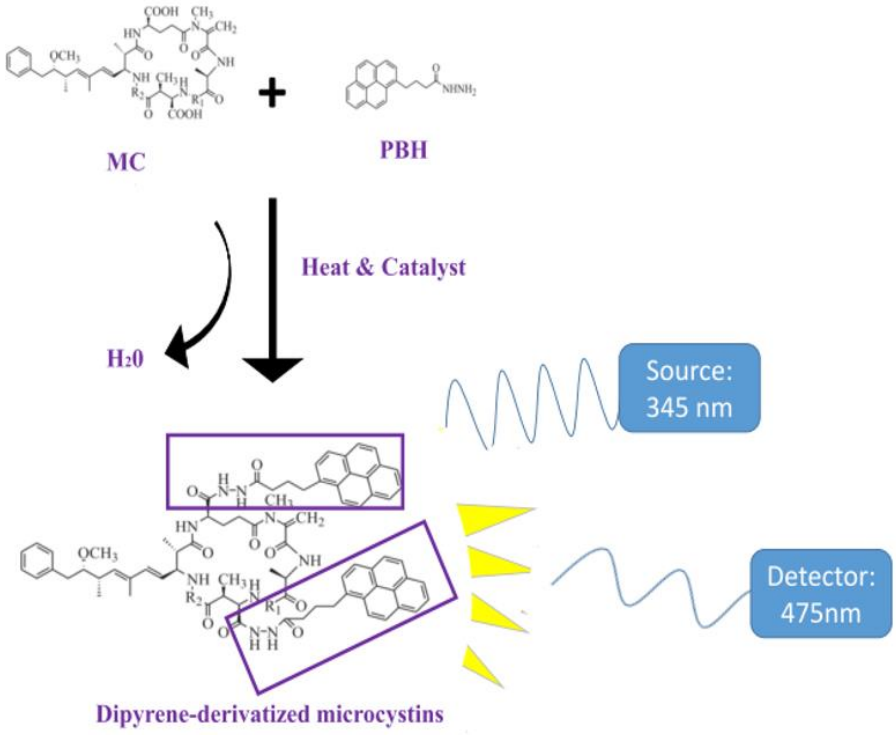

Figure 12: Derivatization of microcystin with PBH. PBH is reacted with microcystin at 60 ˚C in the presence of the catalyst 4-(4, 6-dimethoxy-1, 3, 5-triazin-2-yl)-4-methylmorpholinium chloride (DMT-MM). A condensation reaction binds 2 PBH molecules to microcystin at two conserved carboxyl groups on the microcystin molecule. When excited at 345 nm, the resulting unique dipyrene structure fluoresces at 475 nm, and can be distinguished from monopyrene structures that fluoresce in the range of 360-420 nm. Adapted from [44].

3.2.2 Microcystin Derivatization: Materials and Methods

Reaction component characterization. Retention time and optical characteristics of each reaction component was examined individually and in combination as outlined in Table 5. Microcystin derivatization required stock solutions of varying concentrations of MC-LR (Cayman chemicals, USA) in 95% acetonitrile (Fisher Scientific, USA)/5% ddH_20, 40 mM PBH (Setareh Biotech, USA) in molecular biology grade DMSO (Fisher Scientific, USA), and 200 mM 4-(4,6-dimethoxy-1,3,5-triazin-2-yl)-4-methylmorpholinium chloride (DMT-MM) (Sigma-Aldrich, USA). Reactions were performed in 1 ml glass HPLC vials (Fisher Scientific, USA)

with volumes of each stock solution listed in Table 5. Reactions were vortexed for 2 minutes and incubated at 60 °C for 30 minutes. Following incubation, the mixture was cooled to room temperature and run on HPLC-FLD/ABS or HPLC-MS.

Table 5: Microcystin derivatization reaction reagent matrix to determine peak height and retention time of reaction components.

	10 µL PBH in DMSO	10 µL DMT-MM in 95% Acetonitrile	Microcystin in 95% Acetonitrile	10 µL DMSO	10 µL 95% Acetonitrile	50 µL microcystin in 95% Acetonitrile
1-Complete Reaction	X	X	X			
2-No PBH		X	X	X		
3-No DMT-MM	X		X		X	
4-No MC	X	X				X
5-Only PBH	X				X	X
6-Only DMT-MM		X		X		X
7-Only MC			X	X	X	
8-Reaction matrix				X	X	X
9-95% Acetonitrile					2X	X

Reaction component shelf life. To evaluate if the microcystin derivatization method was suitable for extended use at ambient temperatures, a matrix of freshly prepared and stored reaction components was constructed (Table 6) whereby each stored reaction component was tested against freshly made reaction components. Stock solutions of each component (microcystin, PBH, and DMT-MM) were made on Day 1 of the shelf life experiment, this stock solution was then stored in the dark at ambient laboratory temperature (~20 ˚C). Each subsequent testing day, a matrix of stored and freshly prepared reagents was combined according to Table 5. Reagent stability was initially tested three times a week for 3 weeks, and then once a week for the remainder of the experiment.

Table 6: Microcystin derivatization shelf life matrix.

Treatment	Stored PBH	Stored DMT-MM	Fresh PBH	Fresh DMT-MM	Fresh MC-LR (100 µg/L)
1-Day 1 PBH and DMT-MM	X	X			X
2-Fresh PBH, Day 1 DMT-MM		X	X		X
3-Day 1 PBH, Fresh DMT-MM	X			X	X
4-Fresh PBH and DMT-MM			X	X	X

For HPLC-FLD/DAD analysis 100 µL volumes were analyzed on a HP (Agilent 1100 series) HPLC system fitted with a Luna C18 (Phenomenex, 3 µm, 150 x 3 mm) separation column, at 1 mL/min flow rate. To discern microcystin fractions, absorbance detection was performed using a HP (Agilent 1100 series) diode array detector (DAD) at 238 nm. Florescence detection was performed using 345 nm excitation and 475 nm emission on a HP (Agilent 1100 series) fluorescence detector.

For HPLC-MS analysis, a Shimadzu HLPC Model 20A was fitted with a Luna C18 column (Phenomenex, 3 µm, 150 x 3 mm) to separate microcystin variants (MC-LR and MC-Dha^{7}-LR (NRC); MC-RR, MC-YR, MC-LA). Microcystin variant standards were obtained from Sigma Aldrich. The mobile phase was composed of 0.1% formic acid and 5 mM ammonium formate in 95% acetonitrile (B) and HPLC water (A). Mobile phase running conditions for separation was equilibration from 0-3 min at 30% B, gradient of 30 to 90% B from 9 time (min)-15 min, step change back to 30% B at 15.01 min and then five minutes for re-equilibration. Total run time 20 minutes. Mass spectroscopy was performed with an ABSciex 4000 QTrap mass spectrometer equipped with a TurboV electrospray ion source. MS parameters were as follows: entrance potential: 10 mV; curtain gas: 15 psi; collision gas: high; ionspray voltage: 5000; source

temperature: 600 °C; ion source gases 1 and 2: 70 psi. Additional MS detection factors for microcystin are listed in Table 7.

Table 7: Microcystin HPLC-MS detection parameters.

Toxin	Parent Ion	Daughter Ion	Declustering Potential	Collision Energy	Collision Cell Exit Potential	Retention Time (min)
Microcystin-LR	995.619	135.3	126	115	26	8.25
	995.619	127.1	126	115	26	8.25
Microcystin-YR	1045.633	135.3	141	107	8	8.55
	1045.633	127.1	141	123	8	8.55
Microcystin-LA	910.617	776.4	106	27	8	9.37
	910.617	135.2	106	87	8	9.37
Microcystin-RR	520	135.1	81	43	8	7.48
	520	70.1	81	129	6	7.48
[Dha^{7}]-Microcystin-LR	981.531	135.3	126	101	22	8.25
	981.531	103.2	126	129	6	8.25

3.2.3 Microcystin Derivatization: Results and Discussion

Initial results indicated the formation of a fluorescent product with a retention time of 5.3 minutes in derivatization reactions containing both microcystin and PBH, which was absent in reactions containing no microcystin (Figure 13). Chromatography peak retention times may have varied day to day due to column temperature fluctuation, as a column compartment was not used. Similarly, samples analyzed using HPLC-MS in enhanced mode showed additional peaks with retention times of 15.45 and 16.15 in reactions containing microcystin (Figure 14.a) compared to negative controls (Figure 14.b-d). However, derivatization of microcystin with PBH did not produce consistent results. Chromatograms from complete reactions were routinely obtained that were indistinguishable from reactions with no added microcystin (Figure 15).

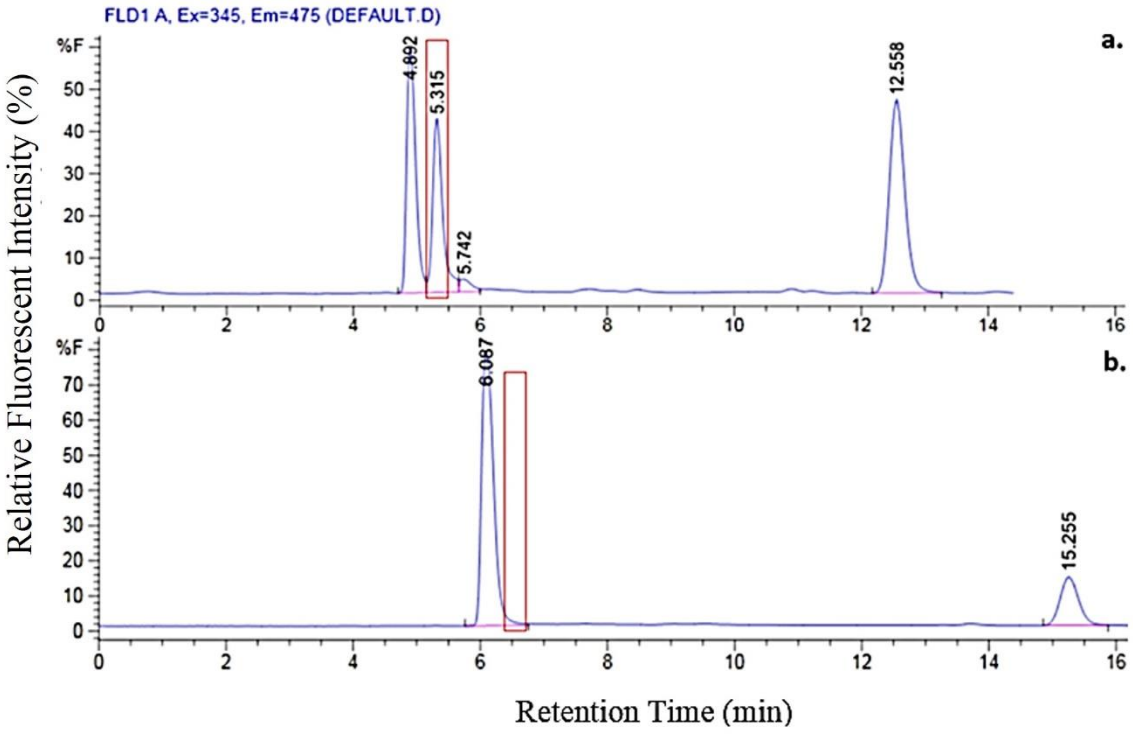

Figure 13: HPLC-FLD detection of MC-PBH derivative. a) Fluorescence chromatogram for complete reaction. b) Fluorescence chromatogram for reaction with no microcystin added.

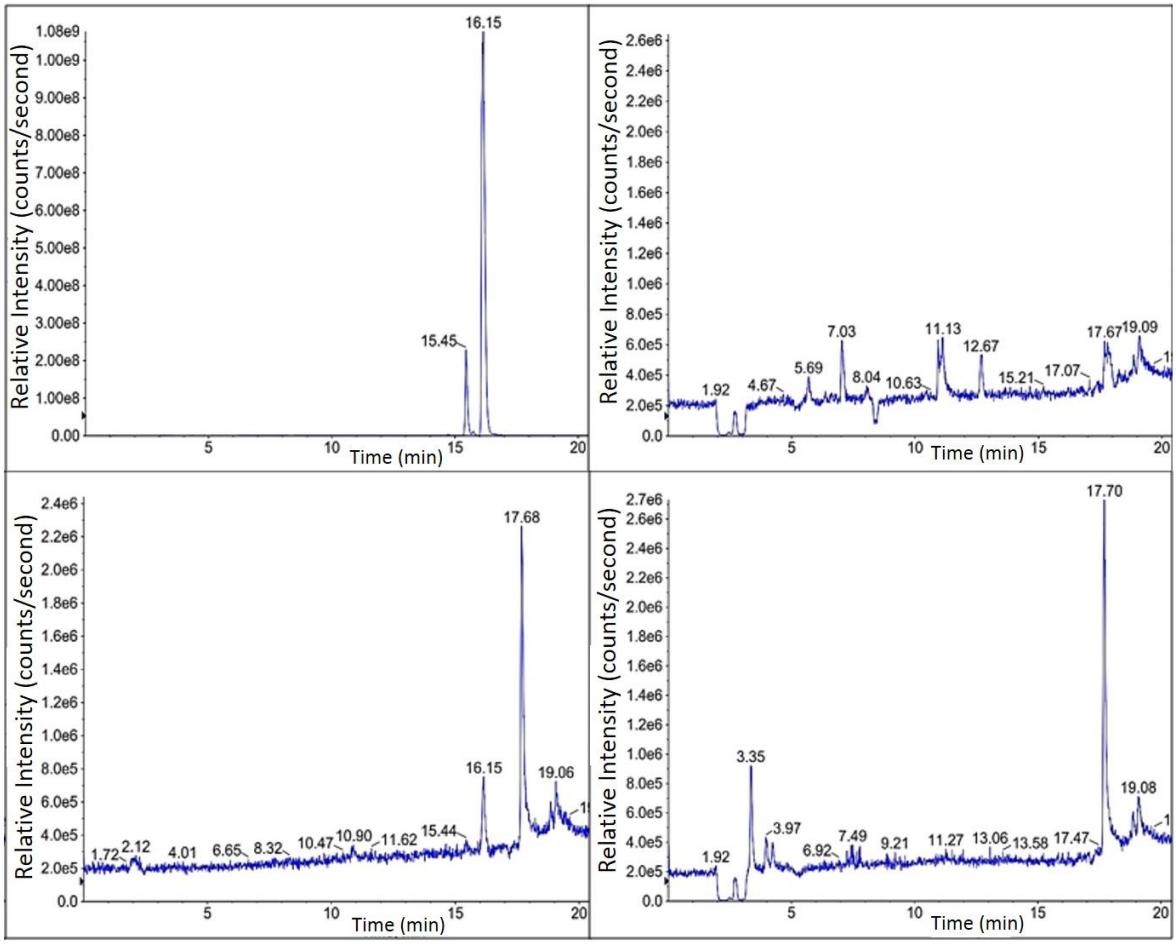

Figure 14: HPLC-MS detection of MC-PBH Derivative with 1, 4, 8, and 2 from matrix listed in Table 5. a) Complete reaction with all reagents. b) Reaction with no microcystin added. c) Reaction matrix with no PBH, DMT-MM, or microcystin. d) Reaction with no added PBH.

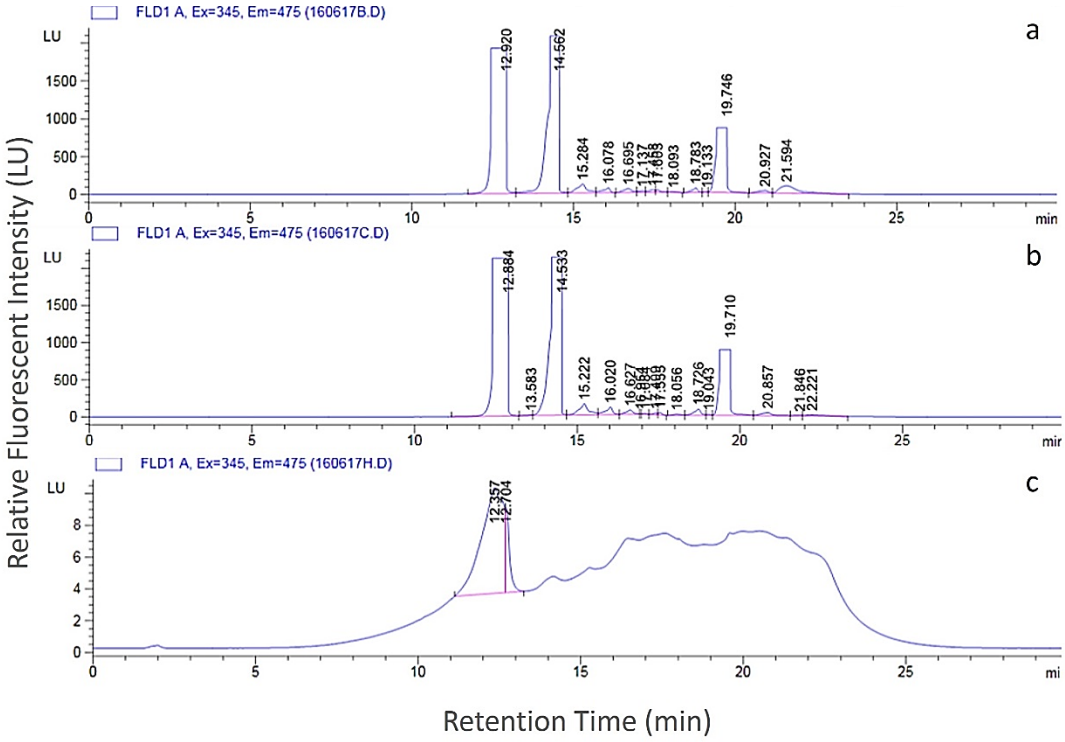

Figure 15: HPLC-FLD chromatograms with reactions 1, 4, and 7 from the matrix listed in Table 5. a) Microcystin added to reaction. b) Microcystin not added to reaction. c) Only microcystin in reaction matrix, without added PBH or DMT-MM (Note difference in scale from a. and b.).

Additional evidence for the inconsistency of the reaction was observed in the shelf life experiments that tested the method's potential to be used in an ambient temperature automated instrument. Figure 16 shows that there was inconsistency in the magnitude of the peak height for what was assumed to be the MC-PBH derivative over time. However, the figure does show that when the reaction with all stored/original reagents failed, addition of fresh catalyst, DMT-MM, allows the derivatization to proceed. This suggests that the reagent with the shortest shelf life is DMT-MM, at about 12 days. If the method was to be further considered for use in a microcystin detection instrument, more research could be done to potentially find a more suitable catalyst for

the reaction. However, the lack of reproducibility makes this method unsuitable for a detection method for an automated *in situ* microcystin sensor.

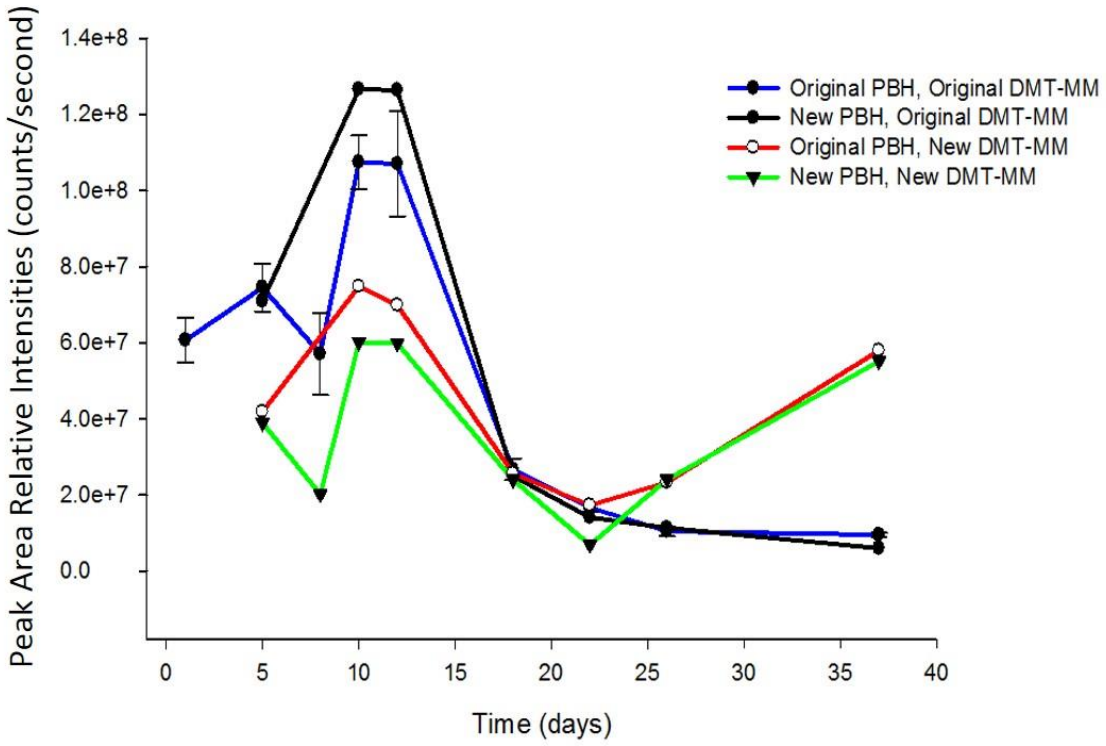

Figure 16: PBH-MC-LR derivatization matrix shelf life experiment.

3.2.4 Cascading Amplification of Nucleic Acids (CANA): Theoretical Operation

CANA is similar to Hybridization Chain Reaction (HCR) [111] [112], a non-enzymatic, isothermal, signal amplification, nucleic acid detection technique that is attractive for use in an automated instrument. Techniques similar to CANA were first developed by Dirks et al. [111], and have been subsequently modified by other groups for a range of applications (i.e. Fluorescent *in situ* hybridization (FISH), DNA signal amplification) [111], [113], [114], [115]. HCR and related techniques rely on signal amplification (Figure 17) rather than amplification of target sequence, which could potentially cut down on contamination/non-specific amplification

[112]. CANA (Smith, 2014, Unpublished), relies on the application of modified molecular beacons, similar to those developed by Tyagi et al. [116] to detect a target nucleic acid sequence by signal amplification (Figure 17). Another advantage of this technique is that it presents the possibility of detecting microcystin in addition to nucleic acids, with modification of Probe 1 to include a microcystin DNA aptamer.

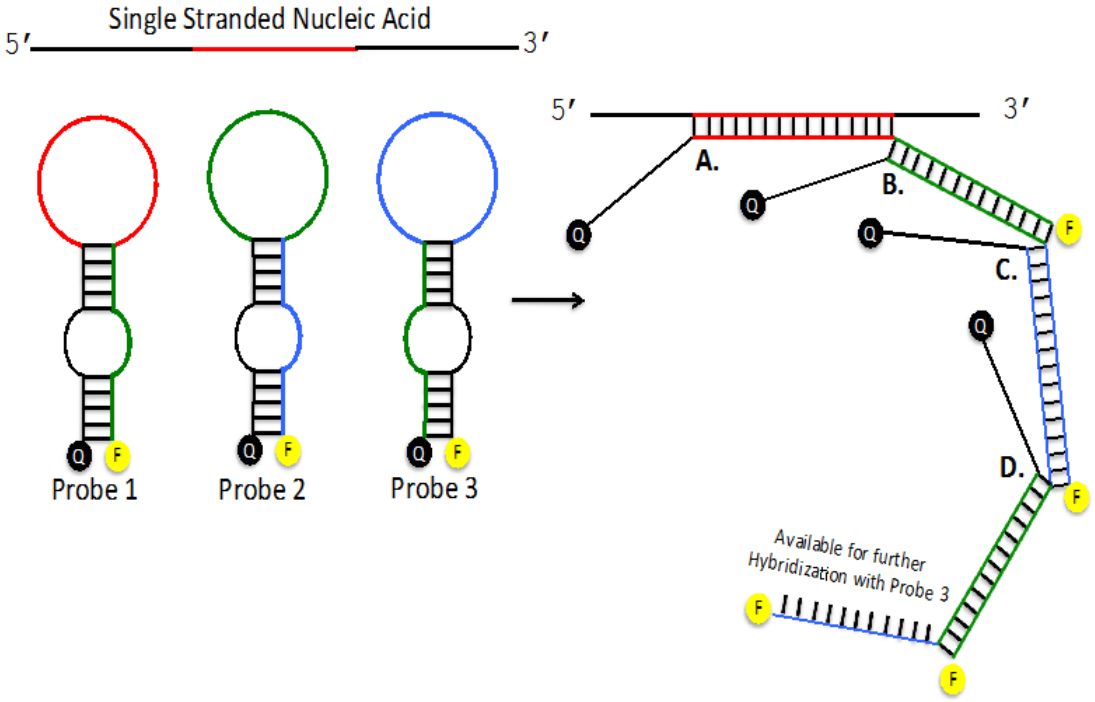

Figure 17: CANA beacon signal amplification. CANA, uses three hairpin probes that contain a fluorophore and quencher that are in close proximity to each other when the probes are in their unbound state. Probe 1 has sequence identity (red) to a region on a, target nucleic acid and unfolds and hybridizes to the target sequence in its presence. The loop region of probe 2 has identity to a region of the unfolded stem of probe 1 (green) and can unfold and hybridize when it is exposed. Probe 2 and probe 3 share identity in their loop and stem structures (blue and green) and following hybridization of probe 1 to the target sequence form a cascading sequence where they sequentially bind to each other. Upon each binding event, the fluorophore is separated from the quencher enabling an increase in fluorescent signal.

3.2.5 Cascading Amplification of Nucleic Acids (CANA): Materials and Methods

Probe design. Three beacons were designed for cascading amplification with the aim of detecting a 19 bp region of the *mcyE* gene from *Microcystis spp.* (Genbank accession HM854746.1) (Figure 18). Beacon design was performed manually and secondary structure checked using the online mfold web server application [117]. Beacons were designed to have delta G ranging between -4.0 and -5.5 kcal/mol, using the folding parameters (temperature 42 ˚C, 70 mM Na^{2+}, 12 mM K^{+}). DeltaG of Probe 1, 2 and 3 were -4.67 -5.2, and-4.1 kcal/mole, respectively. Beacon sequences were interrogated using the NCBI nucleotide database to ensure that they were specific only to their target sequences. All beacons and oligonucleotides were synthesized with HPLC purification by IDT (USA) and contained a 5' fluorophore (5(6)-Carboxyfluorescein, (denoted as 56-FAM) and a 3' quencher Iowa Black quencher (denoted as 31ABkFQ) (Table 8).

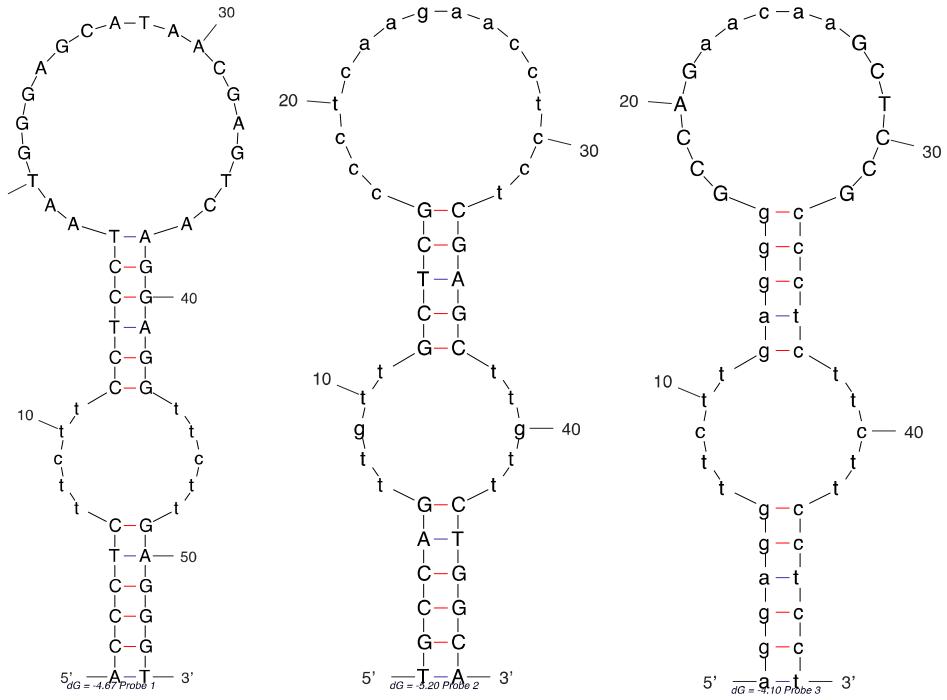

Figure 18: **Secondary structure of probes from mfold web server for nucleic acid folding and hybridization prediction** [117]**.**

Table 8: CANA probe sequences.

Probe	Sequence
Probe 1	/56-FAM/ACCCTCttcttCCTCCTAATGGGAGCATAACGAGTCAAGGAGGttcttGAGGGT/3IABkFQ/
Probe 2	/56-FAM/TGCCAGttgttGCTCGccctcaagaacctcctCGAGCttgttCTGGCA/3IABkFQ/
Probe 3	/56-FAM/aggaggttcttgagggGCCAGaacaaGCTCCGccctcttcttcctcct/3IABkFQ/

CANA reaction conditions: CANA reactions contained 50 nM Probe 1, 50 nM Probe 2, and 50 nM Probe 3. Initial testing of the method targeted a 55 nucleotide long single stranded DNA oligo nucleotide with identity to the *mcyE* gene from *Microcystis spp*. For no template negative controls the input DNA was replaced with the equivalent volume of molecular grade water (MoBio Laboratories, USA). A reaction buffer containing 20 mM Tris-HCl, 2 mM NaCl, 0.01% SDS, 20% formamide was used to bring the reaction to final volume of 25 µL. Reactions were incubated at 42 °C in a DNA Engine Opticon (MJ Research, USA) continuous fluorescence detector. Fluorescence readings were taken every 1 minute for times ranging from 30 to 90 minutes. A matrix of reaction conditions using various combinations of probe and template was conducted in order to evaluate and characterize the performance of the method (Table 9).

Table 9: CANA beacon and template matrix of reactions.

Treatment	Probe 1	Probe 2	Probe 3	Template
1-All components	X	X	X	X
2-Without 1, with template		X	X	X
3-Without 2, with template	X		X	X
4-Without 3, with template	X	X		X
5-All probes, no template	X	X	X	
6-Without 1, no template		X	X	
7-Without 2, no template	X		X	
8-Without B3, no template	X	X		

3.2.6 Cascading Amplification of Nucleic Acids (CANA): Results and Discussion

Initial, testing of the CANA method using a standard curve ranging from 0 to 10,000 copies of input DNA produced increasing signal amplification that was proportional to input DNA concentrations (Figure 19). However, in subsequent experimentation these results proved difficult to reproduce, and resulted in un-proportional signal amplification. A matrix of reaction components varying combinations of probe and template was performed in order to determine what reaction component or condition was contributing to the non-specific signal amplification. Non-specific amplification was seen in reactions performed with no template and with only two out of three probes (Figure 20), suggesting insufficient probe stringency. Further investigation of the method is warranted with significant redesign of the probe structures. Increasing probe stringency could be performed by lengthening the stem structure and/or by decreasing the number of nucleotides in the open loop section of the probes.

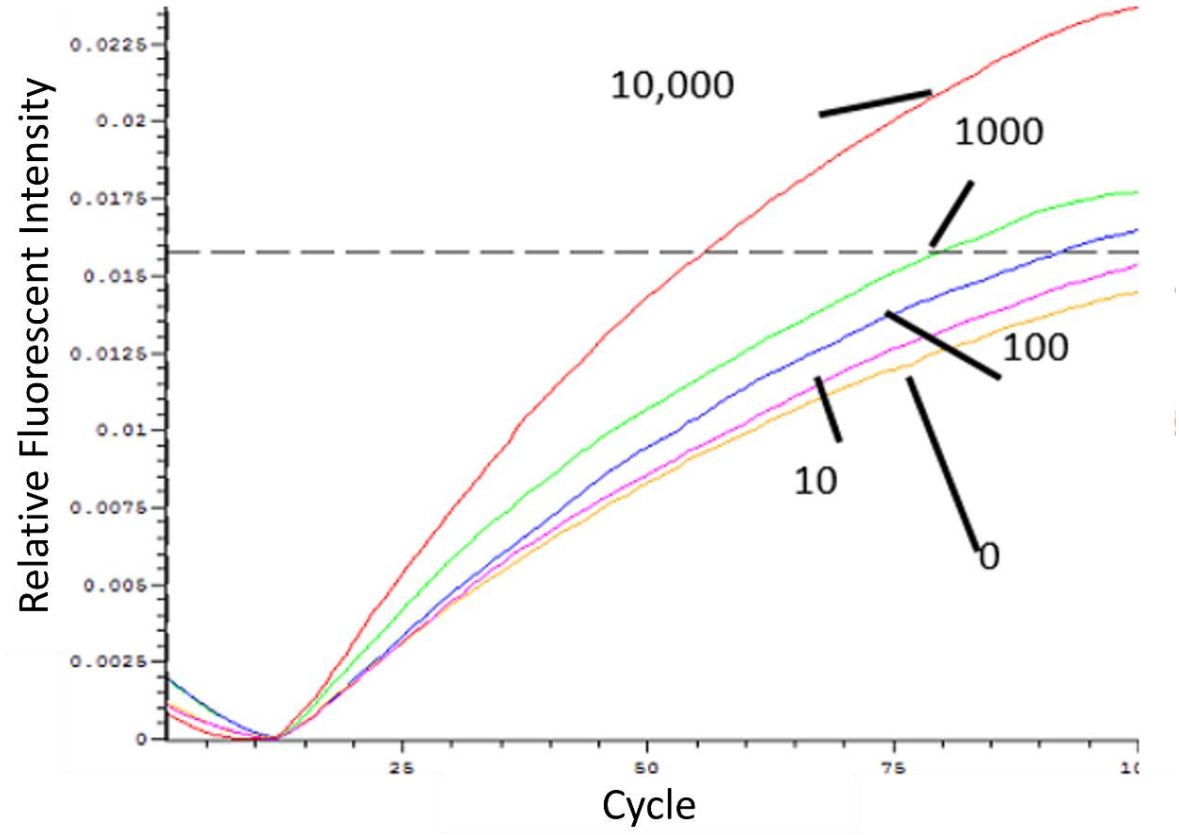

Figure 19: CANA signal amplification plots. a) Preliminary standard curve (10,000, 1,000, 100, 10, and 0 template copies).

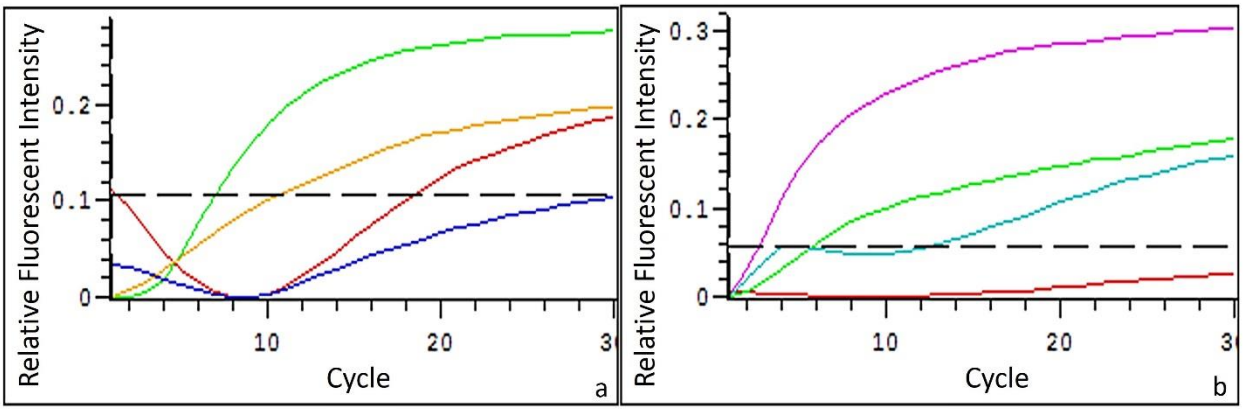

Figure 20: NEFSA Amplification plots. a) Amplification plot showing amplification with no template. Green and red have template and probes 1, 2, and 3. Yellow and blue have no template and probes 1, 2, and 3. b) Amplification plot showing amplification with two out of three beacons. Green and red have template and probes 1, 2, and 3. Pink and blue have template and only probes 2 and 3.

3.2.7 Strand Displacement Amplification (SDA): Theoretical Operation

Strand Displacement Amplification (SDA) [118] is an isothermal DNA amplification technique that requires target DNA, two sets of primers (S1 & S2, B1 & B2 in Figure 21), exo-nuclease deficient DNA polymerase, restriction enzyme, and dNTPs (dATP, dGTP, dTTP, and a modified alpha-thiol-dCTP). The modified dCTP allows for the restriction enzyme to nick, instead of fully cutting the DNA as it would if all standard unmodified nucleotides were present. S1 and S2 have restriction enzyme sites included at their 5' end, as well as identity to the target sequence. Primers B1 and B2 have identity to the target DNA and play an important part in the first round of amplification by enabling strand displacement of the newly amplified fragments containing the primers with introduced restriction sites [60]. While the SDA method relies on the action of two enzymes for amplification, it potentially has shelf life limitations. However, the isothermal nature of the reaction makes it an attractive candidate for an automated detection mechanism

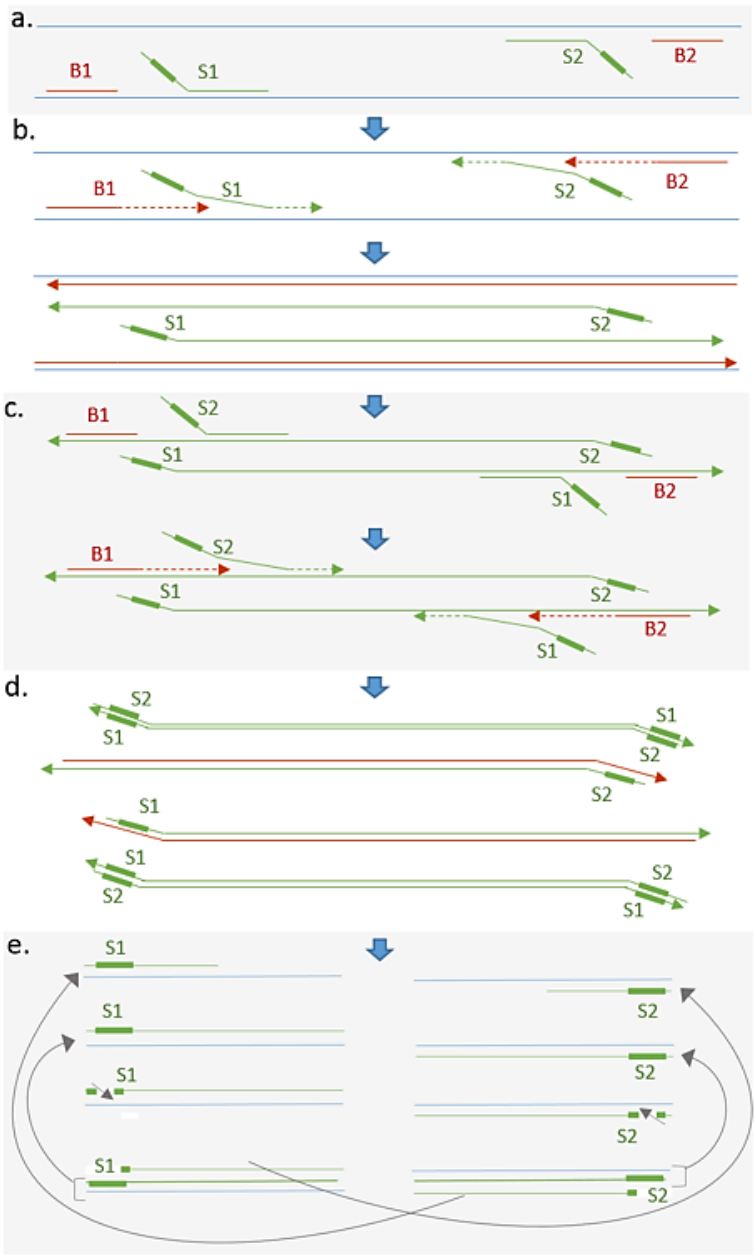

Figure 21: Strand displacement amplification. Adapted from [60]**.**

a) Double stranded target DNA (blue) is denatured, primers S1 & S2 (green) bind, and B1 & B2 (red) bind. S1 & S2 have restriction sites, indicated by the thicker line at the overhang of the primer.

b) Primers are extended by exo- nuclease deficient DNA polymerase with dATP, dGTP, dTTP, and alpha-thiol dCTP. B primers displace the strand formed from the S primers. This results in two double stranded segments without restriction sites, and two single stranded segments with restriction sites.

c) Primers S1, S2, B1, and B2 bind again to the single stranded segments with restriction sites.

d) Segments are extended to form four double stranded segments with restriction sites.

e) S primers bind to target sites. Strands are extended. Nicking enzyme nicks at the S primer sites. As extension occurs again at the nicking site, the downstream strand is displaced. S primer can then bind again to this strand and the process will repeat.

3.2.8 Strand Displacement Amplification (SDA): Materials and Methods

SDA reaction conditions: SDA reactions contained a final concentration of 1x isothermal reaction buffer, 0.4 mM each dNTP, 0.8 mM alpha-thiol-dCTP, 1x EvaGreen (Biotinum, USA), SDA_F/SDA_R primers (0.5 µM), Bump_F/Bump_R primers (0.5 µM), Bst 2.0 warm start (0.3 U/µL), Nt.BspQI (0.2 U/µL), *mcy*E template (100, 1,000, 10,000 copies) in a final reaction

volume of 25 µL. Bst 2.0 warm start, dNTPs, isothermal reaction buffer and Nt.BspQ1 were purchased from New England Biolabs (USA). Alpha-thiol-dCTP was purchased from TriLink Biotechnologies (USA). Master mix of template and all reagents except enzyme were incubated a DNA Engine Opticon™ continuous fluorescence detector (MJ research, USA) at 92 °C for one minute, before cooling to 30 °C for one minute. Bst 2.0 warm start and Nt.BspQI were then added in appropriate concentration to each reaction. SDA reactions were then incubated at 37 °C for 60 minutes with an optical read every minute.

SDA primer design. Multiple primer sets were developed for use in SDA reactions that amplify slightly different regions of the *mcyE* target sequence. The relative orientation of the primer sites are highlighted in Figure 22, with the specific primer sequences listed in Table 10. Primer sequences were tested in various forward and reverse combinations (i.e. Bump_R_G1 & Bump_F_A2) to amplify sequences of varying length: B1F:B1R, 127 base pairs; B1F:A2R, 220 base pairs; B1F:G1R, 387 base pairs; AF:A2R, 111 base pairs; AF:G1R, 278 base pairs; G1F:G1R, 71 base pairs. All primers were tested for homo and heterodimer formation using the online tools provided on the IDT website and were tested against the NCBI nucleotide database for specificity to the target gene sequence. All primers were synthesized by IDT (USA) and purified with standard desalting.

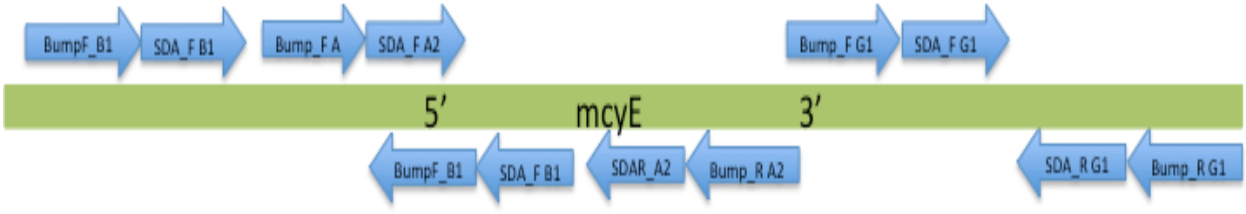

Figure 22: Relative primer orientations on *mcyE* gene.

Table 10: SDA Primer sequences.

Name	Sequence (5' to 3')
SDA_F B1_Nt.BspQ1	ACCGCATCGAATGCATGCGCTCTTCACGATTTAGGCAAGCAAACT
SDA_R B1_Nt.BspQ1	GGATTCCGCTCCAGACTTGCTCTTCAGGGAGCATAACGAGTCAA
SDA_F A2_Nt.BspQ1	ACCGCATCGAATGCATGCGCTCTTCATTGACTCGTTATGCTCCC
SDA_R A2_Nt.BspQ1	GGATTCCGCTCCAGACTTGCTCTTCAAATCTCAGCAATTTCYAGAG
SDA_F G1_Nt.BspQ1	ACCGCATCGAATGCATGCGCTCTTCAGACCTGCACTCCCTGAG
SDA_R G1_Nt.BspQ1	GGATTCCGCTCCAGACTTGCTCTTCACGGGGTGCAACATAATTAGAAK
Bump_R G1	CTAACGAGATTGGATTCTAAATAATTC
Bump_F G1	CTTAACTCGACATGGGAAACTT
Bump_R A2	TTGGCAAGAAATTCTCGAA
Bump_F A	YCCCGGAGAAATTGAATATC
Bump_R B1	GGGAGCATAACGAGTCAA
Bump_F B1	CAA AAA CTC TCT TTA GAA CCG G
SDA_R B1_BsoBI	GGATTCCGCTCCAGACTTCTCGGGTGGGAGCATAACGAGTCAA
SDA_F B1_BsoBI	ACCGCATCGAATGCATGCCTCGGGCGATTTAGGCAAGCAAACT
SDA_R A2_BsoBI	GGATTCCGCTCCAGACTTCTCGGGAATCTCAGCAATTTCYAGAG
SDA_F A2_BsoBI	ACCGCATCGAATGCATGCCTCGGGTTGACTCGTTATGCTCCC
SDA_R G1_BsoBI	GGATTCCGCTCCAGACTTCTCGGGCGGGGTGCAACATAATTAGAAT
SDA_F G1_BsoBI	ACCGCATCGAATGCATGCCTCGGGACCTGCACTCCCTGAG

3.2.9 **Strand Displacement Amplification (SDA): Results and Discussion**

SDA failed to produce amplicons of the predicted sizes after extensive method optimization experiments. Furthermore, SDA amplification routinely produced a high molecular weight nonspecific amplification product from an unknown origin. This amplification product was present in reactions that contained only nucleotides, restriction enzyme and DNA polymerase, but lacked template and SDA primer sets. He et al. [119] found similar amplification products when they were attempting to amplify a 130 bp target sequence from

lambda phage DNA. However, in this study, the correct amplification product was also obtained [119]. It was suggested that the band could be due to contamination involved in enzyme production, and could be reduced by decreasing restriction enzyme concentration and Mg^{2+} concentration.

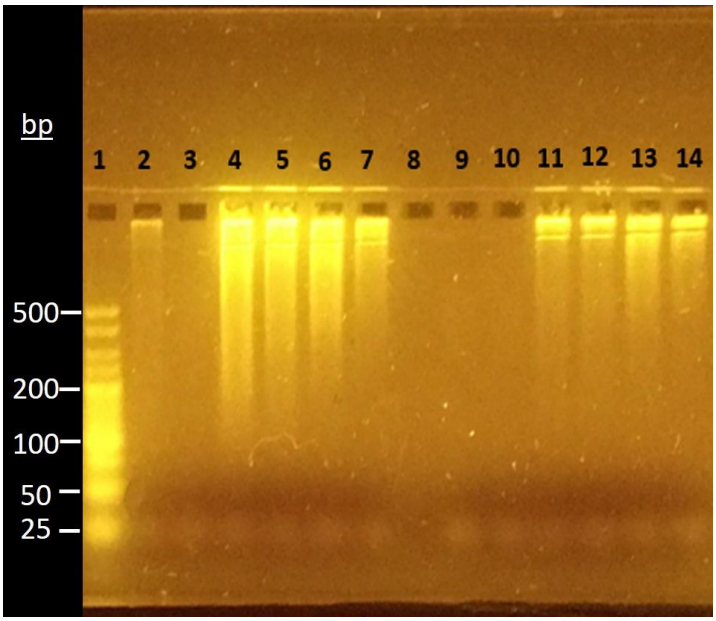

Figure 23: Agarose gel electrophoresis of Gradient SDA (55, 65, and 70 °C) reactions using B set primers, with and without template. Lane 1: ladder. Lanes 2, 3: 55 °C without template. Lanes 4, 5: 65 °C without template. Lanes 6, 7: 70 °C without template. Lane 8: empty. Lanes 9, 10: 55 °C with template. Lanes 11, 12: 65 °C with template. Lanes: 13, 14: 70 °C with template.

In attempt to optimize reaction conditions, B1 and B2 primer concentrations were adjusted between 0.05 µM and 0.5 µM, Nt.BspQI concentration was adjusted between 0.04 units/µL and 0.08 units/µL and buffer concentrations were altered to reduce salt concentration. However, the reaction conditions were not able to be optimized such that predicted length amplicon could be obtained. In order to determine the cause of the amplification, several controls were run. The reaction was run with and without template at varying temperatures (Figures 23). High molecular weight amplification occurred in all of these conditions when the temperature was above 55 °C. Additionally, SDA was run with reactions without template and without

primers. These reactions also produce high molecular weight bands at temperatures above 55 ºC (data not shown). If further experimentation were to be performed, Bst 2.0 warm start concentration could be decreased to attempt to decrease non-specific amplification. Alternatively, a different strand displacing polymerase could be investigated.

3.2.10 Hybridization Schemes Using Colorimetric Detection: Theoretical Operation

A variety of hybridization schemes to capture target molecule and produce either direct or indirect colorimetric signal were attempted. Colorimetric signal was produced from an enzyme linked reporter probe acting on a substrate. In all hybridization schemes presented, the enzyme used was horseradish peroxidase (HRP) and the substrate used was 3, 3, 5, 5´-tetramethylbenzidine (TMB). Extensive shelf-life testing was performed on this enzyme/substrate pair. All reaction scheme possibilities listed in Table 11 can be performed using competitive or non-competitive hybridization reaction mechanisms. Non-competitive methods are performed using sandwich hybridization, giving a signal that is directly proportional to the concentration of the target analyte. Competitive methods rely on competition of sample target molecule and pre-enzyme bound purified target molecule for binding sites, with a signal that is inversely proportional to the concentration of the target analyte.

Table 11: Hybridization reaction schemes.

Scheme	Linking Method/ Attachment Surface	Capture Molecule Type	Reporter Probe
1.Media packed column	**a**.Streptavidin linked sepharose beads	**i**.Biotin linked *mcy*E probe	HRP linked *mcy*E probe
		ii.Biotin linked microcystin aptamer	HRP linked microcystin aptamer
	b.Streptavidin linked silica beads	**iii**.Biotin linked *mcy*E probe	HRP linked *mcy*E probe
		iv.Biotin linked microcystin aptamer	HRP linked microcystin aptamer
2.Glass capillary tube	**a**. Microcystin silanized on glass	**i**.MC-LR	HRP linked microcystin aptamer or Adda-specific antibody
	b. Oligonucleotide silanized on glass	**ii**.Amine linked *mcy*E probe	HRP linked *mcy*E probe
		i**ii**.Amine linked microcystin aptamer	HRP lined microcystin aptamer

3.2.11 Hybridization Schemes Using Colorimetric Detection: Materials and Methods

McyE probes and microcystin aptamers. Probes targeting *mcy*E were either biotin linked or amine linked depending on which hybridization scheme was being used. Microcystin aptamers were synthesized based on previously published [51], [50] microcystin aptamer sequences (Table 13) with both amine linked groups and biotin linked groups. Several aptamer sequences were tested because the exact binding sites between aptamer and microcystin is unknown. Sequences for *mcy*E probes and aptamers are listed in Tables 12 and 13, respectively. Six carbon spacer Amine label is denoted by /5AMMC6 and biotin label is denoted by /5BiosG. All oligonucleotides were synthesized by IDT. Amine labeled oligonucleotides were purified using standard desalting while biotin labeled oligonucleotides were HPLC purified.

Table 12: *Mcy*E probe sequences.

Name	Sequence (5' to 3')
***mcy*ECompAmine**	/5AmMC6/CGCATGTTACCCTCGTATTGCTCAGTCATGCG
***mcy*E_captDirect**	/5AmMC6/TTCAATTTCTCCGGGATCAATTCGATAACCATTGACCTTAACTTGATTATCTTTTCGTCCCATAAACTCAATGATAC
***mcy*E_captComp**	/5AmMC6/GTTTGATTATTCACTTGAACGGGTAAAACAATCGCTCTTTCAATGGGAGCATAACGAGTCAATTGATATTCAATTTCTCCGGG

Table 13: Microcystin DNA aptamers [51]**,** [50]**.**

Name	Sequence (5' to 3')
MC17-Amine	/5AmMC6/TTTTTGGGTCGAAAGTGGAGGGATACAGAGGAGGGGTTCGGCCCAGGCATGTCTTG [51]
MC17-Biotin	/5BiosG/TTTTTGGGTCGAAAGTGGAGGGATACAGAGGAGGGGTTCGGCCCAGGCATGTCTTG [51]
MC25-Amine	/5AmMC6/TTTTTGGGTCCCGGGGTAGGGATGGGAGGTATGGAGGGGTCCTTGTTTCCCTCTTG [51]
MC25-Biotin	/5BiosG/TTTTTGGGTCCCGGGGTAGGGATGGGAGGTATGGAGGGGTCCTTGTTTCCCTCTTG [51]
AN6-Amine	/5AmMC6/GGCGCCAAACAGGACCACCATGACAATTACCCATACCACCTCATTATGCCCCATCTCCGC [50]
AN6-Biotin	/5BiosG/GGCGCCAAACAGGACCACCATGACAATTACCCATACCACCTCATTATGCCCCATCTCCGC [50]
RC22-Amine	/5AmMC6/CGCCAATCTCAAAGCCCGCCACCTGCCCCTCACTGCCCACCTGTGGAATCCATGTCGCTC [50]
RC22-BIO	/5BiosG/CGCCAATCTCAAAGCCCGCCACCTGCCCCTCACTGCCCACCTGTGGAATCCATGTCGCTC [50]

Scheme 1 methods. Streptavidin linked sepharose beads (GE Healthcare Streptavidin Sepharose High Performance, Sweden) and 0.5 µm diameter streptavidin coated silica microspheres, (Bangs Laboratories, USA). Biotin labeled oligonucleotide probes or aptamers were linked to beads according to the manufacturer's instructions. Once linked, a column was constructed to contain the beads using a 0.5 inch section of (1 mm ID) PFA tubing (Dupont, USA), with a 0.2 µm frit-in-feral (IDEX Health and Science, USA) placed on either end of the tubing to enable the column to be fitted to the fluidic control apparatus.

Scheme 2 methods. Glass capillary tubes (Corning PYREX® melting point tubes) used for solid support had overall dimensions of 1 mm inner diameter and 100 mm length. Three different capture molecules were silanized to the inside surface of the capillary tubes. Silanization of amine-linked aptamer and amine-linked probe was carried out according to protocol detailed by Guo et al. [120]. Guo et al. used pre-cleaned glass, so in this procedure glass capillary tubes were cleaned according to protocol listed by Wei et al. [121]. MC-LR was silanized onto the inside of the glass capillary tubes by the method detailed by Herranz et al. [77]. The only modification to these protocols was that glass capillary tubes were used in place of pre-cleaned microscope slides. Once silanized, the capillary column was fitted to the fluidic control apparatus.

Fluidic connections and control. Columns from both scheme 1 and scheme 2 were fitted to the pumping apparatus using compression fittings and a low pressure union (IDEX Health and Science, USA). A male to barb threaded fitting and Flexelene 135C FLXC1-2 tubing (Eldon James, USA) was then used to connect this capillary column assembly to a SP200 model peristaltic pump (APT Instruments, USA) in order to pull fluid through the column. Control of the pump was achieved using an Arduino Mega (Arduino, Italy) microcontroller, and a custom interface shield. The shield contained an H-bridge and 24 VDC power supply that interfaced the 5 VDC logic of the microcontroller with the 24 VDC power requirements of the pump and enabled the pump to perform forward and reverse fluid flow. Software controlling forward and reverse movements of the pump was written in C in the Arduino Integrated Development Environment.

Hybridization protocol for Scheme1/Scheme2. Following connection to the pump, hybridization was performed by first blocking the attachment surfaces with several variations of

blocking buffer (Appendix A) to prevent non-specific binding. Once blocked, target molecule was added to attachment surfaces and allowed to incubate for times ranging from 30-120 minutes. Solutions were then rinsed with high stringency and low stringency wash solutions before adding enzyme-linked reporter probe/antibody (Appendix A). The reporter probes/antibodies were allowed to incubate for times ranging from 30-120 minutes. Solutions were again rinsed with high stringency and low stringency wash solutions before addition of substrate. Substrate was added and allowed to incubate for 20 minutes on column/capillary tube. At 20 minutes, the solution was removed from the column/capillary tube and absorbance measured at 650 nm using a microplate reader (BioTek Synergy H4 Hybrid Reader).
More involved methods for hybridization and regeneration were attempted for glass capillary tubes. During the hybridization step, the tube was heated to 42 °C to aid in probe binding. For probe regeneration, the column was heated to 92 °C for two minutes and flushed with wash buffer. A high salt solution, 2M NaCl was also tested for column regeneration.

Enzyme/substrate shelf life. HRP was suspended in commercially available storage buffer StabilZyme ® (Surmodics, USA). One portion was kept at 4 °C and another portion was stored in the dark at room temperature. Every 3-5 days for a period of 55 days, 1 µL of 0.1, 1, and 10 µg/L room temperature HRP and 1 µL of 4C HRP were each incubated with 100 µL of TMB for 20 minutes. Absorbance of the reactions was then measured at 650 nm using a microplate reader (BioTek Synergy H4 Hybrid Reader).

3.2.12 Hybridization Schemes Using Colorimetric Detection: Results

After extensive testing with all combinations of blocking buffers listed in Appendix A, blocking buffer strength for oligonucleotide experiments was unable to be optimized. Low stringency blocking buffers resulted in non-specific probe binding and high stringency buffers

resulted in no probe binding. However, an experiment binding HRP linked adda-specific antibody to MC-LR silanized glass capillary tube (Scheme 2.a) did yield a positive result. Following a 20 minute incubation with substrate TMB the solution had an absorbance at 650 nm reading of 0.44 AU units compared to the negative control at 0.067 AU. This suggests that the issue was most likely due to insufficient blocking conditions, not with the silanization attachment chemistries used.

Enzyme shelf life experiments showed that HRP enzyme and TMB substrate were active at ambient temperature for the duration of the experiment, to 55 days. Room temperature HRP solutions at concentrations of 0.1 µg/L, 1 µg/L, and 10 µg/L had consistent optical densities (at 650 nm, after 20 minute incubation) at roughly 0.4, 0.6, and 2.2 relative absorption units, respectively. The 10 µg/L HRP solution stored at 4 °C also had consistent optical density (at 650 nm, after 20 minute incubation) readings at roughly 2.2 relative absorption units (Figure 24). This suggests that this system would be sufficient for use on-board an automated *in situ* instrument. However additional laboratory work is required to find the optimal blocking, hybridization and washing conditions for each assay.

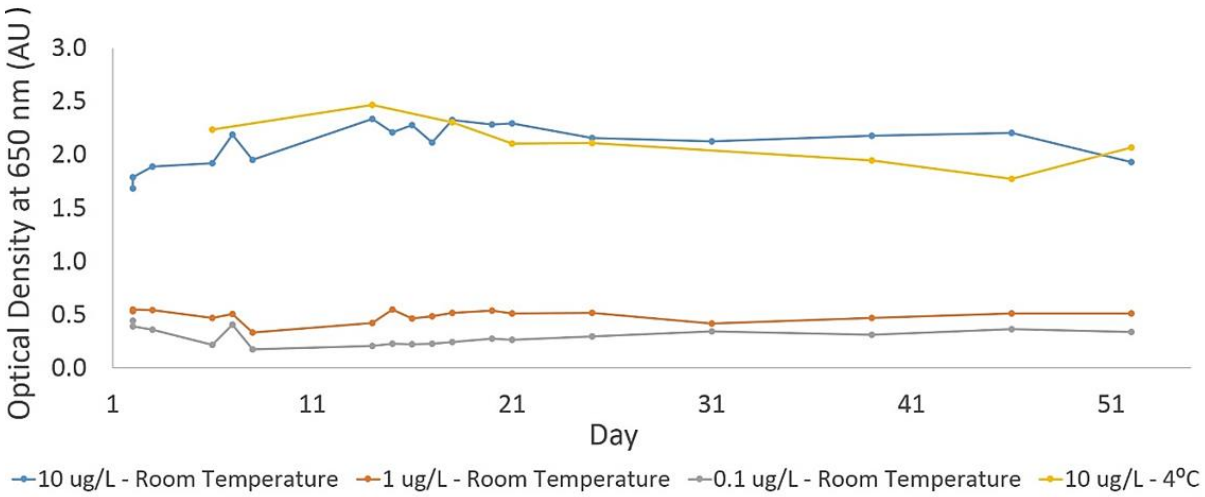

Figure 24: Shelf life experiment for HRP enzyme and TMB substrate at varying concentrations and temperatures. Optical densities were measured at 650 nm following a 20 minute incubation.

3.2.13 Nicking Enzyme Assisted Fluorescence Signal Amplification (NEFSA): Theoretical Operation

NEFSA is a detection technique that is composed of 3 main reaction components, a DNA aptamer with a hairpin (HP) structure, a quenched fluorescent probe, and a nicking restriction enzyme [122] (Figure 25). In the presence of its specific target, the DNA aptamer undergoes a conformational change that exposes a probe binding site. Following hybridization of the probe to this site, a nicking enzyme is able to cleave at a site internal to the BQP probe, resulting in disassociation of the two probe fragments. This causes the fluorophore to be separated from the quencher, resulting in an increase in fluorescence signal [122]. This detection strategy has particular utility for *in situ* sensor applications as it has the potential to detect both nucleic acid and toxin targets. Xue et al. [122] developed this technique for use on the protein thrombin, but similar methods have been used to detect DNA targets [123]. Additionally, this method represents

a signal technique that does not rely amplification of the target molecule. This property has the potential to reduce carry over contamination that could cause cross sample false positives.

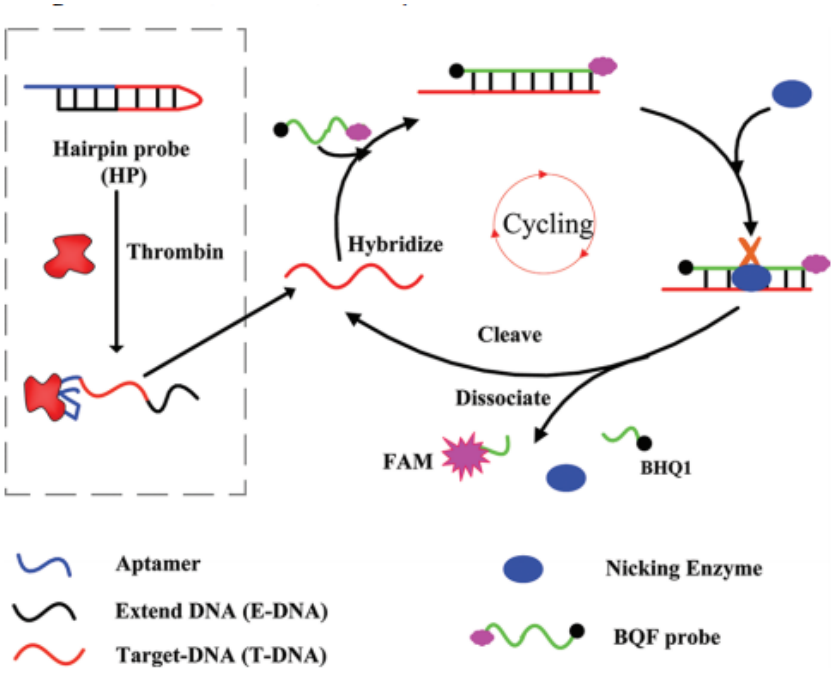

Figure 25: **Nicking Enzyme Assisted Fluorescence Signal Amplification (NEFSA) requires target protein (or nucleic acid), DNA hairpin probe, BQF fluorescent probe with quencher, and nicking enzyme.** When the target molecule and hairpin probe are combined, the hairpin unfolds, causing the hybridization site on the hairpin to be exposed. The BQF probe has identity to this hybridization site. It is also designed with a restriction site for the nicking enzyme so that once bound, the nicking enzyme will cleave between the fluorophore and the quencher. When the probe is cleaved and the two segments are displaced, a fluorescent signal is generated and the process can repeat itself. This cycling leads to an increase in fluorescence over time. Reprinted with permission from Xue, Liyun; Zhou, Xiaoming; Xing, Da. "Sensitive and Homogeneous Protein Detection Based on Target-Triggered Aptamer Hairpin Switch and Nicking Enzyme Assisted Fluorescence Signal Amplification." Analytical Chemistry (2012). Copyright (2012) American Chemical Society.

3.2.14 Nicking Enzyme Assisted Fluorescence Signal Amplification (NEFSA): Materials and Methods

Reaction conditions. Reagent master mix was made at the following final concentrations: 10X reaction buffer (1X), nicking enzyme (0.5 mM), probe (3 µM), HP aptamer or HP *mcyE* probe (0.1 µM) with a 25 µL total reaction volume. For reactions targeting DNA targets, single stranded DNA template with identity to *mcyE* gene from *Microcystis spp.* (Genbank accession HM854746.1) was added at varying concentrations: 10,000, 1000 and 100 copies. For reactions targeting microcystin, the toxin was added at 1,000, 100, and 10 µg/L. Reactions were incubated in a DNA Engine Opticon (MJ research, USA) continuous fluorescence detector at 37 °C for one hour with an optical read taken at 1 minute intervals.

Probe design. Three probes targeting s small section of the *mcyE* gene from *Microcystis spp.* (Genbank accession HM854746.1) were designed with varying secondary structure stringency. Three reporter probes were also designed with various secondary structure configurations ranging from linear probes with minimal secondary structure to molecular beacon type configurations with traditional stem loop structures. Aptamer probes were designed based on microcystin aptamers listed in the literature [50]. Hairpin, reporter, and aptamer probes are listed in Table 14.

Table 14: NEFSA *mcy*E hairpin, reporter, and aptamer probes.

***mcy*E hairpin probes**	**Sequence (5' to 3')**
***mcy*E probe 1**	GGGAGCATAACGAGTCAATTGATATTCAATTCTTGCTCCTCAGC AAGAATTGAATATCAA
***mcy*E probe 2**	GGGAGCATAACGAGTCAATTGATATTCAATTCTTGCTCCTCAGC AAGAATTGAATAT
***mcy*E probe 3**	GGGAGCATAACGAGTCAATTGATATTCAATTCTTGCACCTCAGC AAGAATTGAATAT
nickAmp_Probe	/56-FAM/TTCTTGCTGAGGAGC/3BHQ_1/
***mcy*E Nick Beacon 1**	/56-FAM/GCTCCAATTCTTGCTGAGGAGC/3IABkFQ/
***mcy*E Nick Beacon 2**	/56-FAM/TGCTGAGGA/ZEN/GCAACAGCA/3IABkFQ/
nickAmp_AptRC6	CACGCAACAACACAACATGCCCAGCGCCTGGAACATATCCTATG AGTTAGTCCGCCCACACTTGCTCCTCAGCAAGTGTGGGCGG
nickAmp_AptMC17	TTTTTGGGTCGAAAGTGGAGGGATACAGAGGAGGGGTTCGGCC CAGGCATGTCTTGTTGCTCCTCAGCAACAAGACAT

3.2.15 Nicking Enzyme Assisted Fluorescence Signal Amplification (NEFSA): Results

NEFSA standard curve reactions (Figure 26) showed signal amplification in both template and non-template reactions, with no discrimination between high and low template concentrations. There are several possibilities for the cause of the non-specific amplification. Firstly, the BQF probe is forming a secondary structure that folds on itself enabling the nicking enzyme to cut and separate the fluorophore from the quencher. Secondly, the nicking enzyme is able to cut single stranded BQF probe in its native unbound configuration. Finally, the hairpin probe is able to unfold in reaction mixture without the presence of target enabling the BQF probe to binding to the hairpin, and the nicking enzyme acts upon the double stranded structure. These possibilities suggest that an alternate nicking enzyme and more stringent probe design for the hairpin and BQF probe should be investigated. After resolving the non-specific amplification, further experimentation is required to determine shelf life and storage conditions of probes and enzyme at ambient temperature to evaluate suitability for automation.

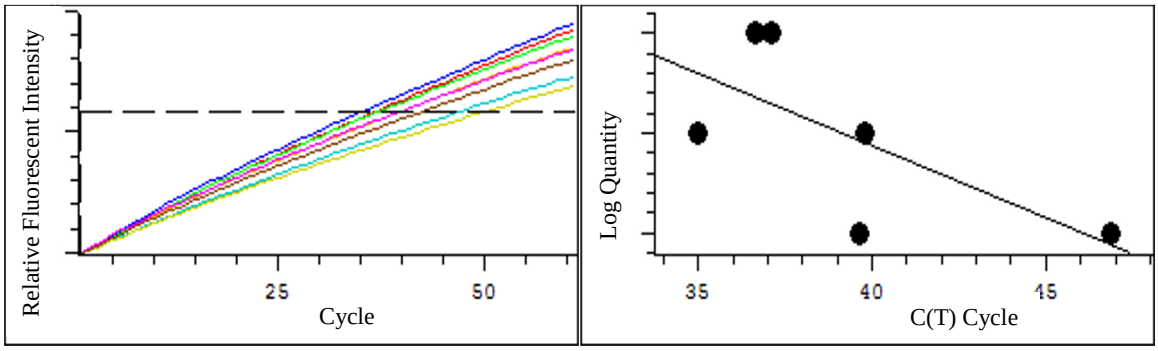

Figure 26: NEFSA standard curve showing no response to change in concentration. A) All concentrations (10^4, 10^3, $10^{2,}$ and 0 copies). B) Standard curve of concentrations vs. C(t), showing no discrimination between high and low template concentrations.

3.3 Conclusion

NEFSA and CANA both have potential to be used for detection of microcystin and its biosynthesis genes, but have shown inconclusive preliminary results. Both techniques are isothermal, which greatly reduces the power needs of the automated instrument. Both methods use a signal transduction methodology for detection rather than amplification of the of their target molecules, potentially decreasing for crossover contamination and simplifying cleaning protocols in an automated instrument. NEFSA requires an enzyme to generate the fluorescent signal, while CANA is an enzyme free method that relies only on the interaction of three probes to generate a detectable signal, making it potentially even more attractive for long term use in an automated instrument that operates at ambient environmental temperatures as it could simplify reagent storage considerations. Investigation of probe design and stringency for both methods, and enzyme type for NEFSA, is required to evaluate the sensitivity of the methods. If the specificity and sensitivity can be optimized, further experimentation on shelf life and storage conditions at ambient temperature will be needed to determine their viability for use in an

automated *in situ* detection instrument to aid in making critical public health decisions about potable and recreational water usage.

4 References

[1] L. V. D'Anglada and J. Strong, "Drinking Water Health Advisory for the Cyanobacterial Microcystin Toxins," Washington DC, 2015.

[2] L. V. D'Anglada, J. M. Donohue and J. Strong, "Health Effects Support Document for the Cyanobacterial Toxin Microcystins," U.S. Environmental Protection Agency, Washington D.C., 2015.

[3] "HAB-related toxin detection in Lake Erie with an Environmental Sample Processor," Great Lakes Environmental Research Laboratory, [Online]. Available: https://www.glerl.noaa.gov//res/HABs_and_Hypoxia/esp.html. [Accessed 22 December 2016].

[4] C. Scholin, G. Doucette, S. Jensen, B. Roman, D. Pargett, R. Marin, C. Preston, W. Jones, J. Feldman, C. Everlove, A. Harris, N. Alvarado, E. Massion, J. Birch, D. Greenfield, R. Vrijenhoek, C. Mikulski and K. Jones, "Remote detection of marine microbes, small invertebrates, harmful algae, and biotoxins using the environmental sample processor (ESP)," *Oceanography,* vol. 22, no. 2, pp. 158-168, 2009.

[5] R. Haselkorn, "Cyanobactera," *Current Biology,* vol. 19, no. 7, pp. R277-R278, 2009.

[6] H. W. Paerl and V. J. Paul, "Climate change: Links to global expansion of harmful cyanobacteria," *Water Research,* vol. 46, no. 5, pp. 1349-1363, 2012.

[7] H. Paerl and T. Otten, "Harmful Cyanobacterial Blooms: Causes, Consequences, and Controls," *Microbial Ecology,* vol. 65, no. 4, pp. 995-1010, 2013.

[8] W. Dodds, W. Bouska, J. Eitzmann, T. Pilger, K. Pitts, A. Riley, J. Schloesser and D. Thornbrugh, "Eutrophication of U.S. Freshwaters:Analysis of Potenital Economic Damages," *Environmental Science and Technology,* vol. 43, no. 1, pp. 12-19, 2009.

[9] L. J. Beversdorf, "Spatial and temporal variation in cyanobacterial population dynamics and microcystin production in eutrophic lakes," *University of Wisconsin-Madison,* vol. 3594892, p. 164 pages, 2014.

[10] J. Graham, J. Jones and S. Jones, "Microcystin in Midwestern Lakes," *Lakeline,* pp. 32-35, 2006.

[11] S. Singh, A. Srivastava, H. M. Oh, C. Y. Ahn, G. G. Choi and R. K. Asthana, "Recent trends in development of biosensors for detection of microcystin," *Toxicon,* vol. 60, no. 5, pp. 878-894, October 2012.

[12] T. Msagati, B. Siame and D. Shushu, "Evaluation of methods for the isolation, detectionn, and quantification of cyanobacterial hepatotoxins," *Aquatic Toxicology,* vol. 78, no. 4, pp. 382-397, 2006.

[13] B. Neilan, E. Dittman, L. Rouhianen, R. Bass, V. Schaub, K. Sivonen and T. Borner, "Nonribosomal Peptide Synthesis and Toxigenicity of Cyanobacteria.," *Journal of Bacteriology,* vol. 181, no. 13, pp. 4089-4097, 1999.

[14] T. Noguchi, A. Shinohara, A. Nishizawa, M. Asayama, T. Nakano, M. Haseqawa, K. Harada, T. Nishiawa and M. Shirai, "Genetic analysis of the microcystin biosynthesis gene cluster in microcystis strains from four bodies of eutrophic water in Japan," *The Journal of General and Applied Microbiology,* vol. 55, no. 2, pp. 111-123, 2009.

[15] R. Kurmayer and G. Christiansen, "The Genetic Basis of Toxin Production in Cyanobacteria," *Freshwater Reviews,* vol. 2, no. 1, pp. 31-50, 2009.

[16] L. Beversdorf, S. Chaston, T. Miller and K. McMahon, "Microcystin mcyA and mcyE Gene Abundances Are Not Appropriate Indicators if Microcystin Concentrations in Lakes," *PLoS ONE,* vol. 10, no. 5, 2015.

[17] S. Wood, A. Ruekert, D. Hamilton, C. Cary and D. Ditrich, "Switching toxin production on and off: intermittent microcystin synthesis in a Microcystis bloom," *Environmental Microbiology Reports,* vol. 3, no. 1, pp. 118-124, 2011.

[18] R. Rastogi, R. Sinha and A. Incharoensakdi, "The cyanotoxin-microcystins: current overview," *Reviews in Environmental Science and Biotechnology,* vol. 13, no. 2, pp. 215-249, 2014.

[19] R. Bouhaddada, S. Nelieu, H. Nasri, G. Delarue and N. Bouaicha, "High diversity of microcystins in a Microcystis bloom from an Algerian lake," *Environmental Pollution,* vol. 216, pp. 836-844, 2016.

[20] P. Vesterkvist, J. Misiorek, L. Spoof, D. Toivola and J. Meriluoto, "Comparative Cellular Toxicity of Hydrophilic and Hydrophobic Microcystins on Caco-2 Cells," *Toxins,* vol. 4, no. 11, pp. 1008-1023, 2012.

[21] A. Perez-Morales, S. Sarma and S. Nandini, "Microcystins production in Microcystis induced by Daphnia pules (Cladocera) and Brachionus calyciflorus (Rotifera)," *Hidrobiologica,* vol. 25, no. 3, pp. 411-415, 2015.

[22] W. Fischer, S. Altheimer, V. Cattori, P. Meier, D. Dietrich and B. Hagenbuch, "Organic anion transporting polypeptides expressed in liver and brain mediate uptake of microcystin," *Toxicology and Applied Pharmacology,* vol. 203, no. 3, pp. 257-263, 2004.

[23] J. Rapala, K. Sivonen, C. Lyra and S. Niemela, "Variation of microcystins, cyanobacterial hepatotoxins, in Anabaena spp. as a function of growth stimuli.," *Applied and Environmental Microbiology,* vol. 63, no. 6, p. 2206–2212, 1997.

[24] A. Campos and V. Vasconcelos, "Molecular Mechanisms of Microcystin Toxicity in Animal Cells," *International Journal of Molecular Sciences,* vol. 11, no. 1, pp. 268-287, 2010.

[25] X. Xu, R. Yu, L. P. Wang, S. Wu and Q. Song, "Sensitive determination of total microcystins with GC-MS method by using methylchloroformate as a derivatizing reagent," *Analytical Methods,* vol. 5, no. 7, pp. 1799-1805, 2012.

[26] P. Lakshamana, N. Gupta and R. Jayaraj, "Screening of certain chemoprotectants against cyclic peptide toxin microcystin-LR," *Indian Journal of Pharmacology,* vol. 36, no. 2, pp. 87-92, 2004.

[27] World Health Organization, "Cyanobacterial toxins: Microcystin-LR in Drinking Water," Guidelines for drinking-water quality, Geneva, 1998.

[28] EPA Office of Water, "2015 Drinking Water Health Advisories for Two Cyanobacterial Toxins," United States Environmental Protection Agency, 2015.

[29] United States Environmental Protection Agency, "Fact Sheet: Draft Human Health Recreational Ambient Water Quality Criteria/Swimming Advisories for Microcystins and Cylindrospermopsin," Office of Water, 2016.

[30] J. Shoemaker, D. Tettenhorst and A. de la Cruz, "method 544: Determination of microcystins and nodularin in drinking water by solid phase extraction and liquid chromatography/tandem mass spectrometry," US Environmental Protection Agency, Cincinnati, 2015.

[31] Supelco, "Bulletin 910: Guide to Solid Phase Extraction," Sigma-Aldrich, 1998.

[32] K. Mehta, N. Evitt and J. Swartz, "Chemical lysis of cyanobacteria," *Journal of Biological Engineering,* vol. 9, no. 10, pp. 1-8, 2015.

[33] M. Agrwal, S. Yadav, C. Patel, N. Raipuria and M. Agrawal, "Bioassay methods to identify the presence of cyanotoxins in drinking water supplies and their removal strategies," *European Journal of Experimental Biology,* vol. 2, no. 2, pp. 321-336, 2012.

[34] C. MacKintosh, K. Beattie, S. Klumpp, P. Cohen and G. and Codd, "Cyanobacterial Microcystin-LR Is a Potent and Specific Inhibitor of Protein Phosphatases 1 and 2A From Both Mammals and Higher Plants," *FEBS letters,* vol. 264, no. 2, pp. 187-192, 1990.

[35] W. Carmichael and J. An, "Using Enzyme Linked Immunosorbent Assay (ELISA) and a Protin Phospatase Inhibition Assay (PPIA) for the Detection of Microystins and Nodularins," *Natural Toxins,* vol. 7, no. 6, pp. 377-385, 1999.

[36] R. Kaushik and R. Balasubramanian, "Methods and approaches used for detection of cyanotoxins in Environmental Samples: a review," *Critical Reviews in Environmental Science and Technology,* vol. 43, no. 13, pp. 1349-1383, 2013.

[37] S. Herranz, M. Marazuela and M. Moreno-Bondi, "Automated portable array biosensor for multisample microcystin analysis in freshwater samples," *Biosensors and Bioelectronics,* vol. 33, no. 1, pp. 50-55, 2012.

[38] H. C. Shi, B. D. Song, F. Long, X. H. Zhou, M. He, Q. Lv and H. Y. Yang, "Automated Online Optical Biosensing System for Continuous Real-Time Determination of Microcystin-LR with High Sensitivity andSpecificity: Early Warning for Cyanotoxin Risk in Drinking Water Sources," *Environmental Science and Technology,* vol. 47, no. 9, pp. 4431-4441, 2013.

[39] K. I. Harada, H. Murata, Z. Qiang, M. Suzuki and F. Kondo, "Mass spectrometric screening method for microcystins in cyanobacteria," *Toxicon,* vol. 34, no. 6, pp. 701-710, 1996.

[40] R. Halvorson, W. Leng and P. Vikesland, "Differentiation of Microcystin, Nodularin, and Their Component Amino Acids by Drop-Coating Deposition Raman Spectroscopy," *Analytical Chemistry,* vol. 83, no. 24, pp. 9273-9280, 2011.

[41] X. Wu, B. Xiao, Y. Gong, Z. Wang, X. Chen and R. Li, "Kinetic study of the 2-methyl-3-methoxy-4-phenylbutanoic acid produced by oxidation of microcystin in aqueous solutions," *Environmetnal Toxicology and Chemistry,* vol. 27, no. 10, pp. 2019-2026, 2008.

[42] X. Wu, B. Xiao, R. Li, Z. Wang, X. Chen and X. Chen, "Rapid quantification of total microcystins in cyanobacterial samples by periodate-permanganate oxidation and reversed-phase liquid chromatography," *Analytica Chimica Acta,* vol. 651, no. 2, pp. 241-247, 2009.

[43] F. Momani and N. Jarrah, "Treatment and kinetic study of cyanobacterial toxin by ozone," *Journal of Environmental Science and Health Part A,* vol. 45, no. 6, pp. 719-731, 2010.

[44] T. Hayama, K. Katoh, T. Aoki, M. Itoyama, K. Todoroki, H. Yoshida, M. Yamaguchi and H. Nohta, "Liquid chromatographic determination of microcystins in water samples following pre-column excimer fluorescence derivatization with 4-(1-pyrene)butanoic acid hydrazide," *Analytica Chimica Acta,* vol. 755, pp. 93-99, 2012.

[45] M. Lee, S. Ramanathan, R. Ismail, S. Mansor, M. Ali and S. Tan, "Stability test for the enzyme immunoassay reagents of Mitragynine," *Asian Pacific Journal of Tropical Disease*, vol. 4, no. 3, p. 244, 2014.

[46] F. Long, M. He, H. Shi and A. Zhu, "Development of evanescent wave all-fiber immunosensor for environmental water analysis," *Biosens. Bioelectron.,* vol. 23, no. 7, pp. 952-958, 2008.

[47] F. Long, M. He, A. Zhu, J. Sheng and H. Shi, "Matrix effects on the microcystin-LR fluorescent immunoassay based on optical biosensor," *Sensors,* vol. 9, no. 4, pp. 3000-3010, 2009.

[48] F. Long, M. He, A. Zhu and H. Shi, "Portable optical immunosensor for highly sensitive detection of microcystin-LR in water samples," *Biosensors and Bioelectronics,* vol. 24, no. 8, pp. 2346-2351, 2009b.

[49] T. Matsunaga, M. Okochi and H. Nakayama, "Construction of an automated DNA detection system for manipulation of Microcystis spp. using spefific DNA probe immobilized on magnetic particles," *Electrochimica Acta,* vol. 44, no. 21-22, pp. 3779-3784, 1999.

[50] A. Ng, R. Chinnappan, S. Eissa, H. Liu, C. Tlili and M. Zourob, "Selection, characterization, and biosensing application of high affinity congener-specific microcystin-targeting aptamers," *Environmental Science and Technology,* vol. 46, no. 19, pp. 10697-10703, 2012.

[51] M. Famulok, "In vitro selection of specific aptamers against MC-LR," *Chin J Prev Med,* vol. 38, no. 6, 2004.

[52] C. Nakamura, T. Kobayashi, M. Miyake, M. Shirai and J. Miyake, "Usage of a DNA aptamer as a ligand targeting microcystin," *Mol. Cryst. and Liq. Cryst.,* vol. 371, no. 1, pp. 369-374, 2001.

[53] Z. Lin, H. Huang, Y. Xu, X. Gao, B. Qiu, X. Chen and G. Chen, "Determination of microcystin-LR in water by a label-free aptamer based electrochemical impedance biosensor," *Talanta,* vol. 103, pp. 371-374, 2013.

[54] V. Pichon and F. Chapuis-Hugon, "Role of molecularly imprinted polymers for selective determination of environmental pollutants—A review," *Analyltica Chimica Acta,* vol. 622, no. 1-2, pp. 48-61, 2008.

[55] M. Weller, "Immunoassays and Biosensors for the Detection of Cyanobacterial Toxins in Water," *Sensors,* vol. 13, no. 11, pp. 15085-15112, 2013.

[56] I. Chiancella, M. Lotierzo, S. Piletsky, I. Tothill, B. Chen, K. Karim and A. Turner, "Rational Design of a Polymer Specific for Microcystin-LR Using a Computational Approach," *Analytical Chemistry,* vol. 74, no. 6, pp. 1288-1293, 2002.

[57] I. Chiancella, S. Piletsky, I. Tothill, B. Chen and A. Turner, "MIP-based solid phase extraction cartridges combined with MIP-based sensors for the detection of microcystin-LR," *Biosensors and Bioelectronics,* vol. 18, no. 2-3, pp. 119-127, 2002.

[58] A. Zeck, M. Weller, D. Bursill and R. Niessner, "Generic microcystin immunoassay based on monoclonal antibodies against Adda," *Analyst,* vol. 126, no. 11, pp. 2002-2007, 2001.

[59] J. Youngblom, "Extended Stability of Taq DNA Polymerase and T4 DNA Ligase at Various Temperatures," *BioTechniques,* vol. 34, pp. 264-268, 2003.

[60] T. G. Walker, "Empirical Aspects of Strand Displacement Amplification," *PCR Methods and Applications,* vol. 3, no. 1, pp. 1-6, 1993.

[61] P. Zhu, B. F. Zhang, J. H. Wu, C. Y. Dang, Y. T. Lv, J. Z. Fan and X. J. Yan, "Sensitive and rapid detection of microcystin synthetase E Gene (mcyE) by loop-mediated isothermal amplification: A new assay for detecting the potential microcystin-producing Microcystis in the aquatic ecosystem," *Harmful Algae,* vol. 37, pp. 8-16, 2014.

[62] E. Casper, S. Patterson, P. Bhanushali, A. Farmer, M. Smith, D. Fries and J. Paul, "A handheld NASBA analyzer for the field detection and quantification of Karenia brevis," *Harmful Algae,* vol. 6, no. 1, pp. 112-118, 2007.

[63] M. Smith and D. Fries, "A Field-Able RNA Extraction and Purification Procedure," *Journal of Rapid Methods & Automation in Microbiology,* vol. 16, no. 1, pp. 13-21, 2008.

[64] J. Clark, J. Harrison, R. Mdegela and J. March, "Extended Stability of Restriction Enzymes at Ambient Temperatures," *BioTechniques,* vol. 29, no. 3, pp. 536-542, 2000.

[65] N. Vilarino, C. Louzao, M. Fraga, L. Rodriguez and L. Botana, "Innovative detection methods for aquatic algal toxins and their presence in the food chain," *Analytical and Bioanalytical Chemistry,* vol. 405, no. 24, p. 7719–7732, 2013.

[66] Y. Xia, J. Zhang and L. Jiang, "A novel dendritic surfactant for enhanced microcystin-LR detection by double amplification in a quartz crystal microbalance biosensor.," *Colloids and Surfaces B: Biointerfaces,* vol. 86, no. 1, pp. 81-86, 2011.

[67] Y. Ding and R. Mutharasan, "Highly sensitive and rapid detection of microcystin-LR in source and finished water samples using cantilever sensors," *Enironmental Science Technol,* vol. 45, no. 4, pp. 1490-1496, 2010.

[68] M. Campas and J. Marty, "Highly sensitive amperometric immunosensors for microcystin detection in algae," *Biosensors and Bioelectronics,* vol. 22, no. 6, pp. 1034-1040, 2007.

[69] S. Wang, Z. Wu, D. Xu, B. Shim, Y. Zhu, F. Sun, L. Liu, C. Peng, Z. Jin, C. Xu and N. Kotov, "Simple, rapid, sensitive, and versatile SWNT−paper sensor for environmental toxin detection competitive with ELISA," *Nano Letters,* vol. 9, no. 12, pp. 4147-4152, 2009.

[70] M. Campas, M. Olteanu and J. Marty, "Enzymatic recycling for signal amplfification: improving microcystin detection with biosnsors," *Sensors and Actuators B: Chemical,* vol. 129, no. 1, pp. 263-267, 2008.

[71] H. Yu, J. Lee, S. Kim, G. Nguyen and I. Kim, "Electrochemical immunoassay using quantum dot/antibody probe for identification of cyanobacterial hepatotoxin microcystin-LR," *Analytical and Bioanalytical Chemistry,* vol. 394, no. 8, pp. 2173-2181, 2009.

[72] J. Zhang, J. Lei, C. Xu, L. Ding and H. Ju, "Carbon nanohorn sensitized electrochemical immunosensor for rapid detection of microcystin-LR," *Analytical Chemistry,* vol. 82, no. 3, pp. 1117-1122, 2010.

[73] P. Tong, S. Tang, Y. He, Y. Shao, L. Zhang and G. Chen, "Label-free immunosensing of microcystin-LR using a gold electrode modified with gold nanoparticles," *Microchimica Acta,* vol. 173, no. 3, pp. 299-305, 2011.

[74] S. Loyprasert, P. Thavarungkul, P. Asawatrerantanajul, B. Wongkittisuksa, C. Limsakul and P. Kanatharana, "Label-free capacitive immunosensor for microcystin-LR using self-assembled thiourea monolayer incorporated with Ag nanoparticles on gold electrode," *Biosens Bioelectron,* vol. 24, no. 1, pp. 78-86, 2008.

[75] X. Sun, H. Shi, H. Wang, L. Xiao and L. Li, "A simple, highly sensitive and label-free impedimetric immunosensor for detection of microcystin-LR in drinking water," *Analytical Letters,* vol. 43, no. 4, pp. 533-544, 2010.

[76] G. Doucette, C. Mikulski, K. Jones, K. King, R. Greenfield, S. Jensen, B. Roman, C. Elliot and C. Scholin, "Remote, subsurface detection of the algal toxin domoic acid onboard the Environmental Sample Processor: Assay development and field trials," *Harmful Algae,* vol. 8, no. 6, pp. 880-888, September 2009.

[77] S. Herranz, M. Bockova, M. Marazuela, J. Homola and M. Moreno-Bondi, "An SPR biosensor for the detection of microcystins in drinking water," *Analytical and Bioanalytical Chemistry,* vol. 398, no. 6, pp. 2625-2634, 2010.

[78] Y. Xia, J. Deng and L. Jiang, "Simple and highly sensitive detection of hepatotoxins microcystin-LR via colirmetric variation based on polydiacetylne vesicles," *Sensors and Actuators B: Chemical,* vol. 145, no. 2, pp. 713-719, 2010.

[79] L. Reverte, D. Garibo, C. Flores, J. Diogene, J. Caixach and M. Campas, "Magnetic Particle-Based Enzyme Assays and Immunoassays for Microcystins: From Colorimetric to Electrochemical Detection.," *Environmental Science and Technology,* vol. 47, no. 1, pp. 471-478, 2012.

[80] W. Ma, W. Chen, R. Qjao, C. Liu, C. Yang, Z. Li, D. Su, C. Peng, Z. Jin, C. Xu, S. Zhu and L. Wang, "Rapid and sensitive detection of microcystin by immunosensor based on nuclear magnetic resonance.," *Biosensors and Bioelectronics,* vol. 25, no. 1, pp. 240-243, 2009.

[81] F. Yan, A. Erdem, B. Meric, K. Kerman, M. Ozsoz and O. Sadik, "Electrochemical DNA biosensor for the detectino of specific gene related to Microcystis species," *Electrochemistry Communications,* vol. 3, no. 5, p. 224–228, 2001.

[82] M. Campas, D. Szydlowska, M. Trojanowicz and J. Marty, "Towards the protein phosphatase-based biosensor for microcystin detection," *Biosensors and Bioelectroncs,* vol. 20, no. 8, pp. 1520-1530, 2005.

[83] O. Sadik and F. Yan, "Novel fluorescent biosensor for pathogenic toxins using cyclic polypeptide conjugates," *Chemical Communications,* vol. 35, no. 9, pp. 1136-1137, 2004.

[84] M. Campas, D. Szydlowska, M. Trojanowicz and J. Marty, "Enzyme inhibition-based biosensor for the electrochemical detection of microcystins in natural blooms of cyanobacteria," *Talanta,* vol. 72, no. 1, pp. 179-186, 2007.

[85] P. Tong, Y. Shao, J. Chen, Y. He and L. Zhang, "A sensitive electrochemical DNA biosensor for Microcystis spp. sequence detection based on an Ag@Au NP composite film," *Analytical Methods,* vol. 7, no. 7, pp. 2993-2999 , 2015.

[86] C. Sengiz, G. Congur and A. Erdem, "Development of Ionic Liquid Modified Disposable Graphite Electrodes for Label-Free Electrochemical Detection of DNA Hybridization Related to Microcystis spp.," *Sensors,* vol. 15, no. 9, pp. 22737-22749, 2015.

[87] H. Changseok, A. Doepke, W. Cho, V. Likodimos, A. Cruz, T. Back, W. Heineman, B. Halsall, V. Shanov, M. Schulz, P. Falaras and D. Dionysiou, "A Multiwalled-Carbon-Nanotube-Based Biosensor for Monitoring Microcystin-LR in Sources of Drinking Water Supplies," *Advanced Functional Materials,* vol. 23, no. 14, p. 1807–1816, 2013.

[88] H. L. Du, X. W. Fu, Y. P. Wen, Z. J. Qiu, L. M. Xiong, N. Hong and Y. H. Yang, "A Label-free Immunosensor for Microcystins-LR Based on Graphene and Gold Nanocage," *Chinese Journal of Analytical Chemistry,* vol. 42, no. 5, pp. 660-665, 2014.

[89] L. Hou, Y. Ding, L. Zhang, Y. Guo, M. Li, Z. Chen and X. Wu, "An ultrasensitive competitive immunosensor for impedimetric detection of microcystin-LR via antibody-

conjugated enzymatic biocatalytic precipitation," *Sensors and Actuators B: Chemical,* vol. 233, no. 5, pp. 63-70, 2016.

[90] J. Zhang, H. Sun, X. Zhang, W. Wang and Z. Chen, "An electrochemical non-enzymatic immunosensor for ultrasensitive detection of microcystin-LR using carbon nanofibers as the matrix," *Sensors and Actuators B: Chemical,* vol. 233, no. 5, pp. 624-632, 2016.

[91] H. He, L. Zhou, Y. Wang, C. Li, J. Yao, W. Zhang, Q. Zhang , M. Li, H. Li and W.-f. Dong, "Detection of trace microcystin-LR on a 20 MHz QCM sensor coated with in situ self-assembled MIPs," *Talanta,* vol. 131, pp. 8-13, 2015.

[92] L. Lebogang, B. Mattiasson and M. Hedstrom, "Capacitive sensing of microcystin variants of Microcystis aeruginosa using a gold immunoelectrode modified with antibodies, gold nanoparticles and polytyramine," *Microchimica Acta,* vol. 181, no. 9, pp. 1009-1017, 2014.

[93] L. Liu, C. Xing, H. Yan, H. Kuang and C. Xu, "Development of an ELISA and immunochromatographic strip for highly sensitive detection of microcystin-LR," *Sensors,* vol. 14, no. 8, pp. 14672-14685, 2014.

[94] J. Tian, H. Zhao, X. Quan, Y. Zhang, H. Yu and S. Chen, "Fabrication of graphene quantum dots/silicon nanowires nanohybrids for photoelectrochemical detection of microcystin-LR," *Sensors and Actuators B: Chemical,* vol. 196, p. 532–538, 2014.

[95] J. Briscoe, S.-Y. Cho and I. Brener, "Part-Per-Trillion Detection of Microcystin-LR Using a Periodic Nanostructure," *IEEE Sensors Journal,* vol. 15, no. 3, pp. 1366 - 1371, 2015.

[96] A. Neumann, X. Wang, R. Niessner and D. Knopp, "Determination of microcystin-LR in surface water by a magnetic bead-based colorimetric mmunoassay using antibody-conjugated gold nanoparticles," *Analytical Methods,* vol. 8, pp. 57-63, 2016.

[97] F. Tan, N. M. Saucedo, P. Ramnani and A. Mulchandani, "Label-free electrical immunosensor for highly sensitive and specific detection of microcystin-LR in water samples," *Environmental Science and Technology,* vol. 49, no. 15, pp. 9256-9263, 2015.

[98] S. Eissa, A. Ng, M. Siajs and M. Zourob, "Label-Free Voltammetric Aptasensor for the Sensitive Detection of Microcystin-LR Using Graphene-Modified Electrodes," *Analytical Chemistry,* vol. 86, no. 15, pp. 7551-7557, 2014.

[99] F. Wang, S. Liu, M. Lin, X. Chen, S. Lin, X. Du, H. Li, H. Ye, B. Qiu, Z. Lin, L. Guo and G. Chen, "Colorimetric detection of microcystin-LR based on disassembly of orient-aggregated gold nanoparticle dimers," *Biosensors and Bioelectronics,* vol. 68, pp. 475-480, 2015.

[100] J. Lv, S. Zhao, S. Wu and Z. Wang, "Upconversion nanoparticles grafted molybdenum disulfide nanosheets platform for microcystin-LR sensing," *Biosensors and Bioelectronics*, vol. 90, pp. 203-209, 2016.

[101] S. Wu, Q. Li, N. Duan, H. Ma and Z. Wang, "DNA aptamer selection and aptamer-based fluorometric displacement assay for the hepatotoxin microcystin-RR," *Microchimica Acta*, vol. 183, no. 9, pp. 2555-2562, 2016.

[102] S. M. Tripathi, W. J. Bock, P. Mikulic and G. Mishra, "Rapid and accurate detection of Cyanobacterial toxin microcystin-LR using fiber-optic long-period grating based immunosensor," *ArXiv e-prints*, no. 1409.4931, pp. 1-12, 2014.

[103] W. Chen, L. Li, N. Gan and L. Song, "Optimization of an effective extraction procedure for the analysis of microcystins in soils and lake sediments," *Environmental Pollution*, vol. 143, no. 2, pp. 241-24, 2006.

[104] M. Barco, L. Lawton, J. Rivera and J. Caixach, "Optimiazation of intracellular microcystin extraction for their subsequent analysis by high-performance liquid chromatography," *Journal of Chromatography*, vol. 1074, no. 1-2, pp. 23-30, 2005.

[105] F. Chu, X. Huang and R. Wei, "Enzyme-linked immunosorbent assay for microcystins in blue-green algal blooms.," *Journal Association of Official Analytical Chemists*, vol. 73, no. 3, pp. 451-456, 1990.

[106] R. Aranda-Rodriguexz, Z. Jin, J. Harvie and A. Cabecinha, "Evaluation of three field test kits to detect microcystins from a public health perspective," *Harmful Algae*, vol. 42, pp. 34-42, 2015.

[107] J. A. Fuhrman, D. E. Comeau, Å. Hagström and A. M. Chan, "Extraction From Natural Planktonic Microorganisms of DNA Suitable for Molecular Biological Studies," *Applied and Environmental Microbiology*, vol. 54, no. 6, pp. 1426-1429, 1988.

[108] J. Marmur, "A procedure for the isolation of deoxyribonucleic acid from micro-organisms," *Journal of Molecular Biology*, vol. 3, no. 2, pp. 208-218, 1961.

[109] Boom, Sol, Salimans, Jansen, Wertheim-Van DIllen and Van Der Noordaa, "Rapid and Simple Method for Purification of Nucleic Acids.," *Journal of Clinical Microbiology*, vol. 28, no. 3, pp. 495-503, 1990.

[110] T. Sereda, C. Mant, F. Sonnichsen and R. Hodges, "Reversed-phase chromatography of synthetic amphipathic alpha-helical peptides as a model for ligand/receptor interactions. Effect of changing hydrophobic environment on the relative hydrophilicity/hydrophobicity of amino acid side-chains," *Journal of Chromatography*, vol. 676, no. 1, pp. 139-153, 1994.

[111] R. Dirks and N. Pierce, "Triggered Amplification by Hybridization Chain Reaction.," *Proceedings of the National Academy of Sciences of the United States of America,* vol. 101, no. 43, p. 15275–15278, 2004.

[112] T. Yamaguchi, S. Kawakami, M. Hatamoto, H. Imachi, M. Takahashi, N. Araki, T. Yamaguchi and K. Kubota, "In situ DNA-hybridization chain reaction (HCR): a facilitated in situ HCR system for the detection of environmental microorganisms," *Environmental Microbiology,* vol. 17, no. 7, p. 2532–2541 , 2014.

[113] J. Ikbal, G. Lin and Z. Gao, "The Hybridization Chain Reaction in the Development of Ultrasensitive Nucleic Acid Assays.," *TrAC Trends in Analytical Chemistry,* vol. 64, pp. 86-99, 2015.

[114] X. Chen, N. Briggs, J. McLain and A. Ellington, "Stacking Nonenzymatic Circuits for High Signal Gain.," *Proceedings of the National Academy of Sciences of the United States of America,* vol. 110, no. 14, p. 5386–5391, 2013.

[115] H. Choi, V. Beck and N. Pierce, "Next-generation in Situ Hybridization Chain Reaction: Higher Gain, Lower Cost, Greater Durability.," *ACS Nano,* vol. 8, no. 5, p. 4284–4294, 2014.

[116] S. Tyagi and F. R. Kramer, "Molecular beacons: probes that fluoresce upon hybridization.," *Nature Biotechnology,* vol. 14, no. 3, pp. 303-308, 1996.

[117] M. Zuker, "Mfold web server for nucleic acid folding and hybridization prediction.," *Nucleic Acids Research,* vol. 31, no. 13, pp. 3406-3415, 2003.

[118] T. Walker, M. Little, J. Nadeau and D. Shank, "Isothermal in Vitro Amplification of DNA by a Restriction Enzyme/DNA Polymerase System," *Proceedings of the National Academy of Sciences of the United States of America,* vol. 89, no. 1, pp. 392-396, 1992.

[119] Y. He and T. Jiang, "Nickase-dependent isothermal DNA amplification," *Advances in Bioscience and Biotechnology,* vol. 4, no. 4, pp. 539-542, 2013.

[120] Z. Guo, R. Guilfoyle, A. Thiel, R. Wang and L. Smith, "Direct fluorescense analysis of genetic polymorphism by hybridization with oligo nucleotide arrays on glass supports," *Nucleic Acids Research,* vol. 22, no. 24, pp. 5456-5465, 1994.

[121] C.-W. Wei, J.-Y. Cheng, C.-T. Huang, M.-H. Yen and T.-H. Young, "Using a microfluidic device for 1 ul DNA microarray hybridization in 500 s," *Nucleic Acids Research,* vol. 33, no. 8, p. e78, 2005.

[122] L. Xue, X. Zhou and D. Xing, "Sensitive and homogeneous protein detection based on target-triggered aptamer hairpin switch and nicking rnzyme assisted fluorescence signal amplification," *Analytical Chemistry,* vol. 84, no. 8, p. 3507–3513, 2012.

[123] J. J. Li, Y. Chu, B. Yi-Hung Lee and X. Sunney Xie, "Enzymatic Signal Amplification of Molecular Beacons for Sensitive DNA Detection.," *Nucleic acids research,* vol. 36, no. 6, p. e36, 2008.

[124] S. Nybom, "Sonja Nybom (2013). Biodegradation of Cyanobacterial Toxins, Environmental Biotechnology - New Approaches and Prospective Applications, Prof. Marian Petre (Ed.), InTech, DOI: 10.5772/55511. Available from: http://www.intechopen.com/books/environmental-bio," *Environmental Biotechnology-New Approaches and Prospective Applications,* 2013.

[125] C. Ward, K. Beattie, E. Lee and G. Codd, "Colorimetric protein phosphatase inhibition assay of laboratory strains and natural blooms of cyanobacteria: comparisons with high-performance liquid chromatographic analysis for microcystins," *Microbiolody Letters,* pp. 465-473, 1997.

[126] S. Handy, B. Yakes, J. DeGrasse, K. Campbell, C. Elliot, K. Kanyuck and S. DeGrasse, "First report of the use of a saxitoxin–protein conjugate to develop a DNA aptamer to a small molecule toxin," *Toxicon,* pp. 30-37, 2013.

[127] "Blue Green Algae," [Online]. Available: http://dnr.wi.gov/lakes/bluegreenalgae/.

[128] J. O'Neil, T. Davis, M. Burford and C. Gobler, "The rise of harmful cyanobacteria blooms: The potential roles of eutrophication and climate change," *Harmful Algae,* vol. 14, pp. 313-334, 2012.

5 Appendix A: Buffers

Table 15: Buffers for hybridization schemes.

Buffers	Reagents
Low strength blocking buffer 1	20 mM Tris, 1 M NaCl, 1 mM EDTA, 0.0005% Triton 100X
Low strength blocking buffer 2	20 mM Tris, 1 M NaCl, 1 mM EDTA, 0.0005% Tween 20
Medium strength blocking buffer	20 mM Tris, 1 M NaCl, 1 mM EDTA, 0.0005% Tween 20, 1mg/mL BSA
High strength blocking buffer 1	20 mM Tris, 1 M NaCl, 1 mM EDTA, 0.0005% Tween 20, 1mg/mL BSA, 1 mg/mL salmon sperm DNA
High strength blocking buffer 2	0.9 M NaCl, 20 mM Tris-HCl, 10% dextran, 0.02% SDS, 55% Formamide, 1% Skim Milk, 1 mg/mL salmon sperm DNA
High strength blocking buffer 3	0.9 M NaCl, 20 mM Tris-HCl, 10% dextran, 0.02% SDS, 55% Formamide, 1% Roche blocking reagent, 1 mg/mL salmon sperm DNA
High strength blocking buffer 4	0.9 M NaCl, 20 mM Tris-HCl, 0.02% SDS, 1 mg/mL salmon sperm DNA, 1% Skim Milk
High strength blocking buffer 5	0.9 M NaCl, 20 mM Tris-HCl, 0.02% SDS, 1 mg/mL salmon sperm DNA, 1mg/mL BSA
Low stringency wash buffer	2X SSC, 0.0005% TritonX100
High stringency wash buffer	0.1X SSC, 0.0005% TritonX100

6 Appendix B: Figure Permissions

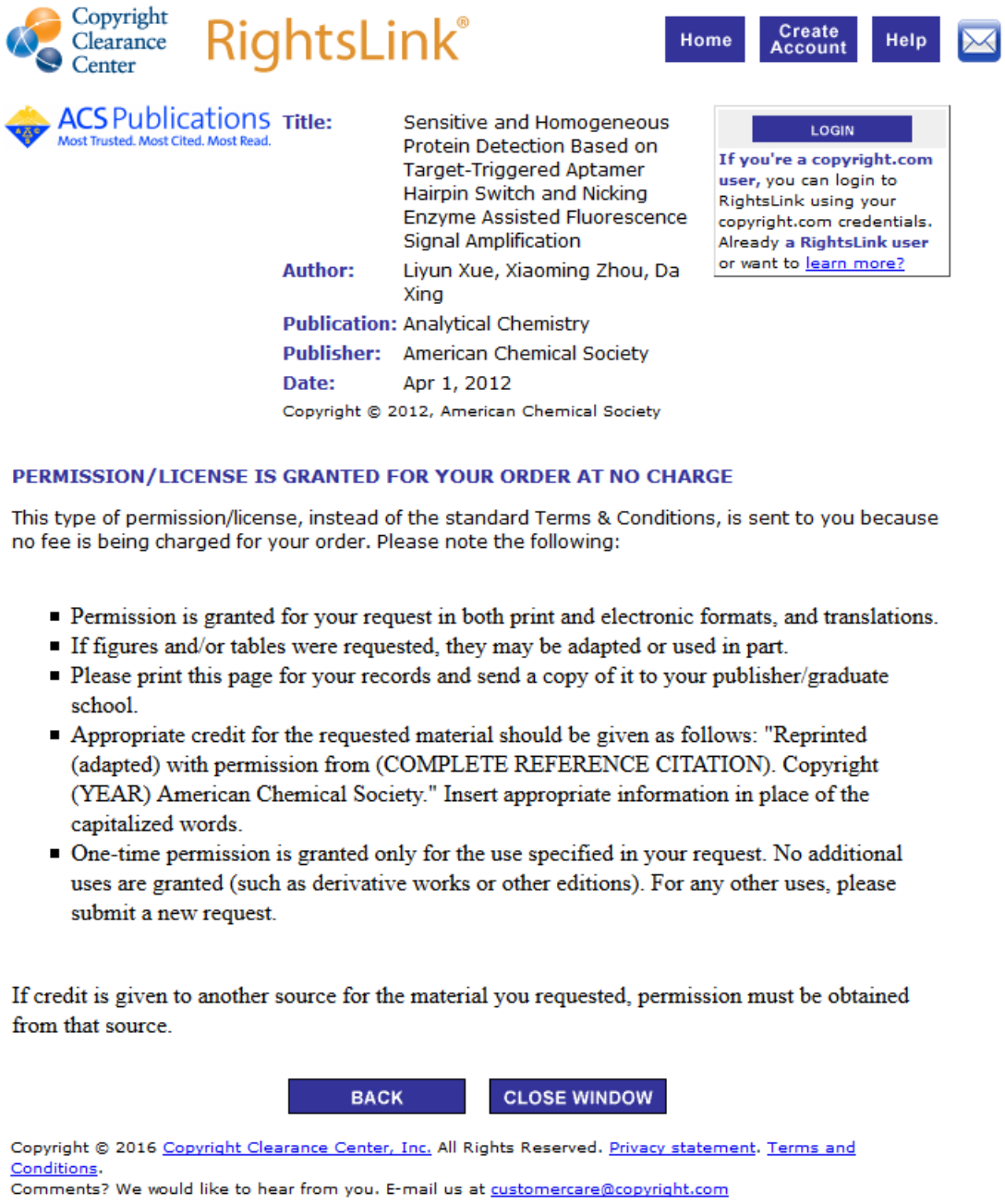

Copyright Clearance Center RightsLink®

Home | Create Account | Help

ACS Publications
Most Trusted. Most Cited. Most Read.

Title: Sensitive and Homogeneous Protein Detection Based on Target-Triggered Aptamer Hairpin Switch and Nicking Enzyme Assisted Fluorescence Signal Amplification

Author: Liyun Xue, Xiaoming Zhou, Da Xing

Publication: Analytical Chemistry

Publisher: American Chemical Society

Date: Apr 1, 2012

Copyright © 2012, American Chemical Society

LOGIN

If you're a copyright.com user, you can login to RightsLink using your copyright.com credentials. Already a RightsLink user or want to learn more?

PERMISSION/LICENSE IS GRANTED FOR YOUR ORDER AT NO CHARGE

This type of permission/license, instead of the standard Terms & Conditions, is sent to you because no fee is being charged for your order. Please note the following:

- Permission is granted for your request in both print and electronic formats, and translations.
- If figures and/or tables were requested, they may be adapted or used in part.
- Please print this page for your records and send a copy of it to your publisher/graduate school.
- Appropriate credit for the requested material should be given as follows: "Reprinted (adapted) with permission from (COMPLETE REFERENCE CITATION). Copyright (YEAR) American Chemical Society." Insert appropriate information in place of the capitalized words.
- One-time permission is granted only for the use specified in your request. No additional uses are granted (such as derivative works or other editions). For any other uses, please submit a new request.

If credit is given to another source for the material you requested, permission must be obtained from that source.

BACK | CLOSE WINDOW

Copyright © 2016 Copyright Clearance Center, Inc. All Rights Reserved. Privacy statement. Terms and Conditions.
Comments? We would like to hear from you. E-mail us at customercare@copyright.com